Determining Optimal Flight Paths for Cellular Network Connectivity for the Transmission of Real-Time Physiological Data in support of Big Data Analytics during Airborne Critical Care Transport

By

Robert Greer, BEng

A Thesis Submitted in Partial Fulfilment
of the Requirements for the Degree of

Master of Science

In

The Faculty of Business and Information Technology

Computer Science

University of Ontario Institute of Technology

February 2017

Certificate of Approval

Abstract

This thesis presents a methodology for determining the optimal flight paths between two geographical points based on distance and cellular reception over the path. This methodology consists of two main concepts: coverage map generation, and path planning. Coverage map generation creates a grid map of the total planning space that contains coverage information for each grid point. Coverage is calculated based on geographical and technical information regarding each cell tower in the planning area. The planning step utilises the coverage map to plan a route based on minimum distance and maximum coverage, which is then smoothed into a feasible route for an aircraft to follow. This methodology is demonstrated in an airborne critical care transport within the Province of Ontario in Canada context. Leveraging available cellular information, this methodology is used to determine optimal paths between various care centres or their closest airport. Evaluation reveals that optimal routes can be found through this methodology.

Keywords: Path Planning, Cellular Networks, Neonatal Transport, Neonatal Intensive Care, Ambulance, Patient Transport, Critical Care Transport, Telemedicine, Physiological Monitoring.

Acknowledgements

Reflecting on the journey that this thesis represents, it is hard not to see that this work represents so much more than just a collection of text. This thesis represents one of the largest challenges in my life and ultimately my greatest triumph. More than just a degree, this these has truly been the springboard on which I have begun my life, and my career. However, none of this would be possible without the support of the many people in my life that supported and guided me through this process.

I would like to thank very special men and women of the McMaster Children's Hospital's Neonatal Transport Team and Dr. Edward Pugh. By exposing me to the incredible world of neonatal transport, you not only inspired this thesis, but you demonstrated the amazing and selfless work you do all day every day. It has truly been an honour to meet and work with you all.

To my supervisor Dr. Carolyn McGregor, thank you for providing me with an opportunity to do this work. The opportunities and experiences you have exposed me to are immeasurable. Your inspiration, and the work you do, has formed the basis on which I have built my career. It has been a true pleasure to do this work under your supervision.

To my co-supervisor Dr. Khalil El-Khatib, thank you for providing the technical insight needed to get through this work.

I would like to thank my friends and family. Your support and encouragement has been unwavering throughout this work. Thank you for the endless motivation and tireless support.

Lastly, and most importantly, I would like to thank Caroline Elias and the entire Elias family. Your love and support through the highs and lows of this work have been immeasurable. Whether it was late nights helping revise sections, or providing a caring ear

when times were tough, your support was something I could always count on. I could not have finished this without you. Thank you, for everything.

List of Figures

List of Tables

List of Equations

List of Acronyms

ATC	-	Air Traffic Control
CDMA	-	Code Division Multiple Access
CDSS	-	Clinical Decision Support System
CNN	-	Canadian Neonatal Network
CP	-	Cyclic Prefix
FDMA	-	Frequency Division Multiple Access
FM	-	Fade Margin
GT	-	Guard Time
NICU	-	Neonatal Intensive Care Unit
OFDMA	-	Orthogonal Frequency Division Multiple Access
RDP	-	Ramer-Douglas-Peucker Algorithm
RSP	-	Radio Signal Propagation
SINR	-	Signal to Interference and Noise Ratio
TA	-	Timing Advance
TDMA	-	Time Division Multiple Access
UAV	-	Unmanned Aerial Vehicle
UE	-	User Equipment
UHF	-	Ultra High Frequency
UMTS	-	Universal Mobile Telecom System
VHF	-	Very High Frequency

1. Introduction

This thesis presents a methodology and set of algorithms to maintain the best possible cellular data connectivity for an aircraft by determining the shortest path between two airports that enables the best possible cellular data connectivity for an aircraft. This research is motivated by the goal of demonstrating usefulness of increasing the quantity of data available to support the clinical decision making process during neonatal transport and the utilization of technology to support that [1]. There have been transport telemedicine technologies that have been developed that aim to address these benefits and increase patient care for transported patients in general, but they have failed to address the airborne aspect of some transports. The reason for this is likely due to a lack of suitable connectivity options for the airborne transport field. The goal of this research is to address the connectivity issues that are present in airborne transport and demonstrate that ground-based cellular network connectivity provides a cost effective and tangible option for use onboard medevac aircraft. By presenting a path planning methodology as a manner of addressing uncovered areas of geography, this thesis presents a viable option for ensuring connectivity for the largest portion of the aircraft route while maintaining distance and speed considerations necessary for aircraft routing.

1.1. Cellular Networks

Cellular networks, and the cellular phones and mobile Internet sticks used to connect to them, have become a pervasive technology in the modern world. Today, people carry their mobile phone with much the same or greater importance as wearing their watch. This need for constant connection has led to the continuous development of cellular network technologies, and wider deployment of networks. Technologies such as LTE (Long Term Evolution) have begun gaining widespread traction and have been providing speeds in excess of 300Mbps to customers [2].

Cellular networks function, on the most basic level, as a two-way communication link between mobile hardware, or a User Device (UD), and fixed cellular tower base station. This connection allows for both voice and data communications to a mobile device, whether it be at rest or under way. Unlike Wi-Fi-based communication, cell networks allow for UD's to transition from one cellular base station to another without the loss of connection as a UD moves and/or the connection to the current tower fades. These features, combined with the high speed and pervasive deployment, make cellular data networks an ideal candidate for use in mobile telemedicine solutions.

Despite the claim by TELUS mobility that their network (amongst the largest in Canada) reaches some 99% of the population [3], there are still large geographical gaps in coverage that make long distance telemedicine difficult (Figure 1-1). These gaps are the result of cellular coverage being focused primarily on areas of greater populations and the roads between them. This theory of installation works well with ground-based usage; however, it proves problematic for airborne use where the same restrictions aren't in place. In this thesis, a solution is presented that aims to address these issues by creating flight routes that maximize distance and speed efficiency that aircraft provide, while making a best-effort to stay within the covered areas.

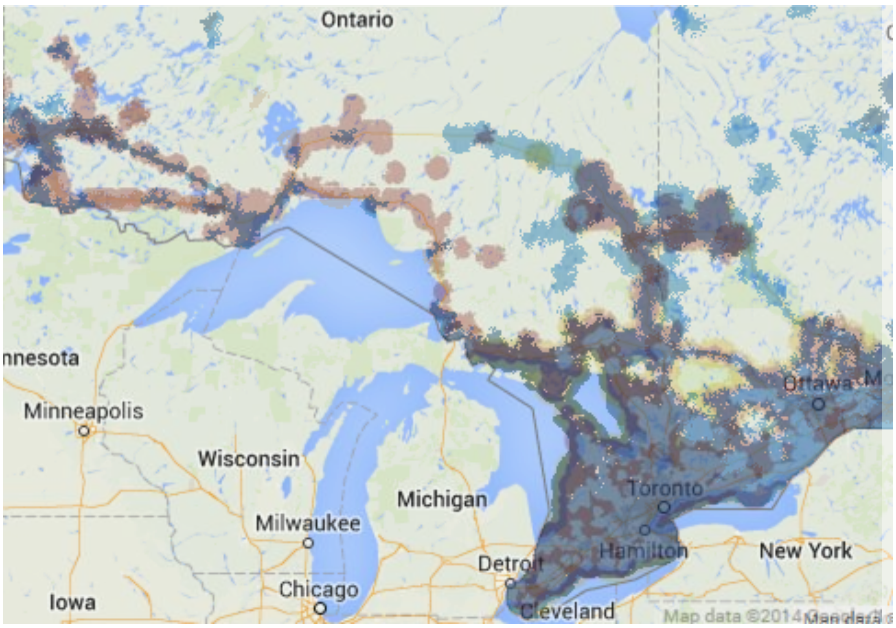

Figure 1-1 - Bell Mobility and Rogers Wireless Cellular Network Coverage

1.2. Telemedicine

Telemedicine, or the broad concept of receiving care remotely by leveraging communication technologies, is not a new topic. For over 30 years, the medical community has been actively seeking to leverage technology to provide better medical care to patients [4]. Efforts have been broad and in a variety of areas, but have largely failed to gain widespread traction.

There are clear benefits to providing care at a distance such as: improved care to underserved rural communities, gaining better insight into the condition of a chronically ill patient living at home, the decrease in travel for rural patients, and lowered overall medical costs. Because of these potential benefits, there have been many attempts to bring telemedicine approaches to various communities, however most have ultimately failed. This is largely due to technological and communication limitations [4]. However, there has been recent success as newer technologies are solving many of the problems that made telemedicine inaccessible.

Progress in airborne critical care transport has not seen the same development, despite this increase in technology and the successes of telemedicine. There are noted benefits to a telemedicine approach in healthcare [5], but it is likely that a lack of viable communications methodologies have prevented substantial development of advanced systems for transport thus far. This thesis proposes a methodology to address these issues to support a telemedicine approach during airborne transport.

1.3. Path Planning

Path planning, in general, has been a mainstay of research topics for many years. Primarily focused on robotics, the amount of research in the area has increased, along with the increased development in robotics as a whole. Path planning itself has long since been discussed in research, but it was not until Dijkstra proposed his path planning algorithm in 1959 [6] that the research field in its present, computational form was born. One of the earliest uses for path planning algorithms, before the computational age, was present in the Depth-First Algorithm investigated by the French Mathematician Charles Pierre Trémaux in the 19th century as a method for solving mazes [7].

Though many of these early algorithms began before computing existed in present form, many of these algorithms have been successfully ported over to the computer science realm [7].

One of the fundamental parts of path planning algorithms is the use of a graph to represent the nodes that can be traversed from a beginning point to an end point. The paths that are traversable between these nodes are referred to as vertices [7]. (See Figure 1-2 - Path Graph Types (A)). In more recent works, such as Dijkstra's algorithm of 1959 [6], the concept of adding a cost for traversing a graph via a particular vertex has enabled the biasing of particular paths to another (Figure 1-2 (B)). This concept has also been furthered to include a direction to restrict vertex traversal to specific directions (Figure 1-2 (C)).

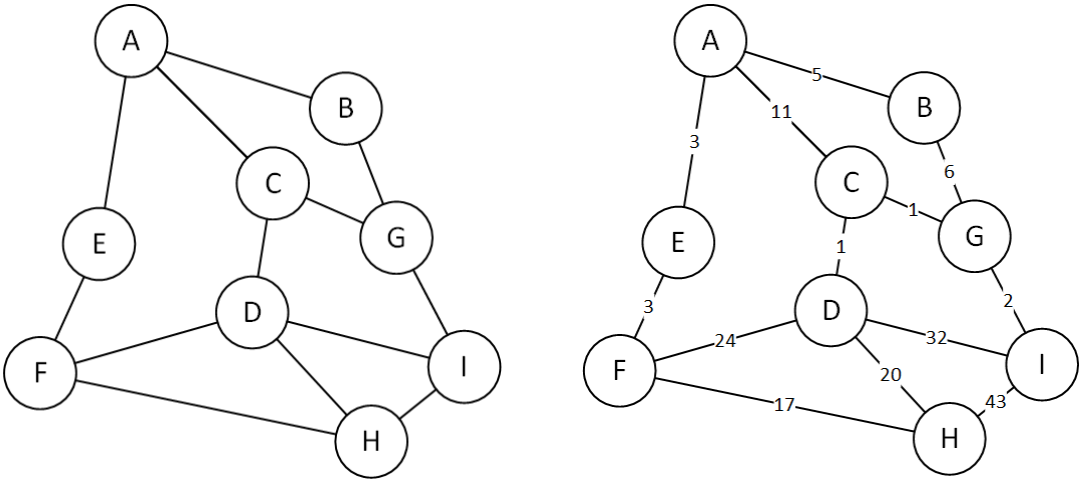

(A) Path Tree **(B) Weighted Path Tree**

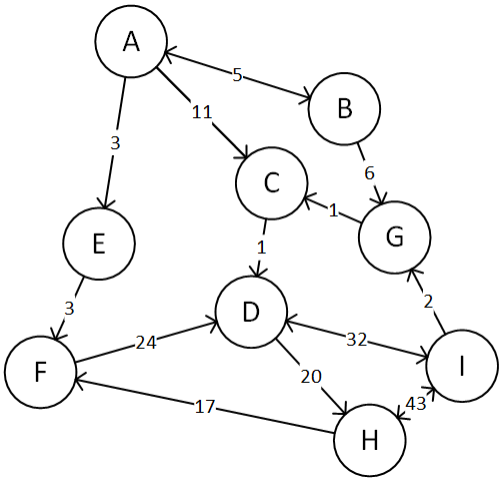

(C) Directional Path Tree

Figure 1-2 - Path Graph Types

One of the key improvements, proposed by Hart et al [8] and the approach proposed for use in this thesis, is the A* algorithm. The A* algorithm implements a Heuristic function that when used in conjunction with the typical path weighting, effectively biases the algorithm to select paths with low heuristic cost. The heuristic function typical provides a lowest possible cost from any node in the graph to the destination [8]. An example of this would be a straight-line distance, across no vertices, to the destination from the node in question. This ensures that the most direct path from a start to end note are traversed first.

Unlike Dijsktra, which must traverse all nodes to find the shortest path [6], the A* algorithm allows for the removal of non-likely nodes from the tree [8]. In more recent developments, research has taken on the task of further refining the fundamental algorithms to further optimize the planning process and decrease the overall size of the tree-space that must be traversed to determine the shortest path [9]–[14].

1.4. Research Motivations

Modern critical care is considered extremely data-intensive. Over the last several decades there have been more and more medical devices integrated into the patient care sphere that produce a high volume of information regarding the patient's current and past state. This new wealth of information has led to a decrease in mortality during critical care visits.

Only recently has the research area emerged that looks at analyzing all of the data that is output by these devices. Traditionally these devices were never continuously monitored. Nurses or physicians typically only looked at these devices during times of increased patient condition criticality, or at a regular interval when collecting vitals. The result of this practice was the loss of a tremendous amount of potentially medically relevant high fidelity medical data that could provide a better insight into a patient's current or future condition.

Recent research has demonstrated this, and that the only feasible way to approach this problem and provide a tangible solution is through the use of stream computing-based algorithms, and big data analytic approaches to make appropriate, continuous real-time use of the data [15], [16]. However, these approaches require low latency and high bandwidth to provide the information in a timely manner as required in critical care. With the continued improvements in cellular networks technologies, they have been shown to provide these requirements [17]. By leveraging this type of connectivity it will allow for higher fidelity and volumes of information to be provided to clinicians that remotely assist

in the transport process. This information will allow for a better insight into a patient's condition and facilitated a better quality of care before admission into the destination intensive care unit.

Though cellular networks can provide the connectivity required to allow for continuous remote monitoring of patients undergoing a critical care transport, there are several challenges that make the application of cellular networks to airborne transport difficult. One of the key problems is that airborne transports often occur over very vast areas, often times where connectivity is limited. For example, airborne transport calls in Ontario often originate from northern tertiary care facilities where there is limited connectivity but are surrounded by vast areas where there is little to no connectivity whatsoever. Other problems include the relatively low cellular tower density in these outlying areas. This leads to cellular connectivity being quite slow and patchy.

This research seeks to address these issues by creating a route that is not only optimal in terms of providing maximum connectivity over its length, but also maximizes the total number of cellular towers that cover all areas of the path to maximise connection probability. Traditional incremental path planning approaches are not practical in this setting given the fact that aircraft are not able to change direction continuously for each cellular tower radius, and as a result holistic planning needs to be taken into consideration. Through the creation of optimal routes, this research aims to demonstrate that airborne transport could feasibly utilise cellular networks to transmit physiological and other medical data continuously throughout a flight. Furthermore, this research aims to demonstrate that utilising a computational path planning approach can generates the routes that maximize signal strength and probability.

1.5. Research Aims and Objectives

The aims and objectives of this research are to propose new flight paths for emergency transport aircraft to utilise in order to:

I. Maximize cellular data connectivity throughout the airborne portion of the transport;
II. Minimize the total route distance to ensure a rapid transport;
III. Enable best possible telemedicine through the transport;
IV. Demonstrate the feasibility of using cellular networks to provide telemedicine connectivity during airborne transport.

1.6. Research Hypothesis

1. A method to enable a flight path to be found that maintains a higher level of cellular connectivity than a direct path can be quantified;
2. The method proposed above is able to determine a flight path that represents the shortest path that maintains highest duration of connectivity;
3. The method proposed above is able to determine a flight path that represents a feasible flight path that could be followed by a manned aircraft;
4. The method proposed above can be demonstrated in the airborne transport domain and provide a tangible method for maintaining optimal cellular connectivity.

1.7. Contribution to Knowledge

In this section, the specific contributions made to the body of Computer Science knowledge are presented.

I. Use of advanced cellular coverage calculations to determine realistic cellular coverage regions for path planning

The first contribution that this thesis provides is that the use of advanced calculations of a cellular tower's specific broadcast range will yield a very realistic coverage map. This ensures that a tower's specific coverage is neither over nor under expressed in a coverage map ensuring more accurate planning.

II. Dynamic creation of cellular coverage maps to represent a region's coverage

The second contribution is the ability to create coverage maps that account for the effects of an aircraft's altitude on the effective broadcast area of a cellular tower. This creates coverage maps that are more realistic than a traditional ground-based estimation of broadcast radius.

III. Use of a path planning approach to maintain cellular connectivity in a manned aircraft

The third contribution is the utilisation of path planning approaches to maintain ground-based cellular connectivity on manned aircraft. Realistic flight paths are generated that represent that optimal blend of connectivity and shortest distance between the origin and destination airports.

IV. Use of path smoothing to create feasible routes for manned aircraft to utilize

The fourth contribution of this thesis is the utilisation of a path smoothing methodology to convert highly complex planned paths, into much less complex paths with fewer steps. These paths provide a much more feasible path for an aircraft to follow.

V. Demonstration using a clinical problem

The final contribution is the utilisation of a clinical problem, lack of connectivity during neonatal airborne transport, to demonstrate the efficacy of the method presented in this thesis. This clinical demonstration provides a unique contribution in the transport domain and could provide a possible solution to the lack of connectivity problem.

1.8. Research Methodology

The research conducted in this thesis follows the Constructive Research Methodology. The constructive method involves the construction of a domain-specific artefact based on pre-existing knowledge in the research domain or related domains. This new artefact results in new knowledge being contributed to the field, and if a solution already exists, the newly proposed solution is notably better than the existing [18] (Figure 1-3).

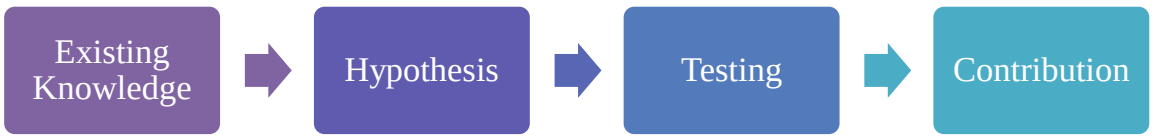

Figure 1-3 - Constructive Research Methodology

The constructive research methodology is implemented in this thesis as follows: (1) existing areas of research such as Airborne Data Networks, Path Planning, Neonatal Transport, and Telemedicine are studied and from them; (2) A set of research hypotheses are determined; (3) Based on the results of existing knowledge, and guided by the hypothesis, a methodology is created for evaluating the hypothesis; and (4) it is implemented for evaluation. Evaluation (5) of the hypothesis was based on the derived methodology and (6) the results presented. The validation of the research hypotheses and the output from the evaluation are used to determine the feasibility for the research domain of Neonatal Critical Care Transport, and it is shown that the results can be significant to other types of medical transport, and aircraft at large.

1.9. Thesis Overview

This thesis has the following structure: Chapter One introduces the research area and defines the research problem and hypothesis. Chapter Two presents a review of related literature and defines the open research area. Chapter Three presents and discusses Neonatal Critical Care Transport – the case study research area. Chapter Four presents the proposed methodology for path planning for optimal network connectivity. Chapter Five presents the implementation of chapter four, and applies it to the case study research area. Lastly, Chapter Six concludes the research and presents a discussion and future research areas.

2. Review of Literature

2.1. Introduction

The purpose of this chapter is present the related works to this research to build context. To accomplish this, there are three main sections presented that describe the three major thematic areas that this research encompasses including: Wireless Data Communication in Aircraft, Path-Planning in Aircraft, and Telemedicine in Patient Transport. The results of the independent reviews are then synthesized in a fourth discussion section and their relevance to this research described.

2.2. Methodology

To retrieve the related research to each of the three main areas of review, literature searches were conducted on a variety of online databases including: IEEE Xplore Digital Library, ACM Digital Library, Ovid Medline, and Google Scholar. On each of these databases, searches were conducted with the keywords and Boolean operators such as 'AND', 'OR', and 'NOT'. In areas where there was either none, or very little academic work, such as wireless data communications in aircraft, information was found on websites of providers or companies in the field to provide context. For each section, papers were found isolated to those published between 1990-2015 except where historical context was required. Keywords used in each section include:

Wireless Data Communication in Aircraft – Aircraft, Airplane, Airborne, UAV, Aerial, Communication, Internet, Airborne, Wi-Fi, 3G, Satellite, Data-Link

Path Planning Activities in Aircraf – Aircraft, Airplane, Airborne, UAV, Communication, Path Planning, Dijkstra, A*, A-star.

Telemedicine in Patient Transport – Telemedicine, Remote Monitoring, Patient, Critical Care, Ambulance, Helicopter, Aircraft.

2.3. Wireless Data Communication in Aircraft

Wireless data communication onboard aircraft is fast becoming as ubiquitous as the Internet itself. The ability to surf the Internet while in flight was once considered fantasy, and then reserved only for the rich in private aircraft. Today, it is now possible to surf the Internet, check emails, or even make a VOIP (voice over internet protocol) call on many domestic North America aircraft. Furthermore, the rise of data communications has led to wireless audio/video feeds providing live news, or even sporting events. All of this is driven by various wireless technologies that have been developed for a wide range of needs, but are now trickling down to the average consumer. In this section, the main technologies available are explored. They include: Satellite, Microwave Downlinks, Cellular, and Military systems.

2.3.1. Satellite

Satellite-based communications for aircraft have long been the natural choice for long-range communications. Single satellites are at extremely high altitudes and are therefore able to cover large swaths of the earth, as well as are versatile enough to service ground, land, and sea-based platforms. There are several major companies that offer wireless internet services for both commercial and private aircraft [19], [20]. Most of these companies rely primarily on the Inmarsat Ka and Ku-band satellite network to provide their data links [19], [21]. These services place one or more satellite's tracking antenna(s) on the top of the aircraft to establish a link to the satellite network. Although they claim speeds in excess of 50mbps, these systems often do not reach those speeds [22]. Furthermore, as is the nature of the very long round trip distance and time with satellite communications systems, these systems are also plagued with very high levels of latency [22]. Latency is a measure of the time it takes for data to begin being transferred after the instruction for transfer. These high-latency could potentially effect the responsiveness of communications and hamper their overall usefulness.

In an attempt to solve this, US-based Company GoGo has implemented a novel hybrid solution. This solution uses antennas placed on the bottom of aircraft to connect to their own surface cellular network. By placing all upload traffic on this network, and reserving the top of aircraft, satellite communications for downloads the system can achieve much higher data rates [23].

Given that satellite communication is a physical up-link (linking in the upwards direction), there is an established limitation for use on rotary wing aircraft. Since an antenna cannot be placed on the highest point of these types of aircrafts, and the effective attenuation and interference from the rotor, there has been no way to obtain a reliable link. In [24], a system is presented for the rapid reacquisition of a signal as the rotor blades interrupt the signal in rotation. The paper demonstrates positive results with its high-customized solution, but does so at lower data rates than a non-interrupted system such as the ones present on fixed-wing aircraft.

2.3.2. Cellular

Despite the increase in speed and prevalence of cellular networks ([2], [25]), there have been relatively few instances where research has been done involving cellular communications from aircrafts. Of the research that was located, all pertained to the use of the technology exclusively on a unmanned platform (UAV) [26]–[28]. The only evidence found of cellular data networks being used to provide a data link to a manned aircraft came from GoGo wireless, mentioned in the preceding section.

In both [26] and [28], cellular networks are utilized for command, control, and relaying of onboard sensor data. Zhi et al. focuses primarily on the relative latency and delay that are present in a cellular based downlink [28]. A methodology for determining current and predicting future transmission delay is presented. Based on these calculations, a more accurate estimate for current position and altitude is presented that compensates for end-to-end delay [28]. Moreover, it is concluded that cellular networks provide a robust,

and high-throughput end-to-end transmission solution for flight data that is of lower latency and cost than satellite solutions [28].

In [26] a cellular-based network is used to relay sensor information from a UAV that tracks aerosol emissions. The system presented allows for both direct connecting to a cellular network, and to connect to adjacent UAVs to provide a data relay effectively increasing its range. This work highlights many of the benefits of utilizing public cellular networks as an air-to-ground link for data communications such as the relatively low latency of the technology [26] compared to satellite systems [24].

Miura et al. [27] present a different approach to utilizing cellular networks aboard UAVs. In this work, the airborne platform is utilized as a relay point for broadcasting a cellular signal to ground-based receivers. Being at high altitude and sending the signal down affords a much longer range per cell than a typical ground based cellular tower, and allows for less signal noise [27]. However, this environment also proves challenging as there can be strong interference from nearby cell towers that broadcast at high power. High power is utilized to ensure signal propagation at ground level, but causes interference on stations at altitude that are much further away than would otherwise be covered at ground level [27].

2.3.3. Microwave Downlinks

Born out of the need to transmit video and audio from media aircraft covering new events, sporting events, etc., Microwave Downlinks are effective solutions for smaller companies and aircrafts. This is due to their portability, small size, and relatively low cost [29]. These systems operate by transmitting data, such as an encoded video signal, to a portable or fixed ground station, and typically have a range in excess of 100km. The signal can also be relayed via other aircraft or base stations to increase the range beyond that. However, due to their requirements for ground-based hardware that can decode their particular signal, their usable range is constrained by the location of fixed ground stations

and the time required to set up portable ground station. As these are a downlink type system, there is no interference with the rotor of a rotary wing aircraft as there is in satellite-based systems [24].

2.3.4. Military

The need for secure communication and tactical information transmission has long been a need for the military. As a result, there have been a myriad of technologies developed over the years to exchange this information between military equipment and installations. Though information on these links is scarce due to their classified nature, there is information about both Link-16 and Link-22, the NATO standard for both tactical voice and information communication available [30]. Link-16 and Link-22 form the most prevalent present-day form of military communication technologies.

Link-16 is a line-of-sight communication technology that takes the features of Link-11 and adds to it secure voice communication, jam resistance, and increased throughput amongst others [30]. The technology provides a message-based communication topology that consists of a hard-coded set of message types and structures. Though this provides no extensibility, it ensures forward compatibility.

Link-22 is a beyond line of sight communication system that aims to provide secure and jam-resistant communication between aircraft, as well as navy, and army equipment. Addressing primarily the line-of-sight requirement of Link-16, Link-22 operates in much the same way, except that nodes on a link-22 network relay received messages. Unfortunately, like Link-16, Link-22 is another fixed message protocol not allowing extensibility [30].

2.4. Path Planning Activities in Aircraft

In this section, studies in airborne path planning are surveyed. Each piece of research is compared on the following topics: Aircraft Platform, Field, Algorithm, Path Constraints, and Communication Technology. The evaluation of research is presented in Table 2-1. Based on the output from this analysis, conclusions are drawn based on relevance to this research and an approach to this research is generated.

Despite the lengthy history of research into the path planning field [7] as mentioned in 1.3, the aircraft-specific domain is somewhat of a more recent phenomenon. This is likely the result of the more recent emergence of Unmanned Aerial Vehicles (UAV). Airborne-specific path planning involves creating flight paths that are not constrained in the same physical way that path planning for vehicles is, for example. Planning activities are generally constrained by things more relevant to the domain of study, such as waypoints, topographical features, or avoidance areas.

Author	Aircraft Platform	Field	Algorithm	Path Constraints	Communication Technology
Adams, et al. [31]	Piloted	Civil	Based on Dynamic Programming	• Distance • Proximity to Other Aircraft • Aircraft Dynamics • Obstacles	N/A
Bortoff [32]	UAV	Military	Voronoi Graph Search	• Distance • Proximity to Radar sites	N/A

Grøtli, et al. [9]	UAV	Civil Oil / Gas	MILP	• Fuel Usage • Position and Speed • Connectivity using SPLAT! • Anti-Collision • Anti-Grounding	Not Defined
Hammouri, et al. [10]	UAV	Not Specific	Voronoi Graph Search	• SINR	Not Defined
Kermani, et al. [33]	UAV	Not Specific	Genetic Algorithm + Fuzzy Logic	• RSP using SPLAT! • Distance • Altitude • Avoiding No Fly Zones	Not Defined
L'Afflitto, et al. [34]	Abstract	Not Specific	Mathematically defines constraints	• Fuel Efficiency • Energy Consumption	N/A
Li, et al. [35]	UAV	Not Specific	Fuzzy Logic	• Distance • "Hazard"	N/A
Lingxiao, et al. [36]	Abstract	Military	Dijkstra	• Distance • Survival Probability	N/A
McGee, et al. [37]	UAV	Civil	Dubin's Paths + Minimum Principle	• Bounded Turn Rate • Constant Wind Vector	N/A
Meng, et al.[11]	UAV	Not Specific	Bi-Directional Sparse A*	• Distance • Straight Line Distance Heuristic	N/A
Meng, et al. [12]	UAV	Military	Genetic Algorithm	• Terrain Avoidance	N/A

Schouwenaars, et al. [38]	UAV	Not Specific	MILP	• Ground Station proximity • Physical Helicopter Dynamics • Obstacle avoidance • Connectivity	Not Defined
Tanil, et al. [39]	UAV	Military	Multiple Population Genetic Algorithm	• Collision Avoidance • Optimum Communication distance • Terrain • Fuel • Radar Detection	Not Defined
Shi, et al. [40]	UAV	Not Specific	Not Described	• Vehicle Dynamics • Altitude • Distance	N/A
Tseng, et al. [41]	UAV	Civil	A*	• Signal Strength	3G
Wang, et al. [13]	UAV	Not Specific	Dubin's Path-Enhanced Sparse A*	• Dynamics • Obstacles • Distance	N/A
Xin, et al. [14]	UAV	Military	Improved A*	• Distance • Threat/Forbidden zones	N/A

Table 2-1: Literature Comparison and Evaluation

2.4.1. Aircraft Platform

The overwhelming majority of papers published in this research domain have been targeted at UAV platforms. The notable exception to this, being [31]. Research in the UAV domain also correlates well with the trend of using constraints such as Distance, Fuel, Terrain, Obstacles, Vehicle Dynamics, Collision avoidance, Weather, and forbidden

areas. In a typical manned aircraft, these aspects are overcome by the pilot's vision, and Air Traffic Control (ATC)-provided Radar services. However, there are aspects of path planning that the human factor cannot address, such as connectivity and radar detection range. Furthermore, [31] addresses the large amount of coordination that is required in congested airspace between aircraft. This is a problem that is primarily addressed by Air Traffic Control, but can become challenging and often results in less than optimal routes.

2.4.2. Domain

Overall, each paper reviewed tended to not be geared specifically towards a particular domain. Of the ones that were, there was an even distribution between the military ([12], [14], [32], [36], [39]) and the civil domains ([9], [31], [37], [41]). Despite the mention of a domain, however, only [9] made reference to any concrete use-case guiding their research work.

2.4.3. Algorithm

In this section, the specific algorithms utilised for path planning, and classes of such, are presented. Based on the papers that were discovered, there are two main types of algorithms/methodologies that are utilized: Genetic Algorithms ([12], [33], [39]), and Dijkstra-based algorithms ([6], [7], [9], [10], [32], [36], [41]). Dijkstra-based algorithm approach path planning as a weighted graph where the algorithm determines optimal route by traversing the graph. The algorithm keeps track of the total cost (sum of all path weights) from the start to end points to find the optimal path (the one with the lowest cost). Dijkstra's algorithm was one of the first path planning algorithms derived and has led to the creation of a whole host of other algorithms, such as A*, which seek to improve upon its performance. Genetic algorithms instead use a model of evolution and meta-heuristic search algorithms to prune a randomly generated set of nodes. Genetic algorithms have been shown to solve search problems with high-dimensionality more quickly than Dijkstra-

type algorithms. The algorithms used tend to also reflect the quantity, complexity, and specific traits of the constraints that are used. A particular example of this is [39], where a particular multi population variant of a genetic algorithm is used to plan the paths of multiple different UAVs, each represented as a population.

Another trend that is evident in the selection of algorithms is the increasing complexity of algorithm used the more recent the paper is. The earlier papers tend to have a more simple set of constraints, and therefore use a more simple version of algorithms ([10], [12], [32], [35]). In more recent papers, and as constraints become more numerous and complex, modifications of the original, simpler forms of algorithms are either utilized or implemented ([9], [13], [14], [38], [39]).

2.4.4. Path Constraints

This category seeks to expose the constraints that various different authors present as a means to effect/bias their respective path planning algorithms. The most commonly used constraint, and also one of the fundamental constraints used in examples of different algorithms is distance [6], [8]. This is common as path planning generally involves finding the shortest physical or duration path between two or more points.

Wireless connectivity is an area that is commonly used as a constraint effecting path planning. Emphasis on this particular constraint varies from paper to paper, however, in [10], [41] it forms the primary constraint for path planning. The approaches utilised to gauge wireless connectivity vary substantially from paper to paper. For example in [10], the pessimistic approach of Signal to Interference and Noise Ratio (SINR) is used to gauge connectivity in the goal of recovering and maintaining connectivity. [41] Utilises the optimistic approach of calculating signal strength based on Link Budgets and Path Loss calculations. Overall it is found that the trend is that optimistic approaches are utilised when locations and physical characters of a network are known, but current dynamics of the signal are not known [9], [33], [41]. The pessimistic approach is utilised generally when

there is not a lot known about the physical characteristics of networks, such as communication equipment type, powers, etc., as in [10], [38].

Another very common constraint used to influence path planning is that of areas of avoidance. Either not defining paths through particular areas or assigning very large path weights biases algorithms biased to not travel particular routes. This is particularly apparent in [12], [14], [36], [38], [39]. In the work of Xin et al [14], the basis of the work is primarily that of avoiding areas that are seen as forbidden or threatening.

The last major areas of constraints that are presented in research are those of a physical or dynamics nature. Constraints such as fuel usage, wind direction and velocity, and the physical dynamics of the aircraft under study themselves. [9], [13], [31], [33], [34], [38], [40] demonstrate these constraints.

2.4.5. Communication Technology

The fifth category looks specifically at which communication technology is utilized in each of the papers that leverage connectivity as a metric in determining path costs. Despite a variety of papers leveraging this metric, only [41] provides a solution based on a concrete technology as opposed to a general "wireless" connectivity ([9], [10], [33], [38], [39]). Along with this more broad, abstract view, none of the papers, including [41], provide any optimization for the technology they are utilizing.

2.5. Telemedicine in Patient Transport

The concept of telemedicine-based approaches to providing more advanced care outside of a hospital setting is not a new one, and has never been a more popular topic of research. In fact, a search for "Telemedicine" on Google Scholar yields "191,000" results (Conducted 13 Aug 2015). The current trend in the research field also shows the gaining popularity of the research area with more and more papers published every year on the

topic [42]. However, the majority of this work is focused around either home-based telemedicine, or in-hospital telemedicine from remote care facilities [42], [43]. The likely reason behind this focus of research is likely to do with the large aging population in the western world. Evidence of this is revealed with the large, recent, distribute of telemedicine research focused in this area [42], [43].

Despite these trends, there is still active research in the area of telemedicine for patient transport. Moreover, there have been studies that established a strong need for such a system [44]. To evaluate the current research and determine its relation to this work, four categories have been utilized: Transport Type, Network Technology Utilised, Type of Data Transmitted, and Support for Big Data Approaches.

Author	Transport Type	Network Technology Utilised	Type of Data Transmitted	Support for Big Data Approaches
Anantharaman, et al [45]	Ambulance	Mobitex	ECG, Vital Signs	No
Curry, et al [46]	Ambulance	Cellular	Audio / Video	N/A
LaMonte, et al [47]	Ambulance	Cellular	Audio / Video	N/A
Lin, et al [48]	Intra-hospital	WLAN	ECG, SpO2, BP, HR	No
Mandellos, et al [49]	Ambulance	Cellular	Various Numeric and Waveform	No
Yamada, et al [50]	Ambulance	Quasi-Zenith Satellite	N/A	N/A
Xiao, et al [51]	Ambulance	Cellular	Audio/Video, "Biosignals"	No
Lam, et al [52]	Ambulance	WiMAX	Audio / Video	N/A

2.5.1. Transport Type

Of all research that was located and analysed, the trend is to develop systems specifically for Ambulance use. Use in other patient transport methodologies, such as air transport, appears to go unmentioned. This is likely due to the relatively high cost, size, and complexity associated with the networking aspect of providing high-speed data to aircraft as mentioned in previous sections.

2.5.2. Network Technology Utilised

The most common network technology used in telemedicine as a whole is Cellular data [53]. One technology that is notably not represented in any great quantity is satellite. Yamada [50] does propose the use of the Japan-based Quasi-Zenith satellite system to provide a telemedicine system backhaul. This system has not been developed any further than a concept at this point.

2.5.3. Type of Data Transmitted

There presently are two trends in the type of data that is transmitted from telemedicine systems, namely Audio/Video feeds, and physiological data. The clinical value of both is quite commonly referenced as the reason for such a system [44]. Based on the existing research, it appears that each independent solution decides on which data to transmit based either on a specific clinical use-case [47], or tries to emulate the patient examination experience [46], [51].

2.5.4. Support for Big Data Approaches

Notably missing from all research found is in this area that involves generating and providing data for the purposes of feeding any Big Data System. Despite the recent push into this area in medicine [54], and the substantial promise, both demonstrated and

theoretical [55], researchers appear reluctant to enter this field within the context of telemedicine as a whole.

2.5.5. Analysis

With the lack of research in the area of airborne transport as a whole, the entire field remains an open research area. One thing that all papers, both in transport telemedicine, and telemedicine as a whole demonstrate is the requirement to send high volumes of data at very high speeds back to a central hospital in order to see the full benefit of the systems. Despite the overwhelming use of Cellular networks to provide connectivity, there is still well-documented evidence that there are connectivity issues associated with the use of cellular networks [56], [57].

2.6. Implications on this Research

The results of this literature review demonstrate the clear motivation behind this research. Section 2.5 shows that there is a real and tangible benefit in providing clinicians with more data in a timely matter, something that presently is not being done. This has been studied many times before in the realm of telemedicine, but no solution has ever need proposed for use during an air-based transport. One of main challenges of this lies in connectivity and how to transmit this data in a timely manner. In 2.3, various connectivity methods were explored, but it is cellular data that provides the only viable option to explore that facilitates the variety of platforms on which transports are carried out. Cellular networks, however, do not always cover an entire transport space, so it is important to maximize connectivity. Section 2.4 provides an overview of the work done in the path planning space pertaining to aircraft. In this, it is shown that there has been much successful work doing path planning with the express purpose of maintaining wireless connectivity.

It is on this basis that the hypotheses are derived. There has been work completed in the many sub-areas of this research, but there has been none that have married all into a

single research domain. It is on this basis that the research presented in this thesis is an open research area.

3. Neonatal Critical Care Transport

The world of healthcare is under tremendous pressure to deliver higher and higher levels of care quality with fewer and fewer resources. One unfortunate side effect of this is high medical error rates [1]. Contributing to this are two major factors: delays in delivering information to the necessary parties in a timely fashion, and the eligibility of hand-written patient charting and notes. In both of these cases, it has been suggested that Information Technology, and the ubiquitous access to it, could provide a means to alleviate both [1]. Despite this, the uptake of information technology in the health care industry has been substantially slower than others [58].

The issue of having information delivered to the necessary parties in a timely manner has been identified as one of the most important aspects to successful neonatal transport [5]. One of the major game-changers that has affected Canadian neonatal transport is the cell phone. Where it was once not possible to communicate between the transport providers and transport facilitators, there is now almost constant access. Technology has seemly not progressed past that.

Much research has been presented that shows how telemedicine systems, as well as audio/video communication systems can provide a tangible benefit to care, and demonstrate vary promising results [17]. Despite this, the subfield of airborne neonatal transport has been left behind. Unless a radio message can be relayed as soon as an aircraft leaves the ground, which is not always the case, there are no means of any type of communication to the transport staff at the facilitating hospital.

This challenge is not an easy one, as Canada is the second largest country in the world, sparsely populated, and has people in very hard to reach areas. Though this provides the ideal use-case for airborne transport, it makes for an extremely complex environment. Ontario, with nearly over 1 million square kilometers, is a prime example of this, and the resulting air transport network they have created is widely regarded as one of the most complex and large in the world [59]. Unfortunately, with the lack of communication

options, and the relatively long durations of transport flights, there is a potential for problems from a lack of communication.

3.1. Background

In the moments following birth, a young child's body undergoes many changes and must adapt extremely quickly in order to sustain life. One of the most notable changes is that the lungs must begin functioning and oxygenating blood. Despite the instinctive nature of these changes, many children do not make the change as seamlessly as others. Furthermore, this becomes even more problematic in premature babies, who are unable to breathe on their own as their lungs are not fully developed. These children, ranging in gestational age between less than 23 weeks to over 42, form the populations that require neonatal intensive care [60]. It is estimated that approximately 10% of all children born will require some level of neonatal care after birth, and 3% of those will require a more advanced and complex level of care [58].

Of the 10% of children that are born with this requirement, some require advanced care that can only be provided in a Neonatal Intensive Care Unit (NICU). In this environment, the children have access to specially trained physicians who can leverage multiple different specialties, imaging, and laboratory services to provide the children with the highest levels of care.

When a mother or the child that is being carried is identified as having a condition that will lead to the need of Neonatal Care, efforts are put in place to transfer the mother, pre-birth, to a facility that will not only provide birthing for the mother, but also the level of care required for the child [61]. However, these efforts are not always successful, and babies can be born in under equipped hospitals. In 2014, there were over 4000 such cases resulting in a child being transferred into a Canadian Neonatal Network (CNN) hospital for more advanced care [62]. This represented over 25% of the total neonatal population treated (see Figure 3-1). Furthermore, there were a further 4300 transfers between CNN

hospitals or tertiary care centers [62]. With over 8000 neonatal patient transfers in Canada on a yearly basis among CNN hospitals (31 reporting), there is a clear need and demonstrated importance for neonatal transport teams.

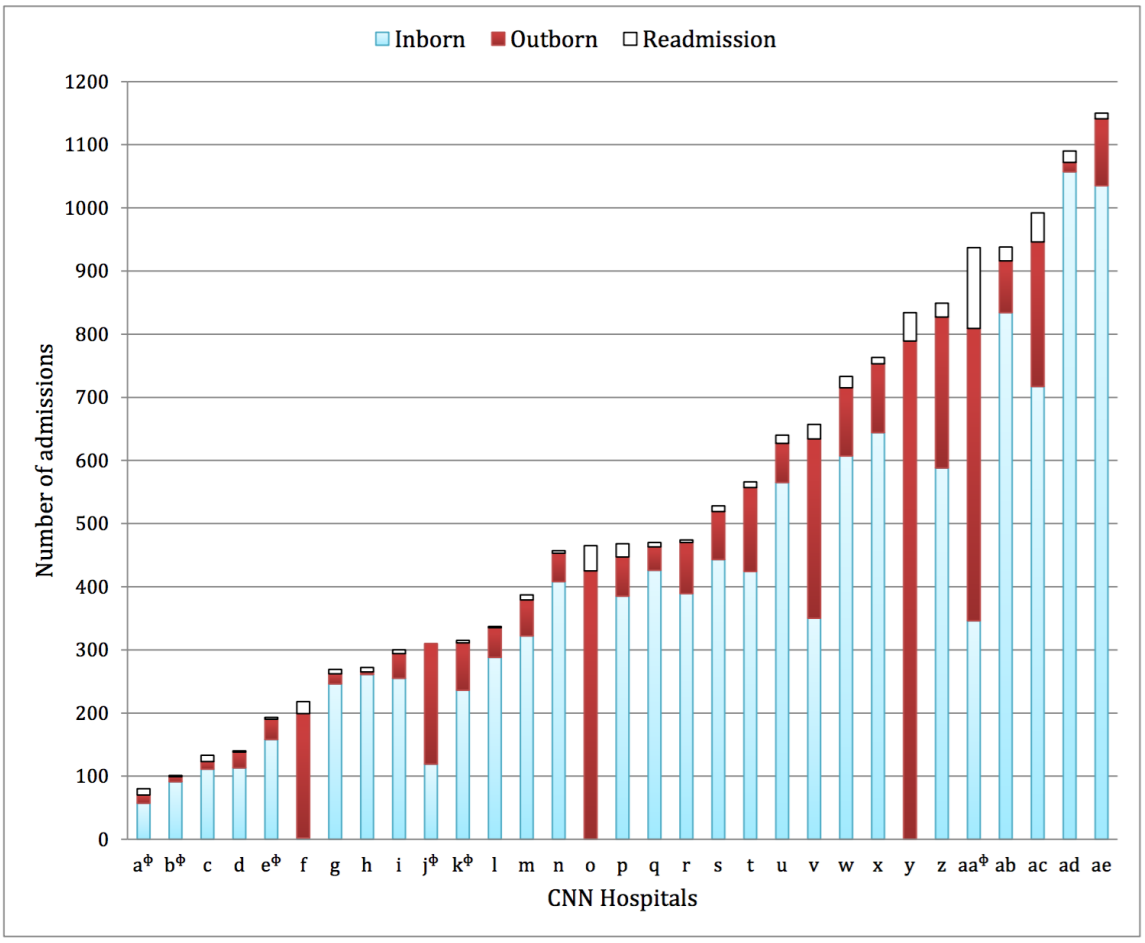

Figure 3-1 - Admissions to Canadian Neonatal Network™ participating sites [62]

Figure 3-1 shows the ratio of admissions to Canadian Neonatal Network sites between inborn (children born within the site) and those whom are outborn (born in another hospital and require transport). Each individual site is represented by each letter on the horizontal axis.

3.2. Team Structure

Facilitating a neonatal transport is not a trivial task, and requires numerous people. In Canada, neonatal transport teams have varying structure, and are often tuned to the needs

of the patients being transported. The universal architecture, however, remains the same [5]: each team consists of a group that resides at the facilitating hospital (group 1), and a group that travels out to complete the transport (group 2). Group 1 comprises of a coordinator and a neonatologist. Group 2 comprises of a variety of team configurations such as Transport Nurse-Transport Nurse (N-N), Transport Nurse-Respiratory Therapist (N-R), Transport Nurse-Physician (N-D), etc. [5]. The following list describes the roles each party plays in a transport.

1. **Transport Coordinator:** Handles the logistics of the transport including organizing transport, finding a bed at an admitting facility, and coordinating team members.

2. **Transport Physician:** The transport physician is a Neonatologist who provides instructions and guidance to the transport nurses/respiratory therapists.

3. **Transport Nurse(s)** Transport nurses are standard neonatal nurses with specialized training. They attend on the transport and are the primary caregivers of the infant.

4. **Respiratory Therapists:** Respiratory therapists are specialized practitioners who manage the respiratory tract of the infant. They manage artificial ventilation as well as recommend a course of action for a variety of respiratory ailments.

3.3. Equipment

The neonatal intensive care unit contains some of the most advanced bedside equipment of any part of a hospital: in order to sustain life in underdeveloped children, this technology is essential. One of the great challenges of Neonatal Transport is how to replicate this environment in a portable form-factor. To accomplish this, transport teams utilize a transport “deck”. This deck is designed in a form factor to fit on a conventional stretcher. This allows it to be transported in both land ambulances, as well as air. On the transport deck, there are a variety of medical devices, which are used to support the infant

and provide as close to an intensive care unit level of care as possible, given the size constraints. The following list presents and describes the various devices found on a transport deck in Ontario:

1. **Incubator:** The incubator provides a warm environment for the infant to reside in. This is particularly important in neonatology where the infants cannot always regulate their own body temperature. The transport nurse in accordance with the core body temperature of the neonate calibrates the temperature of the incubator.

2. **Patient Monitor:** The patient monitor is the device that connects to the patient and provides vital information regarding the patient's physiological state. Information such as Electrocardiogram, Pulse Rate, Respiration Rate, and Blood Oxygen Saturation. This information supports clinical decision making by Reparatory Therapists, Transport Nurse's, and Physicians.

3. **Transcutaneous CO_2:** This device monitors the levels of CO_2 that are present in the infant's blood. Utilising a non-invasive probe placed on the infant's skins, this device continuously generates concentration numbers that are used by respiratory therapists, transport nurses, or transport neonatologists to identify breathing problems, or to adjust ventilator settings to ensure proper oxygenation of blood and removal of CO_2.

4. **Nitric Oxide:** Blends of nitric oxide and oxygen are used in the treatment of with pulmonary hypertension – a common condition effecting the extremely premature. The blends are fed into the air supply used by the ventilator.

5. **Ventilator:** This device is used to support breathing in infants that are not to sustain breathing on their own. Connected via an endotracheal tube placed in the trachea via nose or mouth, this device provides the appropriate concentration of oxygen directly

into the lungs. During transport, the ventilator is monitored and adjusts by either a transport nurse, or respiratory therapist.

6. **Infusion Pumps:** This device controls both rate and quantity of medications or fluids that are infused directly into the venous system.

Despite the multitude of devices, and the extremely high level of care that they can provide, transport teams are still limited. By not travelling with all specialists, a large amount goes un-interpreted or unseen, which can prove problematic.

3.4. Ontario Neonatal Transport Framework

In Ontario, neonatal transports are conducted by one of four neonatal transport teams based at: McMaster Children's Hospital (Hamilton), The Children's Hospital of Eastern Ontario (Ottawa), The Hospital for Sick Children (Toronto), and London Health Sciences Centre Children's Hospital (London). Each of these teams is responsible for providing transport series to the hospitals in the surrounding area, as well as an area of northern Ontario.

To facilitate transports of criticality and/or distance requiring air transport, the province's air ambulance provider "Ornge" is utilised. Ornge utilizes its fleet of over 20 rotary and fixed-wing aircraft. The fleet consists of AgustaWestland AW-139 and Sikorsky S-76 Helicopters, as well as Pilatus PC-12NG fixed-wing aircraft. Due to the high demands on the system, Ornge has a standing agreement with various contractor companies in Ontario. These contractors provide over 40% of the total transports carried out in the province [63]. These contractors have a varying fleet of fixed-wing aircraft including Mitsubishi MU-2, Pilatus PC-12, among others.

Pilatus PC-12NG [64]

AgustaWestland AW-139 [65]

3.5. Discussion

There are clearly defined advantages with providing timely access to physiological and other information to all relevant parties in an infant's care [66]. This problem is greatly exacerbated in neonatal transport, where access to information from a physician can be hours away. Due to this, it is becoming increasingly important to begin closing that gap. To begin this, however, the problem of connectivity must be solved. Before data can flow, a means must be created. The overarching goal of this research is to address this in the most disconnected type of transport: air. Neonatal transport provides no greater place to test this research. With the varying environment, both aircraft and geographic, the transport provides an excellent test environment and provides the ability to contribute to real, tangible change in an industry otherwise forgotten.

4. Coverage Grid Map

Path planning algorithms, including A*, rely on a path map to determine nodes and paths that can be traversed while finding a path from a source to a target node. In the case of planning for an aircraft, the geographical space is opened and non-constricted by typical physical construct such as a road. To address this, one must impose a virtual map path space that overlays the existing area. In this research, the idea of a grid map is implemented. Commonly used in path planning in open spaces, a grid map allows for a structured environment to be created in an opened environment. An example of these grid maps in research are to create no-go areas in a map [9], [14], [32], [33], [39].

In this research, the grid map is used to:

- Define a map to traverse while planning
- Transpose earth-bound coordinates into a flat, Cartesian plane
- Define the coverage quality at all points in the search area

The grid map used in this research presents a virtual grid that is overlaid over the physical earth space that is under investigation (Figure 4-1). In the following sections, the physical definition of grid map is presented. The grid map contains an equally spaced set of square “tiles” that are fixed size. Furthermore, the determination of the coverage radius, and area of the grid that is “covered” by each cell site is presented. The output of this section is a grid map that can be utilised for path planning.

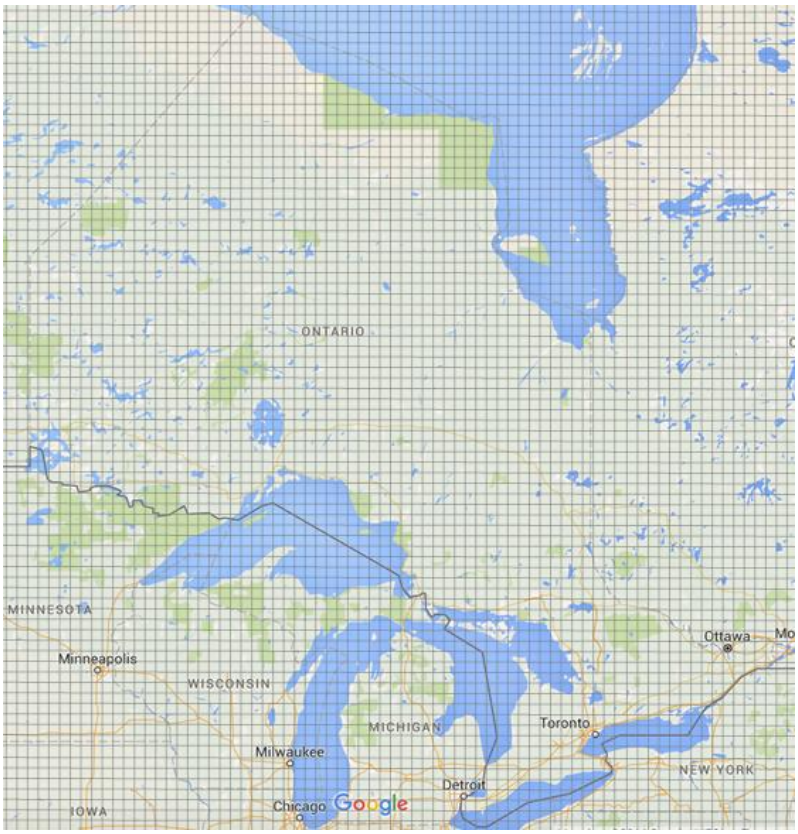

Figure 4-1: Coverage Grid Map Example

4.1. Overview

The following activity diagram (Figure 4-2) provides an overview of the Coverage Grid Map generation. The output of this activity is a fully qualified map, which is used in Chapter 5 for path planning.

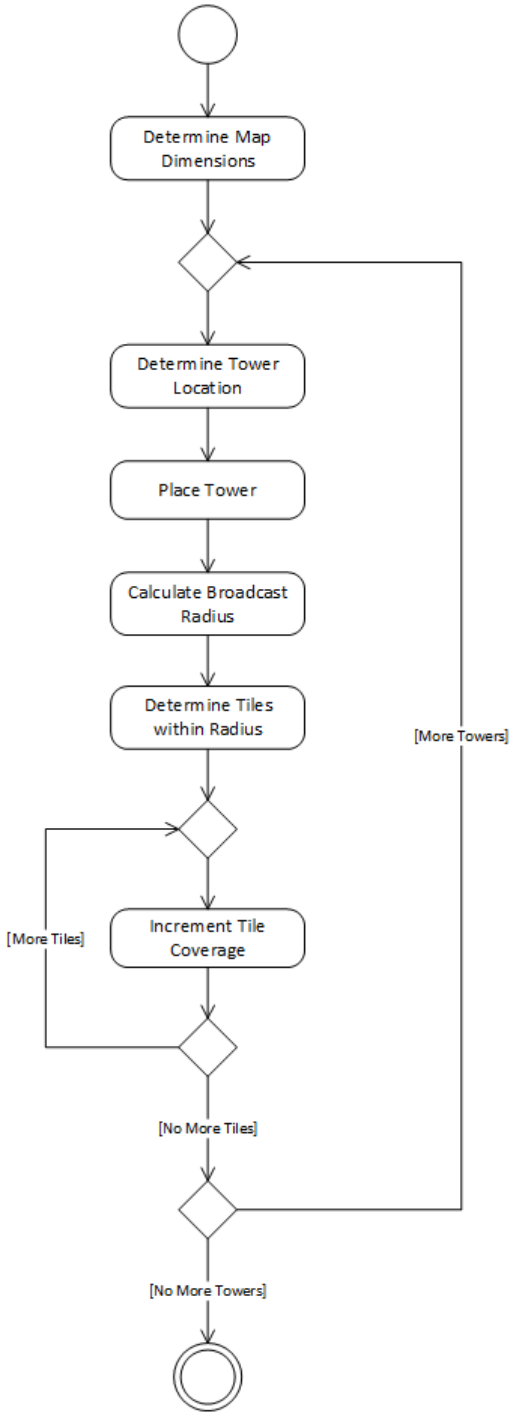

Figure 4-2: Coverage Map Generation Activity Diagram

Define Map Dimensions (4.1.1) – This process determines the size of the overall map space based on the bounding longitude and latitude dimensions and the tile size. The output is a set of height and width dimensions in number of tiles that are used to define the map.

Determine Tower Location (4.1.2) – This step determines which tile a particular cell tower is located in.

Calculate Broadcast Radius (4.1.3) – The broadcast radius is determined in this step by account for the various physical, geographical, and technical factors that determine the maximum range.

Determine Nodes within Radius (4.1.3.5) – Based on a tower location and an associated coverage radius, this step determines which tiles are within the coverage radius.

Increment Tile Coverage (4.1.3.5) – Once the tiles that are covered are located, the quantity of towers, which cover that particular tile, is incremented.

4.1.1. Defining Dimensions

The grid map is constrained to be a bounding box around the area of path planning. It consists of a 2-dimensional collection of square tiles within this bounding box. To define the bounding box, we require the following points:

$$X_1 = Lowest\ Longitude\ (in\ Radians)$$
$$X_2 = Highest\ Longitude\ (in\ Radians)$$
$$Y_1 = Lowest\ Latitude\ (in\ Radians)$$
$$Y_2 = Highest\ Latitude\ (in\ Radians)$$

With these points defined, we can calculate the maximum distance between both latitude and longitude. Both latitude and longitude on the earth are defined as degrees from a fixed point. Latitude is defined as 0-90 degrees either north or south from the equator (0 degrees). Lines of latitude are evenly spread across the earth. Longitude is defined as 0-180 degrees east or west from the prime meridian (0 Degrees). The distance between these lines are maximum at the equator and 0 at the poles. As a result of this, the distance between

coordinate pairs is not a trivial Euclidean distance. To calculate true distance, one must utilise the haversine distance formula.

Haversine Distance Formula

The haversine distance formula calculates the distance over ground of the shortest path between two points $p(\phi_1, \lambda_1) and\ p(\phi_2, \lambda_2)$ over the earth [67]:

$$haversine(\phi_1, \phi_2, \lambda_1, \lambda_2) = 2r \sin^{-1}\left(\sqrt{\sin^2\left(\frac{\phi_2 - \phi_1}{2}\right) + \cos(\phi_1)\cos(\phi_2)\sin^2\left(\frac{\lambda_2 - \lambda_1}{2}\right)}\right)$$

Equation 4-1 - Haversine Distance Formula

Where d is the minimum distance between the two points, r is the radius of the earth (6378 km), ϕ_1 and ϕ_2 are the latitude components of the two points, and λ_1 and λ_2 are the longitude components of the two points.

The overall dimensions of the coverage map can be found utilizing the haversine formula and the size of each tile. The calculation for this is:

$$P_x = \frac{haversine(X_1, X_2, Y_1, Y_1)}{\rho}$$

$$P_y = \frac{haversine(X_1, X_1, Y_1, Y_2)}{\rho}$$

Equation 4-2: Coverage Map Dimensioning Equations

Where P_x is the X component of the coverage map dimension, P_y is the Y component of the coverage map dimension, ρ is the size of the tile square in km, $haversine(X_1, X_2, Y_1, Y_1)$ gives the maximum distance of the longitude, and $haversine(X_1, X_1, Y_1, Y_2)$ gives the maximum distance of the latitude.

With P_x and P_y we can define the map as:

$$M\langle P_x, P_y \rangle$$

By having a map that is based on tiles of a fixed size rather than coordinate based, and transposing objects into them via the haversine formula, all distances within the coordinate map can be done through the Euclidean distance formula.

The Euclidean distance formula is:

$$D(x_1, y_1, x_2, y_2) = \sqrt{|x_2 - x_1|^2 + |y_2 - y_1|^2}$$

Equation 4-3: Euclidean Distance Equation

where the D is the distance between the points (x_1, y_1) and (x_2, y_2).

4.1.2. Determining Tower Locations

To determine the location on the coverage map where each cell tower is located, the offset of the tower's geographical coordinates from a fixed origin point must be calculated. The origin point is any one of the four corners of the coverage map and must be the same point used for all location calculations on the grid. For the calculation purposes, we will take the minimum latitude and longitude to be the origin or (0,0) point of our coverage matrix.

$$O(x, y) = p(X_1, Y_1)$$

To determine the X, and Y location on the coverage map of a tower, or the center of the coverage radius, the following equations are utilised:

$$X = round\left(\frac{haversine(O_x, O_y, T_x, O_y)}{\rho}\right)$$
$$Y = round\left(\frac{haversine(O_x, O_y, O_x, T_y)}{\rho}\right)$$

Equation 4-4: Coordinate Translation Formulas

Where X is the distance of the tower T from the origin O in the x-direction, and Y is the distance of the tower T in the y-direction. This results in a tower being located at tile:

$$T(X, Y)$$

4.1.3. Determining Cell Broadcast Radius

Determining the radius of a cell towers broadcast is a non-trivial task. There are many factors that come into play, each of which can affect the total range of a broadcast independently or with each other. Some of these factors include:

- Output power of the transmitter
- Quality of the receivers hardware
- Height of the tower over terrain or surrounding structures
- Required data rates at the receiver [68], [69]
- Absorption or reflection of nearby structures
- Interference from adjacent cell sites [68], [69]
- Transmission technology being utilized [68]–[71]
- Directionality characteristics of antennas
- Azimuth and Elevation each tower is pointing

In this research however, the cell equipment is located on an airborne platform. The advantage of this is that many of the factors mentioned above become less of a problem, for example interference and attenuation from nearby structures. Some factors are more a problem, however, such as interference from nearby cell sites that typically wouldn't reach

into another cell's coverage zone on the ground. In the following sections the three major factors that dictate the maximum range of a cell signal are presents. These limitations include physical, geographical, and technological factors. Each of these sections present a manner for determining the maximum range a cell could reach.

As a baseline, one should calculate the physical limit that could theoretically be reached based on the technical properties of both the user equipment and the cell tower (physical limitations). This should then be checked against any technological limitations that limit the maximum range (technical limitations) to ensure that it is not exceeded. If this value is exceeded, the technical limit can be taken as the maximum range. Based on the characteristics of geography, the currently determined maximum range should be checked to ensure there are no limiting factors (geographical limitations). The following sections discuss the particular factors and methods for each of these three categories of limitations.

4.1.3.1. Physical Limitations

The physical environment in which wireless communication occurs has a dramatic effect of the quality, and power of an RF (Radio-Frequency) signal. There has been much research and many models presented for modeling the effect of builds, vehicles, and other physical obstructions in various different environments have on a wireless signal. In an urban city, for example, cell signals broadcast at very high powers can have a range of only a few hundred meters where as in a rural environment a low power signal and propagate for tens of kilometers [71].

In the ground-to-air situation presented in this thesis, many of the losses from physical obstructions are not present. As a result of this, physical limitations of wave losses through free space play a crucial role in calculating the maximum effective broadcast distance.

In radio communications, there are two major factors that come into consideration when determining if communication is possible between a transmitter and a receiver: the amount of power broadcast, and the minimum amount of power that is required to be received. Based on these factors, the amount of loss that can be incurred can be derived from the total broadcast power of the transmitter in relation to the minimum power received. This power loss is known as path loss. The path loss is derived from a link budget equation, which accounts for the various factors that increase or decrease the path loss amount. It is from this path loss, that the maximum distance between the transmitting and receive nodes can be calculated. The path loss equations are presented below for both the uplink (Table 4-1) and downlink (Table 4-3) legs.

Transmitter - UE		
a	Maximum TX Power (dBm)	
b	TX Antenna Gain (dBi)	
c	Body loss (dB)	
d	EIRP (dBm)	= a + b - c
Receiver – Node B		
e	Node B noise figure (dB)	
f	Thermal Noise (dBm)	= *k (Boltzmann)* X *T (290 K)* X *B (3.84 Mcps)*
g	Receiver Noise Floor (dBm)	= e + f
h	*SINR (dB)*	
i	Receiver Sensitivity (dBm)	= g + h
J	Interference Margin (dB)	
K	Cable loss (dB)	
L	RX Antenna Gain (dBi)	
m	Fast Fade Margin (dB)	
n	Soft Handover Gain (dB)	
Maximum Path Loss (dB)		= d – i – j – k – l – m - n

Table 4-1: Uplink Link Budget [69]

Field	Description
A	Maximum transmission power of the UE. This is dependent on the technology and the power class on which it is operating.
B	The antenna gain of the UE is dependent both of the type of antenna being used, as well as the frequency band.
C	Body loss is the loss incurred from UE being located close to the head of the user. It effects the voice link budget.
D	The EIRP or Effective Isotropic Radiated Power is a function of fields A,B, and C. The EIRP represents the effective total power emitted from the transmitter.
E	The noise figure is a measure of the degradation of the SNR resulting from the various components in the system wide transmission system chain.
F	The thermal noise factor accounts for the agitation induced by atmospheric temperature on a electromagnetic waves created by the transmitter. Thermal noise is a factor of both temperature and the quantity of data being transmitted.
G	The receiver noise floor is the sum of all noise and undesired signals on the receiver end.
H	The signal to interference and noise ratio is the ratio of signal strength to the sum of all interference and noise signals.
I	Receiver sensitivity is the minimum received signal strength given a defined SINR that can be utilised.
J	Interference margin allows for the increase in Thermal Noise resulting from nearby users.
K	Losses incurred due to the cable between the transmitter and its antenna
L	The antenna gain of the transmitter is dependent both of the type of antenna being used, as well as the frequency band.
M	Power reserved to allow headroom for Power Control Operation (not used in LTE)
N	Soft Handover Gain is the effective increase in headroom from being simultaneously connected to multiple ground stations as part of a diversity scheme.

Table 4-2: Downlink Link Budget Description [69]

Transmitter - UE		
a	Maximum TX Power (dBm)	
b	TX Antenna Gain (dBi)	
c	Cable loss (dB)	
d	EIRP (dBm)	= a + b - c
Receiver – Node B		
e	Node B noise figure (dB)	
f	Thermal Noise (dBm)	= *k (Boltzmann)* X *T (290 K)* X *B (3.84 Mcps)*
g	Receiver Noise Floor (dBm)	= e + f
h	*SINR (dB)*	
i	Receiver Sensitivity (dBm)	= g + h
J	Interference Margin (dB)	
K	Control channel overhead (%)	
L	RX Antenna Gain (dBi)	
m	Body Loss (dB)	
Maximum Path Loss (dB)		= d – i – j – k – l – m

Table 4-33: Downlink Link Budget [69]

Field	Description
A	See A above
B	See B above
C	See K above
D	See D above
E	See E above
F	See F above
G	See G above
H	See H above
I	See I above
J	See J above
K	The control channel overhead factor accounts for the performance drop from other users utilizing the same cell site.
L	See L Above
M	See C Above

Table 4-4: Uplink Link Budget Description [69]

Broadcast Distance

The link budgets described in the preceding section define the maximum attenuation or path loss that can be incurred while still maintaining a signal and specific data rate. From this path loss, the maximum distance of the broadcast can be calculated. These calculation form the basis of some the most important aspects of planning for cellular networks [68], [69]. Due to this, there has been much work in this area to devise the most appropriate model for converting this path loss into a predicted range. One of the founding models in this area is the free space path loss equation (FSPL). This model predicts the range of a signal based on the frequency of the signal and a specific power. The loss calculations in this equation are based on the natural attenuation that happens to any

wireless signal as it travels through the air. It does not, however, account for normal factors that would occur in a variety of different environments.

To address this, certain models have been created with the aim to address factors such as human created objects, diffraction, refraction, reflection, and others that exist in normal environments and provide a more realistic estimation of range. The Okumura-Hata model is an example one of these models. The main problem with these models, however, is that they are aimed at the typical cellular network deployment. That is that cell towers are located higher than a user's equipment. In this research, the opposite is true. Due to this constraint, there are no other models besides FSPL that will allow distance to be estimated.

The FSPL equation is a reasonable estimate in this case, however. In the typical macro-cell network design, cell towers are placed much higher than where a user would be. This is particularly important in rural areas to increase the effective range covered by each cell tower. In urban areas, this is less important as cells tend to be much smaller, but is often placed in high spots to decrease interference and attenuation from nearby structures. A much desirable side effect from this is that it leaves the path from tower to and aircraft in the sky very much unobstructed. Based on this, this research assumes that the path from tower to aircraft is free obstruction at all times. In Equation 4-5 the FSPL equation is presented. This equation, when used in conjunction with the maximum path loss determined from the link budgets, provides an estimate at the expected range of a particular cell tower.

$$d = 10^{\frac{1}{20}[\, l - 92.45 - 20\log(f)]}$$

where

$$d = Maximum\ Broadcast\ Radius\ (km)$$
$$l = Maximum\ Path\ Loss\ (dBm)$$
$$f = Frequency\ of\ Cell\ Service\ (Ghz)$$

Equation 4-5: Broadcast Radius Equation

4.1.3.2. Technical Limitations

Based on the protocol utilised for transmitting data across the major cellular network technologies, there are various limitations imposed that directly affect the maximum transmission distance of a particular cell. These physical limitations are usually rooted in the maximum round trip time (RTT), and allow for a certain broadcast frame in a time-division-based cell system. In a typical cell situation, there are large amounts of attenuation from geographic and man-made objects and interference from other nearby transmitters. Due to this, it is uncommon for physical distance limitations to come into play before limitations are reached in the link budget [72].

This, however, is not the case when transmitting to an aircraft. Aircrafts, which travel at relatively high-altitudes, enjoy minimal interference and encroachment into their first Fresnel zone. Due to this, the link budget generally does not become a factor before the cell radius from a protocol standpoint [71]. This situation, for the same reason as an ocean-borne network, has lead revisions of standards aimed at increasing the theoretical range defined in protocols [71].

In the following sections, the protocol-based limitations of three of the most prevalent cellular data technologies are presented. The results of the survey of each technology are amalgamated in Table 4-6.

GSM (2G)

GSM networks operate on the principle of Time Division Multiple Access (TDMA). On each cell, each user is assigned a time-slot on which they receive, and a time-slot on which they transmit. In GSM, each user can broadcast in one of eight time slots, and in those, in one eight of the time period of the slot. This results in 64 time advance (TA) slots per time period. Each of these periods consists of a single 3.69 microsecond bit-period. With the speed of light being a fixed value, as well as the fixed duration of these time slots, a maximum theoretical range of approximately *35 km* can be found [70].

There was an attempt that demonstrated expanding this out to 121 km by Motorola in 1997, but this technology failed to gain traction [73].

HSPA / HSPA+ (3G)

HSPA, or High-Speed Packet Access, came as an evolution of universal mobile telecom system (UMTS), which is based on 3G. In standard HSPA, there is a system limitation of approximately 60 km [71]. Recognizing the factors of non-link budget dependent environments, release 7 of the HSPA standard (known also as HSPA+ or evolved-HSPA), opened this limit up to 240 km. This is limited, however, in practical terms to 180 km due to the inability to achieve measurement accuracy beyond that [71].

LTE (4G)

The maximum cell radius for an LTE-based 4G network is dependent on the Preamble Format implemented on the particular network. Each of the four main preamble formats varies in the duration of its cyclic prefix (CP) and guard time (GT) [72]. The maximum cell radius is derived from the maximum round-trip time being equal to the GT. Considering that GT is a multiple of the concretely defined T_s (sampling period), by making use of the speed of light, the maximum distance that can be covered results in the cell radius [72]. In the following table, the maximum cell radii are provided along with their associate CP and GT durations.

Preamble format	Number of allocated subframes	CP duration		GT duration		Max. delay spread (μs)	Max. cell radius (km)
		in μs	as multiple of T_S	in μs	as multiple of T_S		
0	1	103.13	3168	96.88	2976	6.25	14.53
1	2	684.38	21024	515.63	15840	16.67	77.34
2	2	203.13	6240	196.88	6048	6.25	29.53
3	3	684.38	21024	715.63	21984	16.67	100.16

Table 4-5 - LTE Field Durations and Related Maximum Cell Radius [72].

Technology	Range Limit (km)			
GSM (2G)	35			
HSPA	60			
HSPA+	180			
LTE	*Format 0*	*Format 1*	*Format 2*	*Format 3*
	14.53	77.34	29.53	100.16

Table 4-6: Cell Technology Range Limits

4.1.3.3. Geographical Limitations

When sending or receiving a signal at very long ranges, the curvature of the earth becomes a factor, as well as the height of both the transmitter and the receiver (Figure 4-3).

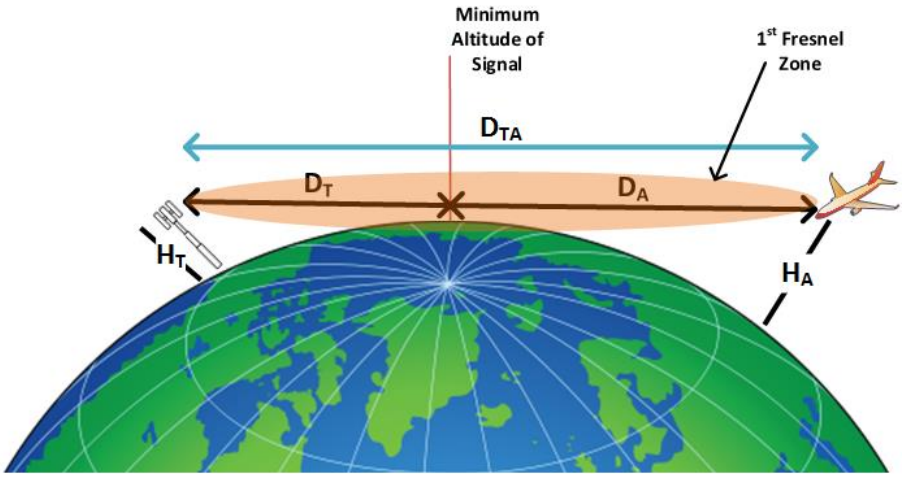

Figure 4-3: Radio Horizon

The following equation determines the maximum broadcast distance based on these factors:

$$d \approx \sqrt{2 \cdot k \cdot R \cdot H_T} + \sqrt{2 \cdot k \cdot R \cdot H_A}$$

$$d \approx 4.12 \left(\sqrt{H_T} + \sqrt{H_A}\right)$$

Equation 4-6: Radio Horizon

Where d (km) is the maximum distance possible for a signal before the earth's surface impedes any signal, k is the modification factor of the earths radius R (km) to account for the air refraction index (k = 4/3 in most cases) [74], H_T is the height of the cell tower antenna (meters) , and H_A is the altitude of the aircraft (meters).

4.1.3.4. Effective Broadcast Radius

The broadcast radius of a cell tower represents the maximum distance from the tower's antenna that a usable signal can be received. However, this is only a valid range when the UE is located at the same height as the tower antenna. To compensate for the altitude of the UE located on the aircraft and to calculate the effective range across the ground, the Pythagorean Theorem can be applied (Figure 4-4) and has been chosen for this research:

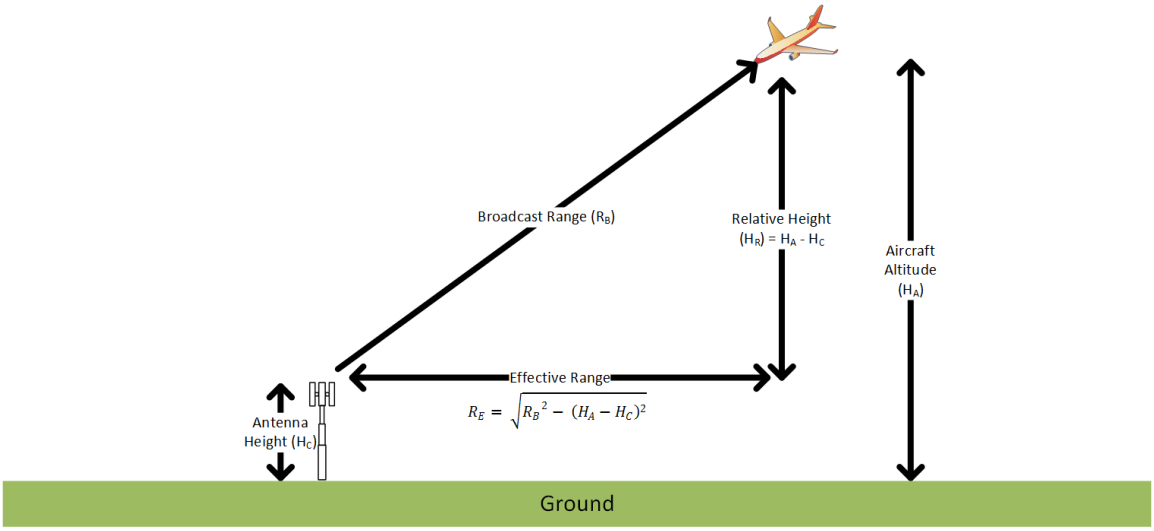

Figure 4-4: Effective Broadcast Range

The resulting equation to calculate the effective broadcast radius across the coverage map is found to be:

$$R_E = \sqrt{{R_B}^2 - (H_A - H_C)^2}$$

Equation 4-7: Effective Broadcast Radius

Where R_E is the effective broadcast radius (m), R_B is the physical broadcast radius (m), H_A is the aircraft's altitude (m), and H_C is the cell tower antenna height (m).

4.1.3.5. Determining Tiles with Broadcast Radius

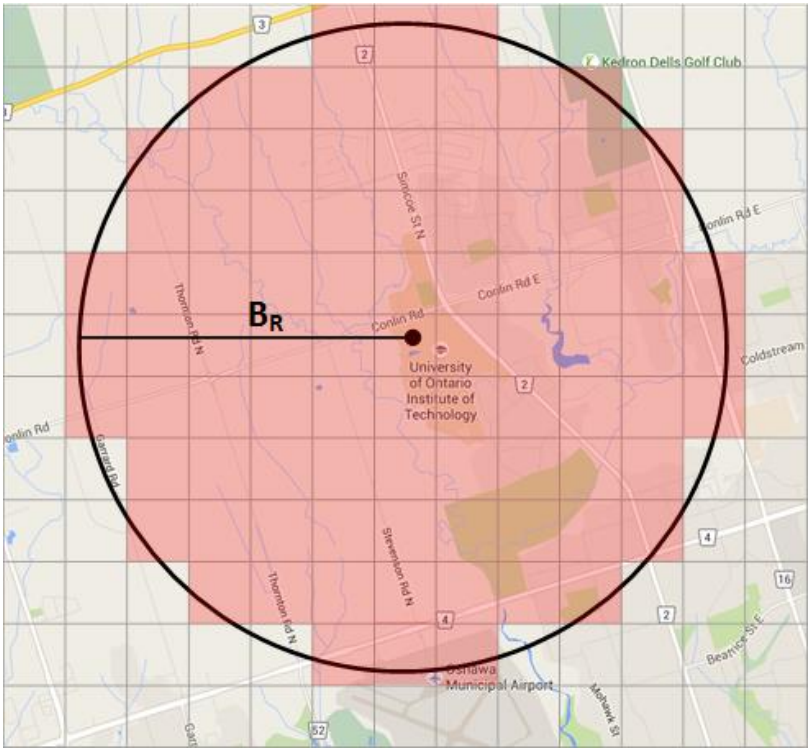

Figure 4-5: Broadcast Radius Tile Coverage

After determining the effective broadcast radius, the next step is to determine which tiles of the coverage map fall within the coverage range (Figure 4-5). To determine this, an algorithm has been created to efficiently make this determination (Figure 4-6):

```
1.  xSize //Size of Coverage Map on x-axis
2.  ySize //Size of Coverage Map on y-axis
3.
4.  /**
5.  Determines the tiles within the coverage area of a Tower
6.  Coverage[][] - array representing the total coverage map's
7.          coverage
8.  mStep - size of each tile (km)
9.  Tx - X position of the tower
10. Ty - Y position of the tower
11. Tr - Effective Broadcast Radius of tower (km)
12. */
13. function populateCoverageArea(coverage[][], mStep, Tx, Ty, Tr)
14.         radius = Tr / mStep
15.         coverage[Tx][Ty]++
16.         for x in [0, Tr]
17.             y = round( sqrt( pow( radius, 2 ) – pow( x, 2 ) ))
18.             for i in [0, y]
19.                 if ( x == 0 && i == 0)
20.                     continue
21.                 if( legal( Tx + x, Ty +i ) )
22.                     coverage[Tx+x][Ty+i]++
23.                 if( i != 0 && legal( Tx + x, Ty - i ) )
24.                     coverage[Tx+x][Ty-i]++
25.                 if( x != 0 && legal(Tx - x, Ty + i ) )
26.                     coverage[Tx-x][Ty+i]++
27.                 if(i != 0 && x != 0 && legal( Tx - x, Ty – i ))
28.                     coverage[Tx-x][Ty-i]++
29.
30. function legal(x, y)
31.         return x >= 0 && y >= 0 && x < xSize && y < ySize
```

Figure 4-6: Pseudocode for Tower Map Coverage Algorithm

The algorithm represented in Figure 4-6 determines which tiles fall within the broadcast range. Since the broadcast radius is a perfect circle with a given radius T_R, from a given tile (T_x, T_y), the number and placement of tiles that are within the range will be the same for each 90° quadrant of the broadcast area. Based on this assumption, the remaining 270° can be determined by determining the offset of each tile in the x-axis, then y-axis, and the x and y-axis from the coordinates of the tower. Given this, it is also possible for a tower to lie on or near the borders of the coverage map. If this is the case, areas outside of the map bounds are considered "covered". These points, however, cannot be expressed in this map. Therefore line 30 of Figure 4-6 presents a function legal(x,y) which determines if a point is within the bounds of the coverage map.

Line(s)	Description
1-2	Size of the coverage map in each direction
14	Determines radius in number of Tiles
15	Increments coverage to the tile on which the tower resides
16	Loops through number of tiles of the radius, which becomes the x-axis positions to investigate
17	Determines the Y-coordinate that represents border of the coverage area given a particular X, and tower position (T_x, T_y) (Equation 4-8)
18	Loops through all points from 0 up to that determined Y-coordinate defining all points in that quadrant that are covered for a given Y.
19	Skips the location of the tower
20-28	Determines if the four quadrant points are legal, and increments their coverage
30-31	Determines if a specified point lays within the coverage map

$$L_y = \sqrt{{T_R}^2 - (L_x - T_x)^2} + T_y$$

Equation 4-8: Determining Y-limit from a given X and Tower Position

5. Path Planning

The A* algorithm is one of the most popular informed-search algorithms. Still actively published on [11], [13], [14], [41], the A* algorithm extended Dijkstra's algorithm to include a heuristic function as a method for guiding the operation of the algorithm [8]. The A* algorithm is known as a best-first search algorithm, meaning that for each iteration it explorers the most promising node first based on a specified function. In addition to this, the A* algorithm utilizes a heuristic function. The purpose of the heuristic function is to estimate the least expensive cost from the current node to the goal node. Heuristic functions are domain specific and are considered valid so long as they never over-estimate the least expensive cost. Both the cost function, and the heuristic costs are combined for each node being explored as per Equation 4-1:

$$f(n) = g(n) + h(n)$$

Equation 5-1: A* Path Cost

Where n is the current node being investigated, $g(n)$ is the sum of all path costs up to n, and $h(n)$ is the heuristic cost from n to the goal node. The basic operation of the algorithm is such that there are two lists of nodes 'opened' and 'closed'. The opened list starts by containing the source node. For each iteration, the nodes that can be reached by the current lowest cost node (first iteration this is the source node) are added to the list as well as their cost $f(n)$. At this point the 'expanded' node is removed from the opened list and placed into the closed list. This process continues until a path is found to the target node, and all other costs in the opened list exceed that of the completed path.

In this work, path planning is performed on the Coverage Grid map that was defined in chapter 4. Nodes in this work are represented by each tile of the coverage map and traversable paths as those between all adjacent nodes on the coverage map including diagonal movements. Unlike many traditional path-planning problems, such as those for

video games, robots, etc., there are no blocked areas of the coverage map. This is due to the very nature of aircraft in the sense that they can fly anywhere within the admissible area (coverage map) and are not blocked by physical or other tangible constraints.

In the following sections, the various components that come into play when planning a path with the A star algorithm are discussed. Section 5.1 discusses how a real world airport's location can be converted into a logical grid location on the coverage map. Section 5.2 defines and discusses the heuristic method utilized in this research. 5.3 defines and discusses the path cost function that is utilised. In 5.4, the path smoothing methodology is presented.

5.1. Determining Source and Destination Airport Positions

To determine the location of the source of designation airports or nodes planning, the corresponding tile to their location must be determined. With the coordinates for both points, the same principle presented in 4.1.2 can be utilised. By utilizing that method, a logical grid location can be found to represent both the start and end points and serve as the guiding principle for the origin and destination points during planning.

5.2. Cost Function

The cost function $g(n)$ for each iteration of the A* algorithm represents the sum of all preceding movement steps costs from the origin $o(x, y)$ to the present node $p(x, y)$ plus the cost of movement to the node under evaluation $n(x, y)$. In the following section, the movement cost function is presented.

5.2.1. Movement Cost Function

The movement cost function is the function that calculates the path cost for traversal from the present node $p(x, y)$, to the node under evaluation $n(x, y)$. The movement cost

much account for both the physical distance cost of traversing between two grid locations as well as number of cellular towers c_n that cover the node under investigation. The movement cost is presented in Equation 5-2:

$$m(p_x, n_x, p_y, n_y) = D(p_x, n_x, p_y, n_y) + \left(\frac{D(p_x, n_x, p_y, n_y)}{c_n + 1}\right)$$

Equation 5-2: Movement Cost Function

The operation of the movement cost function relies on the physical traversal distance between the current node and node under investigation by leveraging the Euclidean distance function $D(x_1, y_1, x_2, y_2)$ (Equation 4-3). Further to the distance component, cellular coverage of node under investigation c_n is represented in the exponential decay formula as an additive second component. Derivation of the limits of the movement cost, to quantify effect of tower count, are presented in 5.2.1.1.

Based on the grid nature of the coverage map and that diagonal movements are allowed, there are 8 nodes from any one node that can be explored. The only exceptions to this is when the present nodes lay on the border of the coverage map. In this event, the only movements permissible are ones that still lie within the coverage map. The movement distance component of the movement cost function leverages the Euclidean distance formula. Due to the uniform spacing and perfect grid of coverage map nodes, the distance to travel between any two nodes in the horizontal and vertical directions can be said to be 1. In the 4 possible diagonal movement directions, the 45-45-90 triangle side length relationships can be used to determine the related cost of the diagonal movements (Figure 5-1).

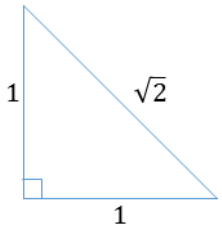

Figure 5-1: 45 Degree Special Triangle

By leveraging this triangle relationship, we can reduce the computational overhead of our movement cost by using $D(p_x, n_x, p_y, n_y) = 1$ for all movements either vertically or horizontally and $D(p_x, n_x, p_y, n_y) = \sqrt{2}$ for all diagonal movements.

5.2.1.1. Movement Cost Function Limit Calculations

The movement cost function works on the premise that in the **worst case** when the number of towers is 0:

$$m(p_x, n_x, p_y, n_y) = \lim_{c_n \to 0} \left(D(p_x, n_x, p_y, n_y) + \left(\frac{D(p_x, n_x, p_y, n_y)}{c_n + 1} \right) \right)$$

$$m(p_x, n_x, p_y, n_y) = \lim_{c_n \to 0} \left(D(p_x, n_x, p_y, n_y) + \left(\frac{D(p_x, n_x, p_y, n_y)}{0 + 1} \right) \right)$$

$$m(p_x, n_x, p_y, n_y) = 2 \cdot D(p_x, n_x, p_y, n_y)$$

Thus the movement cost of node under evaluation becomes twice the Euclidean distance of $D(p_x, n_x, p_y, n_y)$

In the **best case**, where c_n is at a maximum, the movement function becomes:

$$m(p_x, n_x, p_y, n_y) = \lim_{c_n \to \infty} \left(D(p_x, n_x, p_y, n_y) + \left(\frac{D(p_x, n_x, p_y, n_y)}{c_n + 1} \right) \right)$$

$$m(p_x, n_x, p_y, n_y) = \lim_{c_n \to \infty} \left(D(p_x, n_x, p_y, n_y) + \left(\frac{D(p_x, n_x, p_y, n_y)}{\infty + 1} \right) \right)$$

$$m(p_x, n_x, p_y, n_y) = D(p_x, n_x, p_y, n_y)$$

Thus in the best case, where there is a maximum number of towers, the movement function becomes $m(p_x, n_x, p_y, n_y)$. Ultimately the function above represents an exponential decay in the second distance factor for each additional tower. The effect of having more and more towers covering a given node under exploration represents a lower increase in heuristic cost. As no coverage is the worst possible case, it should have the highest cost of movement. Since a tower count greater than one for a given space is good, it is not necessarily equally better than going from no towers to one tower. In fact subsequent towers beyond one do not do anything for a given cellular signal other than increase the probability of coverage being attained (Excepted in the case of MIMO connections, which are not covered in this research). Therefore, this thesis proposes that exponential decay in the effect of subsequent towers beyond one is the correct approach to accounting for total cellular towers for each possible node of traversal.

5.3. Heuristic Function

The heuristic function at its core is meant to estimate the lowest possible cost from any point to the goal. The function itself is a product of the domain onto which it is applied. When choosing a heuristic method, there are a multitude of options for a wide variety of domains. The domain of this thesis is no different. The goal of the heuristic function is to estimate the absolute minimum cost of movement from the current position to the goal node. A heuristic function is considered valid if and only if it never overestimates the minimum of cost of the movement.

When considering the most appropriate heuristic function to utilize in planning, one must find a balance between speed and accuracy. For the example of a non-player character in a video game, it is important for the path generated for its movement to be computed extremely quickly. This is especially important because the destination can be constantly moving. However, with this example, it is less important for the path to be optimal and most accurate but rather generated extremely quickly.

In the case of aircraft within the context of this research, the need for extremely quick path generation is not particularly important. With aircraft there will never be an instant departure, in fact it could take upwards of an hour to have an aircraft readied for departure. This is time that could be spent planning a path. Beyond this, it is less important that a path be able to be recalculated on the fly extremely quickly. If a path were to be changed, there would be a certain amount of time required to obtain clearance to deviate from a path – and this would like happen at most once during a flight. Based on this, it is fair to assume that the heuristic function would make more sense to be skewed towards overall optimal distance and coverage rather than performance of the planning itself.

Beyond performance trade-offs, there is a body of heuristic methods that optimize the shape of the final path by again trading off accuracy of the overall route. Examples of these heuristics are the diagonal distance function, or simply the addition of a tie breaking cross product. Though in principle it is better to generate simple paths, in this particular research, the constraints imposed by having an aircraft leave this method for generating appropriate paths not particularly realistic. Section 5.4 provides an alternate, post-processing approach that utilizes path down sampling to provide paths that are feasible for real aircraft. Since the post-processed smoothing is required to generate feasible routes for an aircraft, it becomes extremely important to lose as little fidelity in the initial planning stages as possible. Since the planning process is effectively a process chain, any loss of fidelity in the path in the early stages of the chain will be magnified further down the chain.

Based on these conditions, a heuristic method was chosen to maximize accuracy in estimating the distance from any point to the destination node. The Euclidean distance

method is one a very common formula used as a heuristic function, and is widely used in examples [8]. The Euclidean distance formula calculates the straight-line distance between any two coordinates, which is always the shortest distance. However, its use of the square-route mathematical operation is also what makes it relatively computationally expensive to compute and therefore makes it slower. However, with the aforementioned relaxation of timing constraints for the sake of ultimate accuracy, it is utilized. The Euclidean distance formula is presented in Equation 4-3.

$$h(n) = D(n_x, t_x, n_y, t_y)$$

Equation 5-3: Heuristic Function

Where $h(n)$ is the heuristic cost, which is the Euclidean distance (Equation 4-3) from the node under evaluation $n(x, y)$ to the goal node $t(x, y)$.

5.4. Smoothing

The output of the planning step is an ordered collection of points that represent each step across the matrix map between the origin and destination points. The number of points varies based on a number of factors such as step size, distance between the origin and destination points, and the cellular coverage across the area. Though this collection of points represents a very accurate representation of the optimal route, it does not represent a traversable route for a physical aircraft.

To put this into perspective, if one were to have a coverage tile map planned around a 1-km tile size, the resulting path would have a route represented by a collection of points every 1-km from the source to the destination. Beyond this, it is quite possible that there are turns that would logically have to be made at every point. If an aircraft were to be travelling at 500km/h, it is unrealistic to think that any of those turns could be made, and if it were possible, the added time, fuel, etc., to execute this route would make it prohibitive.

In the event that an aircraft was flying under Instrument Flight Rules (IFR) in poor conditions, it would further not be possible to file a flight plan with a route that contained as many points and the raw-planned route would contain.

To address the problem of there being too much fidelity in the planned route, this research presents two separate smoothing methodologies that effectively down-sample the original route into an approximation of the original route that contains far fewer points and thus makes it more realistic. These smoothing methodologies optimize either for distance or coverage, and operate by iteratively down sampling the paths while ensuring the resulting path doesn't deviate from a predefined coverage drop allowance.

The base algorithm used for path smoothing in this work is the Ramer-Douglas-Peucker Algorithm [75], [76]. The algorithm is presented in the following section and subsequent sections explain how coverage is calculated on the down sampled route, and the two methods for accessing coverage.

5.4.1. Ramer-Douglas-Peucker Algorithm

The RDP algorithm proposes that a curve comprised of several line segments can also be approximated by a smaller set of points [75], [76]. The similar curve determined by the algorithm is subset of the points defining the original curve. The smoothing effect of the RDP algorithm is illustrated in Figure 5-2.

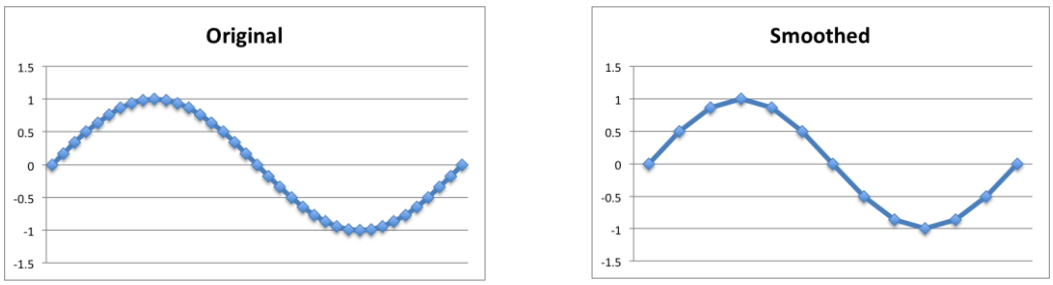

Figure 5-2: Original vs. Smoothed Path Example

The RDP algorithm is performed on a collection of points based on a user-defined ε parameter. The ε parameter is a distance dimension that represents that threshold over which a point cannot be removed. The algorithm functions by first isolating the first and last point as constant points that cannot be removed. These first and last points are then converted into a line segment from which other points have their distance calculated to. If the furthest point from the line segment is lower than ε then all other points are removed including itself. If the distance is greater than ε, then the algorithm is recursively called with all points from the origin to the furthest point, and again with the all points from the furthest point to the end.

In this work, the smoothing operation leverages the RDP algorithm and determines the maximum ε that can be utilized while still maintaining cellular coverage to being no less than a certain percentage of the baseline coverage. The smoothing operation works by iteratively attempting higher and higher ε and evaluating the coverage on the smoothed path against the baseline coverage until either coverage has fallen below the minimum allowable drop, or only one of the origin and destination points remain. The maximum allowable drop is defined as a percentage of the baseline planned coverage that represents a lower threshold of coverage. The operation of the algorithm is illustrated in Figure 5-3.

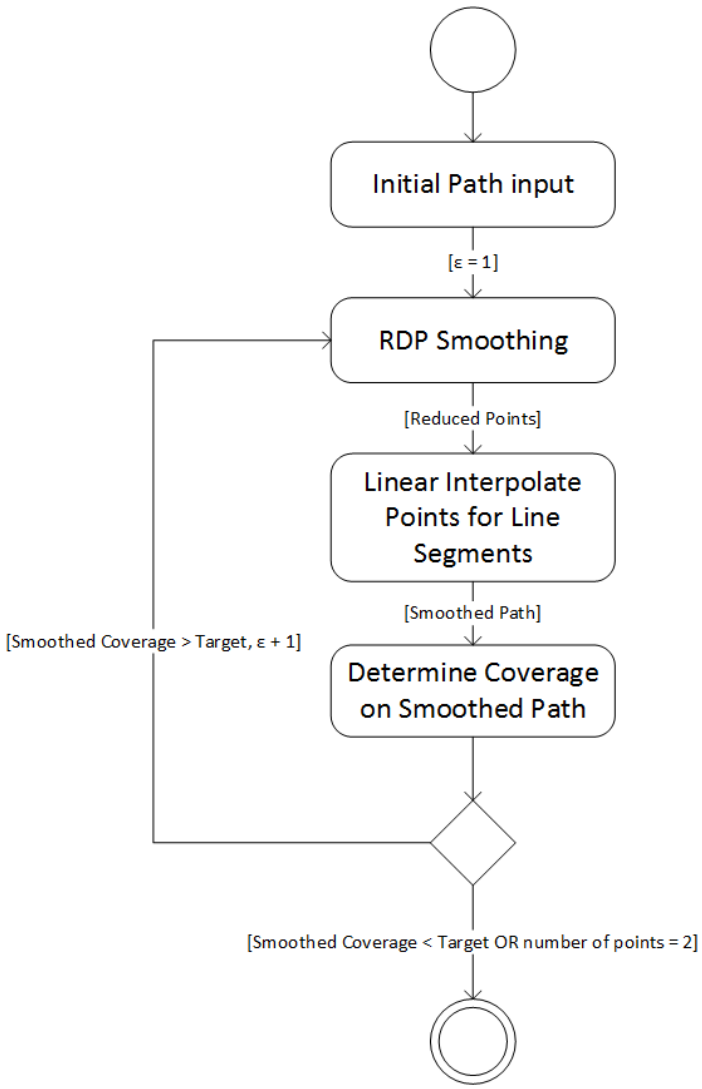

Figure 5-3: Smoothing Activity Diagram

5.4.2. Accessing Coverage during Smoothing

In this work, there are two methods that are used to determine coverage across a path. They are described in the preceding two sections. Each method receives the input of a continuous path from the source to destination points. Assessing coverage during the smoothing starts with assessing the baseline coverage. The baseline path, or planned path, is a continuous path that contains all points across the coverage matrix from source to destination. As the path is iteratively smoothed, points are removed. The effective path

after smoothing contains a line sparse set of points that is not continuous across the coverage matrix. This sparse set effectively creates a set of line segments between pairs of points. To assess the coverage of each of these line segments, the underlying points on the coverage matrix must be interpolated. For this, the sparse set of line segments are paired up in a connected fashion (P1, P2), (P2, P3), etc. For each of these pairs, the standard line-equation is determined with the equation:

$$Y = \left(\frac{P_{2Y} - P_{1Y}}{P_{2X} - P_{1X}}\right)(X - P_{1X}) + P_{1Y}$$

Equation 5-4: Path coordinate interpolation formula

Where:

$$P_{1x}, P_{1Y}: Coordinates\ of\ P_1\ of\ the\ point\ pair$$
$$P_{2x}, P_{2Y}: Coordinates\ of\ P_2\ of\ the\ point\ pair$$
$$X: x\ coordinate\ under\ investigation$$
$$Y: y\ coordinated\ corelated\ to\ X$$

The equation defined above is used to determine the intermediary points between the coordinate pairs by being utilised repetitively with X values defined as all whole numbers between P_{1X} and P_{2X}. The resulting Y coordinates along with defined X values, define all intermediary points on the coverage matrix.

With all point pairs interpolated and their intermediaries defined; coverage can be determined on each path. To assess coverage, there are two methods presented in this research, the “Average” method, and the “Ratio” method. In the following two sections, each of these methods are defined.

5.4.2.1. Path Length Average Coverage

The average coverage method assesses coverage by determining the average number of cell towers covering each coverage matrix point on the path. The average coverage is determined with the following equation:

$$C = \frac{\sum_{i=0}^{n} c(i)}{n}$$

Equation 5-5: Average Coverage Equation

Where:

$$n: Number\ of\ points\ in\ path$$
$$c(i): Number\ of\ towers\ covering\ point\ i$$
$$C: Average\ coverage\ per\ point$$

5.4.2.2. Path Length Coverage Ratio

The coverage ratio method is similar in to the average method in the sense that it is calculating the average coverage of the path over the entire path. The ratio method differs; however, as it calculates the coverage based on a binary covered or not covered and doesn't account for the number of towers covering a particular point on the coverage matrix. In the following equation, the ratio method is defined:

$$C = \frac{\sum_{i=0}^{n} f(i)}{n}$$
$$f(i) = \begin{cases} 0, & c(i) = 0 \\ 1, & c(i) \geq 1 \end{cases}$$

Equation 5-6: Coverage Ratio Equation

Where:

$$n: Number\ of\ points\ in\ path$$

$$f(i): State\ of\ coverage\ of\ a\ particular\ point$$

$$c(i): Number\ of\ towers\ covering\ point\ i$$

$$C: Average\ coverage\ per\ point$$

6. Case Study

In chapters 4 and 5, a set of algorithms and designs were presented to prepare for determining cellular coverage map of a specific area, and utilizing that coverage map to determine an optimal route of travel ensuring the shortest possible distance with greatest possible coverage. The goal of this chapter is to implement what was presented in both chapters 4 and 5 in the context of neonatal airborne transport in Ontario to evaluate the efficacy.

Airborne neonatal transport in Ontario provides an excellent basis for a case study for a variety of different reasons. Despite having the largest population of any province in Canada, and the second largest land mass, Ontario has large amounts of sparsely populated area, particularly in the north. The result of this is a correlated lack-of, or minimal cellular coverage in many of these areas [2], [25], [77]. Beyond a lack of cellular coverage, these sparsely populate areas also lack the advanced care facilities located in urban centers many hundreds or thousands of kilometers away. The result of this is a frequent need for aircraft-based neonatal transports to more advanced care facilities.

The goal of this case study is to design aircraft flight paths that transport aircraft could utilize to maximize the potential for cellular connectivity. With cellular connectivity, a telemedicine system could operate and provide better insight to transport physicians based at the facilitating hospital, and allow them to provide clinical insight and decision making to the transport team in the air. These generated paths will then be evaluated on distance, cellular coverage, and plan-time in comparison to a typical direct route to evaluate the feasibility of each path.

This chapter is structured as follows: In 6.1 the clinical problem requiring this type of a solution is presented. Section 6.2 presents the experimental hypotheses and their relation to the thesis hypotheses. In 6.3 specific details of the implementation for this specific case study are presented and then evaluated in 6.4. In 05 the results presented and in 6.6 those results are discussed.

6.1. Clinical Problem

Each and every day, there are many children born across the Province of Ontario. The majority of these children are born without the need for any advanced care. However, every year in Canada approximately 25% of all neonatal patients will require transport to a more advanced care facility [62]. In outlying and low-populated areas of the province, particularly in northern Ontario, neonatal transports that are carried out typically involve travelling large distances and far longer than a typical transport in Southern Ontario. The reasons for this is primarily a lack of population to support the advanced care facilities such as the ones located in southern cities such as Toronto, or Hamilton.

Studies have shown that the rates of medical errors increase when relevant medical data is not provided to the appropriate parties in a timely manner [1]. This is particularly important in neonatal transport [5]. In a typical neonatal transport conducted in Ontario, the main source of contact and transmission of information is done via a cellular phone back to a facilitating hospital and their transport physician. This solution greatly limits the quantity and quality of the data that can be communicated and it is not possible at all during an air-based transport.

There have been many benefits reported when utilizing telemedicine-based approaches to improving care during transport, particularly in the pediatric world [44]. Despite this, studies that have been completed, or systems designed, have focused nearly exclusively on ambulance-based ground transport (2.5.1). These approaches have demonstrated a wide varied of different data types and formats, however connection limitations have prevented them for ever being used on other modes of transport.

The goal of this study is to evaluate the potential of creating flight paths for the transport aircraft to utilize that will maximize cell connectivity to the ground for the duration of the transport. By enabling air-to-ground communications over a cellular

network, it will enable a data-based telemedicine approach to transmitting vital patient and transport information to the ground to be analyzed by transport physicians. With the added insight, physicians will be able to communicate more accurately to the transport team, support and enable clinical decisions to be made and communicated during flight and improve patient care overall.

6.2. Experimental Hypothesis

In chapter 1, thesis hypothesis are presented that frame the overarching hypothesis that this research presents as a whole. Hypothesis 1-2 provides a tangible evaluation guidelines and hypothesis 3 relates this work to the domain of manned aircraft transport and hypothesis 4 specifically to airborne critical care transport. The following experimental hypothesis provide concrete areas of evaluation that together build toward the evaluation of the Thesis hypothesis:

1. Planning matrix generation time will exponentially increase for each halving of the matrix tile size;

2. Planning matrix file size will increase exponentially for each halving of the matrix tile size;

3. Planning matrix generation time and file size are independent of altitude;

4. Planning time will increase exponentially with a halved matrix tile size;

5. Planned route coverage will increase with a decrease in matrix tile size;

6. Planned route distance will decrease with a decrease in matrix tile size;

7. Planned route will be the same when planned in either direction;

8. Smoothed path will contain fewer points when done on a path planned with a smaller matrix tile size.

9. Smoothed path distance will lower with a decrease in matrix tile size;

10. Path smoothing will result in the same path regardless of direction;

11. Smoothed path coverage will be equal to or less than that of the original planned path;

12. Smoothed path coverage will be greater on routes planned with a smaller matrix tile size;

Hypothesis 5, 7, 9-12 pertains to thesis hypothesis 1, which shows that an optimal path can be found with respect to cellular coverage. Hypothesis 6 pertains to thesis hypothesis 2, which quantifies the path as being the optimal in terms of distance with respect to duration of coverage. Hypothesis 8-12 pertain to the thesis hypothesis 3, which states that a feasible flight path can be found that a manned aircraft could follow. Hypothesis 1-4 specifically looks at the factors that make the routes and planning tangible for use in airborne transport as outlined by thesis hypothesis 4.

Thesis Hypothesis	Experimental Hypothesis'
1	5, 7, 9, 10, 11, 12
2	6
3	8, 9, 10, 11, 12
4	1, 2, 3, 4

Table 6-1: Thesis to Experimental Hypothesis Mapping

6.3. Implementation

In the following two sections, the case-study specific implementation of the algorithms and designs discussed in chapters 4 and 5 are presented. Section 6.3.1 presents the specific implementation details of the "Coverage Matrix Map Generator". This application is responsible for determining the cellular coverage across the entire province of Ontario based on the existing cellular infrastructure of the three major national cellular carriers (Telus, Rogers, and Bell Canada) in relation to a theoretical user equipment set that could be implemented on a transport aircraft. Section 6.3.2 presents the implementation of the path planner application. This application computes flight paths for transport aircraft based on the coverage matrix and source and destination airports or heliports that are realistic points for a neonatal transport to occur.

6.3.1. Coverage Matrix Map Generator

Based on the algorithms and design presented in Chapter 4., the map generator creates coverage maps based on the altitude of planned aircraft, location and broadcast radius of each cell transceiver, and the location of each airport. These maps are persisted as an output of this application to be consumed by the path planner.

The map generator in this case study creates a coverage map for the Province of Ontario. Overall coordinates that present the east-west and north-south bounds of the map are presented in Table 6-2. These bounds create the limits for both the overall tile map and the area of consideration for cellular towers.

Latitude (Degrees)		Longitude (Degrees)	
Min	**Max**	**Min**	**Max**
41.676556° N	56.856944° N	-74.320648° W	-95.153056° W

Table 6-2: Coordinate Limits for Ontario

In the following sections, details of how each component of the coverage map was realized are presented. These sections include the identification of cellular towers existing in Ontario, the identification of their specific cellular technology, calculation of their broadcast range, and converting their coverage range into their coverage matrix coverage form. Further identification of ORNGE aircraft are presented, as well as their average cruise altitude.

6.3.1.1. Cell Tower Identification

In Canada, the frequencies that cellular phone networks operate on are considered restricted. As a result of this, special permissions and permits must be obtained for their use. The Canadian Government Agency "Innovation, Science and Economic Development Canada" handle all restricted frequency spectrum assignments within Canada for cellular networks.

Cell network operators that have been assigned spectrum for their cellular network and actively operate on them must register the technical characteristics and locations of their hardware. This data is compiled into a database called the "Technical and Administrative Frequency Lists" (TAFL). This database is publically available and can be queried to find out this information. For the purpose of this study, the national TAFL database of cellular towers was obtained. This database provides an excellent source that can be used to determine the location and characteristics of all cellular towers located in Ontario for use in this study.

In this study, the TAFL is leveraged to identify the total set of towers for Canada and was reduced down to those that exist in Ontario only. This was accomplished by selecting towers that existed only within the coordinates presented in Table 6-2.

Field	Description	Units
RX	Receive Frequency	MHz
TX	Transmit Frequency	MHz
Latitude	North Latitude	Degrees
Longitude	West Longitude	Degrees
ERP	Effective Radiated Power	dBw
Gain	Antenna Gain	dBi
Height	Height of the Antenna	Meters
Loss	System Losses	dB
Azimuth	Antenna Azimuth Orientation	Degrees
Elevation	Antenna Elevation Orientation	Degrees
Carrier	Name of the carrier who owns the equipment	

Table 6-3: Parameters Provided By TAFL Database

Based on this restriction, a database was created for this study that contained all Ontario towers. In the TAFL, a cell site (or tower) is defined as each unique piece of hardware that transmits and receives on a particular frequency pair. Most true unique cell sites in Canada consist of three or more directional antennas that are oriented evenly to provide 360 degrees of coverage; there are typically multiple entries in the TAFL database for each logical cell site. For the propose of this case study cell sites in the database are compressed to a single site based on the criteria that they broadcast and receive on the same frequencies, are at the same coordinates, and form a combined 360 degrees of coverage. Based on this criterion, a single logical site is placed in the study database that has the same location and frequencies, and has the lowest ERP. With this, each cell tower in the study database is treated as an omnidirectional transceiver. This effectively reduces the total number of cells by a factor of 3 in most cases.

rx	tx	lat	long	erp	gain	height	carrier	loss	power
881.52	836.52	41.7628	-82.6875	22.9	3	42	BELL MOBILITY INC.	3	12.9
840	885	41.7628	-82.6875	13	1	36	TELUS Communicatio	1	13
842.5	887.5	41.7628	-82.6875	13	1	36	TELUS Communicatio	1	13
1880	1960	41.7628	-82.6875	13	1	36	TELUS Communicatio	1	13
1885	1965	41.7628	-82.6875	13	1	36	TELUS Communicatio	1	13

Table 6-4: Example of Cell Tower Database

The compression of towers into omnidirectional transceiver described above resulted in a total of 38514 transceivers being identified across 6177 unique cell sites. These towers, and the pertinent technical information for each of them as described in this section, come together to form a cellular tower database. An example of this is Table 6-4.

One particular deficiency in the TAFL database is specifying which particular cellular technology each tower is operating with. To make this determination, the TX/RX frequencies are compared to the known frequency bands utilized by each technology in Canada. A table has been created that lists the frequency ranges and the associated technology for each of the three major cellular providers in Ontario: Bell, Rogers, and TELUS. In the following table, a list of frequency ranges and their associated technology is presented:

Technology	Provider	TX (Mhz)	RX(Mhz)
LTE	Rogers	699 – 716	729 – 746
		1710 – 1755	2110 – 2155
		2500 – 2570	2620 – 2690
	TELUS	1710 – 1755	2110 – 2155
		2300 – 2400	
		3400 – 3600	
	Bell	1710 – 1755	2110 – 2155
		2500 – 2570	2620 – 2690
		699 – 716	729 – 746
		777 - 787	746 - 756
		N/A	717 - 728
HSPA+	Rogers	1850 - 1910	1930 - 1990
		824 - 849	869 - 894
	TELUS	1850 - 1910	1930 - 1990
		824 - 849	869 - 894
	Bell	1850 - 1910	1930 - 1990
		824 - 849	869 - 894
GSM	Rogers	1850 - 1910	1930 - 1990
		824 - 849	869 - 894

Table 6-5: List of Cellular Technologies By Frequency in Ontario[1]

It has been found that all HSPA networks in Ontario by the three major providers have all been upgraded to HSPA+ [2], [25], [77]. The only provider in Ontario that operates a GSM network is Rogers[2]. Since GSM is the direct precursor to HSPA+ networks, they rely on the same frequency bands [68]. This makes it impossible by use of frequency alone to determine which technology is in use. However, Rogers has been discontinuing use of their original GSM network for the past several years. In Ontario, the last remaining area

[1] http://www.ic.gc.ca/eic/site/smt-gst.nsf/eng/h_sf01714.html

[2] https://www.ic.gc.ca/eic/site/smt-gst.nsf/vwapj/DGSO-002-13-Rogers.pdf/$file/DGSO-002-13-Rogers.pdf

of Rogers's coverage network that is a GSM-only network the town of Kapuskasing [25]. By isolating the towers that cover just this town, it can be determined that the overlapping frequency bands located anywhere outside of that town can be assumed to be HSPA+.

6.3.1.2. Aircraft

The cruising altitudes used in this study for each aircraft type represent an average flight plan filed altitude based on the latest filed flight plan for each aircraft registered to ORNGE. The aircrafts registered to ORNGE were found in the Transport Canada ' Canadian Civil Aircraft Register Database'[3] by isolating the listed aircraft by the owner's name of either "Ornge Global Air Inc." or "7506406 Canada Inc." – Both of which are the legal corporate names of Ornge. With the aircraft register isolated, the registrations numbers that were registered to the aircraft types of either "Pilatus PC-12" or "AgustaWestland AW-139" were identified. This extraction occurred 1 February 2016.

Based on the registration numbers found, a search of the FlightAware[4] website for each aircraft registration was conducted (1 February 2016). The average flight plan filing altitude was recorded and forms the cruising altitude for the case study simulation presented in this section. Table 6-6 provides a list of the identified Registration Numbers and the average Cruising Altitude that were identified.

[3] http://wwwapps.tc.gc.ca/saf-sec-sur/2/ccarcs-riacc/DDZip.aspx

[4] http://www.flightaware.com

Aircraft	Type	Cruising Altitude (ft)	Registration Numbers
PC-12	Airplane	20000	C-GRXB, C-GRXD, C-GRXE, C-GRXH, C-GRXM, C-GRXN, C-GRXO, C-GRXR
AW-139	Helicopter	5000	C-GYNF, C-GYNG, C-GYNH, C-GYNJ, C-GYNK, C-GYNL, C-GYNM, C-GYNN, C-GYNO, C-GYNP

Table 6-6 - ORNGE aircraft

6.3.1.3. Cell Tower Broadcast Distance Calculations

The coverage map generator utilises the cell tower database described in 6.3.1.1 as an input of cell towers for which the broadcast range will be calculated. For each of these cell towers, the coverage map generator determines the broadcast distance as described in Section 4. In 4.1.3.1, the particular physical limitations are defined in the form of link budget equations. For the purposes of this research, the values used to solve the link budget equations are from [68] where Holma et al. present link budget values that provide a good benchmark for distance planning. Where concrete values are known, such as with User Equipment, and the from the TAFL database for cell towers, the values of those are used in place of those presented. In the following tables, the uplink and downlink budget values utilized in this case study are presented.

	UPLINK	HSPA+	LTE
	Data Rate (kbps)	64	64
	Transmitter – UE		
A	TX Power (dBm)	26.0	26.0
B	TX Antenna gain	6.0	6.0
C	Body Loss (dB)	0.0	0.0
D	EIRP	32.0	32.0
	Receiver - NodeB		
E	Node B Noise Figure (dB)	2.0	2.0
F	Thermal Noise (dB)	-108.2	-118.4
G	Receiver Noise (dBm)	-106.2	-116.4
H	SINR (dB)	-17.3	-7.0
I	Receiver Sensitivity (dBm)	-123.4	-123.4
J	Interference Margin (dB)	3.0	1.0
K	Cable loss (dB)	From DB	From DB
L	Rx antenna Gain (dBi)	From DB	From DB
M	Fast Fade Margin (dB)	1.8	0.0
N	Soft handover gain (dB)	2.0	0.0

Table 6-7: Uplink Budget Values [69]

	DOWNLINK	HSPA+	LTE
	Data Rate (kbps)	1024	1024
	Transmitter – Node B		
A	TX Power (dBm)	From DB	From DB
B	TX Antenna gain	From DB	From DB
C	Cable Loss (dB)	From DB	From DB
D	EIRP	Derived	Derived
	Receiver - UE		
E	UE Noise Figure (dB)	7	7
F	Thermal Noise (dB)	-108.2	-104.5
G	Receiver Noise Floor (dBm)	-101.2	-97.5
H	SINR (dB)	-5.2	-9.0
I	Receiver Sensitivity (dBm)	-106.4	-106.5
J	Interference Margin (dB)	4.0	4.0
K	Control Channel Overhead (%)	20.0	20.0
L	RX antenna Gain (dBi)	6.0	6.0
M	Body Loss (dB)	0.0	0.0

Table 6-8: Downlink Budget Values [69]

The data rates defined in Table 6-7 and Table 6-8 of 64kbit/s upload and 1024kbit/s download represent the minimum acceptable data rates for a telemedicine system to have minimum functionality in a continuous manner to support physiological data transmission [78]. In the same tables, the User Equipment specification comes from [68] where specifications of a theoretical non-handled base station is presented in the highest power bands.

6.3.1.4. Implementation Specifics

Implementation of the coverage map generator was completed using the Java programming language and the Eclipse Luna development environment. The application was created as a stand-alone application to generate coverage maps for the Province of

Ontario. The application takes two parameters: a planned altitude, and a step size. The altitude parameter is used to adjust effective broadcast distance as described in 4.1.3.4 based on the cruising altitude of the transport aircraft. The step size represents the resolution of the coverage map based on geographic distance across the ground.

The cell tower database was created and implemented within a MySQL database as described in 6.3.1.1. This database is used during map generation to provide the list of cell towers and their parameters. These parameters, as well as those presented for the link budget equations presented in the previous section are utilized to determine the effective cell broadcast radius.

The application creates an in-memory matrix that is the size of the maximum height and width as defined as the haversine distance (Equation 4-1) in each of the coordinate directions defined in Table 6-2. For each cell tower, the underlying points are determined and an integer representing the number of tower covering that particular point is incremented.

Upon completion of the tower coverage determinations, the matrix is serialized with the Kryo Java Serialization Library[5], compressed with the Apache Commons Compress™ library using the GZip Algorithm[6], and saved to a file on disk.

6.3.2. Path Planner

The path planner was developed as an independent application from the map generator. The path planner takes in source and destination airport, as well as a coverage matrix map file as parameters. The path planner was developed based on the algorithms

[5] https://github.com/EsotericSoftware/kryo

[6] https://commons.apache.org/proper/commons-compress/

presented in section 5, and outputs a smoothed path represented as a collection of points coordinates on the coverage matrix representing the line segments on which to travel.

For the purposes of evaluation, the path planner was used to plan several routes and at several different altitudes. In the following section the methodology for determining routes is presented.

6.3.2.1. Routes

In Ontario, there are four transport teams that handle neonatal transports. Each team is allocated a region of the province, generally geographically close to the hospital at which they are based, for which they are responsible. The regions are known as LIHN's (Local Integrated Health Network). The geographical location and the LIHN allocations are presented in Figure 6-1 and Table 6-9 respectively.

Figure 6-1: Location of Ontario LIHN's[7]

Transport Team	Team Location	LIHN's Covered
McMaster Children's Hospital	Hamilton	3, 4, 6
The Hospital for Sick Children	Toronto	5, 7, 8, 9, 12, 13
Children's Hospital of Eastern Ontario	Ottawa	9, 10, 11, 13, 14
Children's Hospital of Western Ontario	London	1, 2

Table 6-9: Distribution of LIHNs to Transport Teams

Based on the distribution of LIHN's to Transport Teams, several routes for each type of aircraft were devised based on likely transport situations that would arise. A split

[7] http://www.lhins.on.ca/

of routes for both fixed-wing and rotary-wing aircraft were created. Airports / Heliports that are close to feeder hospitals were identified, and their locations and identification codes were found using the Canadian Flight Supplement Handbook[8]. Special consideration was given to ensure that routes are biased towards those that occur in sparsely cellular covered areas [2], [25], [77].

[8] http://www.navcanada.ca/EN/products-and-services/Pages/aeronautical-information-products-canadian-airports-charts.aspx

Route #	Type	Origin	Origin Code	Destination	Destination Code
1	**Airplane**	**Hearst Municipal Airport**	**CYHF**	**Timmins Victor M. Power Airport**	**CYTS**
2	**Airplane**	**Timmins Victor M. Power Airport**	**CYTS**	**Hamilton John C. Munro International Airport**	**CYHM**
3	**Airplane**	**Kapuskasing Airport**	**CYYU**	**Toronto City Centre Airport**	**CYTZ**
4	**Airplane**	**Thunder Bay International Airport**	**CYQT**	**London International Airport**	**CYXU**
5	**Airplane**	**Geraldton (Greenstone Regional) Airport**	**CYGQ**	**Thunder Bay International Airport**	**CYQT**
6	**Airplane**	**Moosonee Airport**	**CYMO**	**Ottawa McDonald-Cartier International Airport**	**CYOW**
7	**Airplane**	**Kenora Airport**	**CYQK**	**London International Airport**	**CYXU**
8	**Helicopter**	**Kenora (Lake of the Woods District Hospital) Heliport**	**CJG6**	**Thunder Bay (Health Sciences Centre) Heliport**	**CTB2**
9	**Helicopter**	**Cobourg (Northumberland Hills Hospital) Heliport**	**CNB4**	**Toronto (Hospital for Sick Children) Heliport**	**CNW8**
10	**Helicopter**	**Sault Ste. Marie Airport**	**CYAM**	**London International Airport**	**CYXU**
11	**Helicopter**	**Kenora Airport**	**CYQK**	**Thunder Bay (Health Sciences Centre) Heliport**	**CTB2**
12	**Helicopter**	**Sault Ste. Marie (Sault Area Hospital) Heliport**	**CSM9**	**Thunder Bay (Health Sciences Centre) Heliport**	**CTB2**
13	**Helicopter**	**Barrie (Royal Victoria Hospital) Heliport**	**CRV2**	**Toronto (Sunnybrook Medical Centre) Heliport**	**CNY8**

Table 6-10 - Routes Under Evaluation

6.4. Evaluation

In this section, the algorithms presented in chapters 4 and 5 are evaluated based on their implementation described in 6.3. The goal of evaluating the algorithms and methodologies is to evaluate the hypotheses presented in 1.6. In 6.4.1 the hardware and software setup of the testing environment is presented, 6.4.2 describes the evaluation methodology for the Coverage Map Generator, 6.4.3 presents the methodology for the path planner, and 6.4.4 the methodology for the path smoother.

6.4.1. Test Setup

All evaluation of the algorithms presented in this work was completed on a 13" early-2015 Macbook Pro Retina with an 2.9Ghz Intel i5 Processor, 16GB of DDR3 1866Mhz Memory, and a 512Gb SSD Hard Drive. All applications were compiled using the Java Development Kit Version 8, and built into executable jar files that were run from the Terminal. Output from the test applications was piped directly to text files.

6.4.2. Coverage Map Generator

The coverage map generator is an independent application from the path planner that's purpose is to build coverage maps at a set step size. In this case study, the map generator will be used to generate maps at the average cruising altitude for both major ORNGE transport aircraft utilized in neonatal transport as defined in Table 6-6. In order to support evaluation of the planning algorithms, the map generator will create maps with the step sizes of 2000m, 1000m, 500m, and 250m.

The map generator will be analysed based on several metrics in order to evaluate hypotheses 1-3, which aim to quantify the dynamics of the matrix map generator:

Dimensions – The overall dimensions of the coverage map will be recorded. The dimension of the coverage map is a correlated to both the dimensions of the Province of Ontario, and the Tile Size.

Processing Times – Several individual processing time metrics will be recorded to track the performance of each part of the map generator. The Matrix Allocation time will record the amount of time required for the system to allocate the memory required to store the matrix. The Processing Time metric represents the amount of time the algorithm requires to calculate coverage radius of each cell tower, determine which points on the matrix fall within that radius, and increment each point of the matrix. The Write Time metric represents the time required to compress the populated coverage matrix representation of the map and write it to a file on disk. To ensure accuracy of timing based metrics, each time recorded will be the average of 10 runs, with results greater than 2 standard deviations removed. Total processing time, defined as the sum of each component processing time will be compared to matrix tile size to evaluate hypothesis 1, which anticipates an exponential increase in total processing time for each halving of the input matrix size. Hypothesis 3 will also be evaluated as to where or not there is a correlation between processing time and the altitude at which the map is generated.

Output Size – The output file size of the resulting populate matrix map is recorded. The output size metrics collected will be compared to matrix tile size, and altitude to evaluate hypotheses 2 and 3. The evaluation of hypothesis 2 will assess the correlation between halving the matrix tile size and the exponential increase in output file size. Hypothesis 3 will assess if there is any correlation between the altitude at which the map is generated, and the output file size.

6.4.3. Path Planning

The path planning evaluation will be carried out on each of the source-destination routes defined in Table 6-10. For each route that is presented, planning will be conducted

at the 2000M, 1000M, 500M, and 250M matrix tile sizes. Furthermore, each route will be planning in both the forward and reverse directions. For each route, direction and matrix tile size combinations, the routes will be planned 10 times for the collection of timing metrics. The path-planning algorithm will be benchmarked using the following performance areas:

Route Distances – To evaluate distance, the direct distance from the source to destination will be collected as well as the total planned route distance for each tile size, route, and direction combination. These distance will be analyzed against the matrix tile size to evaluate hypothesis 6, which hypothesizes that there will be a correlated drop in planning distance with each halving of the matrix tile size. In support of hypothesis 7, distance will be correlated to direction to evaluate any differences.

Planning Time – Planning time will be recorded to identify performance characteristics based on the route with respect to route distance. For each of the 10 runs that are completed, the planning time will be considered the average of the runs that have times that do not fall outside of the 2 standard deviations from the sample mean. The timing benchmarks support hypothesis 4, which states that there will be an exponential increase in planning time as matrix tile sizes are halved.

Path Coverage – Path coverage will be determined based on the method described 5.4.2.1. The path coverage will be determined for both the direct route and the planned route to assess what, if any, improvement there is on the planned route versus the direct route. The method is used to assess the change in coverage to evaluate hypothesis 5, which states that coverage should increase with a decrease in tile size. Furthermore, the coverage of each planned path will be compared in forward to reverse directions to ensure there are no differences in support of hypothesis 7.

6.4.4. Path Smoothing

There are various metrics that will be used to analyse the smoothing portion of path planning. The goal of the smoothing portion of planning is to decrease the complexity of the planned path as much as possible while still maintaining coverage within a certain percentage. In this case study, a 5% drop in total route coverage was utilised as a target for all smoothing activities. Smoothing will be completed using both the Average and Ratio methods presented in chapter 3. The following list presents the smoothing-related metrics that will be collected to determine the efficacy of the smoothing methodology presented. The metrics collected will further be used to evaluate hypotheses 8-12, which aim to evaluate the efficacy of the smoothing portion of this research.

Smoothed Paths Coverage – For each smoothing algorithm, there will be a resulting path that is generated that represents the smoothed path. For each of these smoothed paths, the average coverage will be determined based on the algorithm presented in 5.4.2.1. The smoothed path coverage metric will be used to evaluate hypothesis 11, and 12. Hypothesis 11 states that smoothed path coverage will be equal to or less than of the originally planned path. In the context of this study, and the 5% total drop limit, this will be considered successful if the path can be smoothed within the 5% target and has a 0-5% total effective drop in the smoothed path. Hypothesis 12 states that smoothed path coverage will be higher on paths planned with a smaller tile size. This hypothesis will be evaluated as such in this section. Further support of hypothesis 10 will be determined if there is no change in the smoothed paths completed in either direction.

Number of Path Points – The number of points that make up the smoothed version of the planned path in comparison to the original number of points is important for determine how much simpler the smoothing algorithm made the path. This metric will be recorded for the original planned path, and for each of the paths that results from the two separate smoothing algorithms analysed. The purpose of this metric is to evaluate hypothesis' 8. Hypothesis 8 states that the smoothing will result in a output path that has

fewer points in it for smaller matrix tile sizes, this matrix aims to directly evaluate this. Furthermore, hypothesis 10 will be evaluated with respect to directionality with the assumption that regardless of direction, the smoothed path will be the same for each path and matrix size combination.

Smoothed Path Distance – Smoothing path distance is the distance of the path from origin to destination after the path has been smoothed. This section aims to evaluate how distance is affected by smoothing activities. Hypothesis 9 states that the smoothed path distance should be smaller when the initial path was planned with a smaller matrix tile size regardless of smoothing methodology. The path distances will be analyzed based on the two smoothing methods that were described in chapter 5 and any correlation between matrix tile size and distance demonstrated. Furthermore, paths will be assessed based on any effects of directionality and the resulting smoothed path distance to validate hypothesis 10.

6.5. Results

Based on the evaluation methodology presented in the previous section, this section presents the results. Results are presented in three sections; the first section presents the results from the coverage map generation process. The second section presents the results of the actual path planning activity. In the third and final section, the results of the smoothing operation completed on the paths generated and presented in section two are presented.

6.5.1. Coverage Map Generation

In this section, the results for the evaluation of the coverage map generator application are presented. Graphics that display location of cell towers and their relative density are provided in Appendix II. An example of the total cellular coverage in Ontario at altitude is provided in Appendix III. The application is evaluated for performance based

on both overall processing time, and the output file size. In Table 6-11, the data generated from the averaging of 10 runs of each altitude and step size pair is presented.

Run #	Altitude	Step Size	Dimensions (HxW)	Matrix Allocation (ms)	Processing Time (ms)	Write Time (ms)	Total Generation Time (ms)	Output Size (kB)
1	20000	2000m	845x864	3.2	577.1	409.2	989.5	120371
2	20000	1000m	1689x1727	11	792.7	854.1	1657.8	355197
3	20000	500m	3377x3453	14.8	1906.8	2822.1	4743.7	1063313
4	20000	250m	6754x6906	84.1	8175.5	10281.1	18540.7	3126791
5	5000	2000m	845x864	3.4	584.3	417.4	1005.1	120504
6	5000	1000m	1689x1727	11.5	841.9	899	1752.4	355305
7	5000	500m	3377x3453	16.5	1968.1	2892.7	4877.3	106329 1
8	5000	250m	6754x6906	81.6	7858.3	10424.4	18364.3	312597 4

Table 6-11: Map Generation Results

Timings

The total time presents the sum of the matrix allocation time, processing time (populating the matrix for cell coverage), and the write time (compress and write to disk). It was found that the total processing time has an exponential relation to the step size. This relationship demonstrates and proves hypothesis 1. This relationship is illustrated in Figure 6-2.

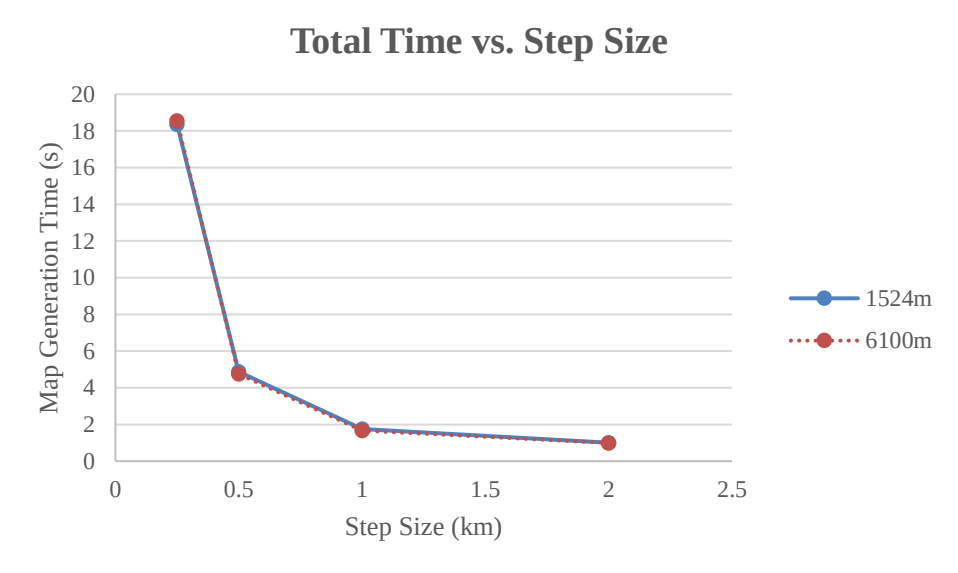

Figure 6-2: Map Generation Total Time vs. Step Size

Figure 6-2 further illustrates that this relationship holds true independently of altitude, which has minimal effect on overall processing time. This is further illustrated in Table 6-12 where the average difference in planning time is only 2.76% at the same step sizes but varying altitude. With this, it can be concluded that processing time is correlated to step sizes and not altitude. This correlates and proves the time component of hypothesis 3, which states that planning type is independent of altitude.

	5000ft	20000ft	Difference	%
2000m	1005.1	989.5	15.6	1.576
1000m	1752.4	1657.8	94.6	5.706
500m	4877.3	4743.7	133.6	2.816
250m	18364.3	18540.7	176.4	0.951

Table 6-12: Total Time vs. Altitude

File Size

The file size presented in the results represents the total raw size on disk of the coverage matrix map that has been serialized, and compressed. Analysis of file size in

comparison to the step size of the matrix map is presented in Figure 6-3. This graph shows the exponential growth of file size as the step size becomes smaller and results in a much larger matrix (shown in Table 6-11). This graph also shows how the same exponential grow rate occurs at various altitudes. The exponential relationship displayed here demonstrates that the proving of hypothesis 2, which states that there will be an exponential increase in file size for each halving of the matrix tile size.

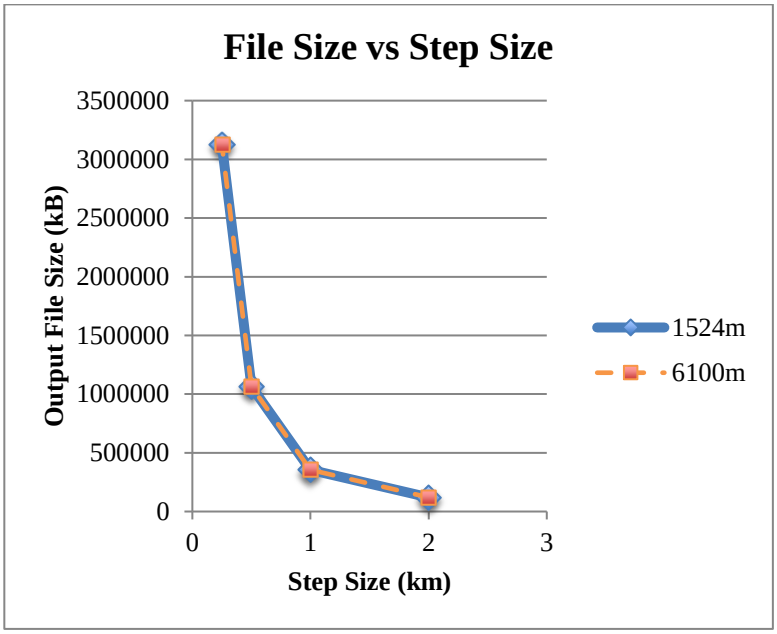

Figure 6-3: Map Generation File Size vs. Step Size

This point is further demonstrated in Table 6-14 where the difference between altitudes for each individual step size is found to average only 0.042% thus demonstrating that altitude is not a factor in file size and that step size is the only factor. This property proves the second component of hypothesis 3, in that the file size for each step size is independent of altitude.

	5000ft	20000ft	Difference	%
2000m	120504	120371	133	0.110
1000m	355305	355197	108	0.030
500m	1063291	1063313	22	0.002
250m	3125974	3126791	817	0.026

Table 6-13: File Size vs. Altitude

6.5.2. Path Planning

Path planning involves creating a path between two points. In most cases, the shortest path in terms of distance is the direct path from point to point. This research presents a path planning methodology that optimizes for both distance and coverage. Paths are generated as a collection of points on a coverage map that are sequentially traversed to move from the start to destination.

Route Number	Type	Altitude (ft)	Origin	Destination
1	**Airplane**	**20000**	**CYHF**	**CYTS**
2	**Airplane**	**20000**	**CYTS**	**CYHM**
3	**Airplane**	**20000**	**CYYU**	**CYTZ**
4	**Airplane**	**20000**	**CYQT**	**CYXU**
5	**Airplane**	**20000**	**CYGQ**	**CYQT**
6	**Airplane**	**20000**	**CYMO**	**CYOW**
7	**Airplane**	**20000**	**CYQK**	**CYXU**
8	**Helicopter**	**5000**	**CJG6**	**CTB2**
9	**Helicopter**	**5000**	**CNB4**	**CNW8**
10	**Helicopter**	**5000**	**CYAM**	**CYXU**
11	**Helicopter**	**5000**	**CYQK**	**CTB2**
12	**Helicopter**	**5000**	**CSM9**	**CTB2**
13	**Helicopter**	**5000**	**CRV2**	**CNY8**

Table 6-14: Planning Routes for Evaluation

Path planning was completed based on the routes, and altitudes presented in Table 6-14. For each route, planning was completed on all four tile-size coverage maps that were generated and documented in the previous section. Planning for each route was completed

in both forward and reverse directions and limited to 12hrs of total planning time. The time limitation was imposed to be a liberal representation of the maximum amount between an initial transport call, when an origin and destination are defined, and the time of departure from the referral hospitals planned origin airfield. As a result of this time limitation, the following routes and their associated tile sizes, and altitudes were not completed (Table 6-15).

Route Number	Direction	Altitude (ft)	Tile Size
7	Forward	20000	250M
7	Reverse	20000	250M
12	Forward	5000	250M
12	Reverse	5000	250M

Table 6-15: Unsuccessful Planning

The overarching goal of this section is to evaluate thesis hypotheses 1 and experimental hypothesis 4-7. Evaluation is done in the following three subsections: Distance, Coverage, and Time.

Distance

Path planning, as mentioned in the previous section, will always result in a path that is longer than the direct path. The goal is, however, to ensure that it doesn't become so much longer than the original path that it becomes unrealistic. In this section, the distance increase over the direct is analyzed based on various factors including planning direction and tile size.

In Figure 6-4 the average increase in path length versus the direct path distance planned at the current tile size is presented. Hypothesis 6 states that the increase in path length should be minimal at smaller tile sizes and increase with growing tile sizes. Based on the planning results, it is found that the 250m-tile size does have the smallest increase in path distance. However, the progressive relationship does not hold true at the larger tile sizes.

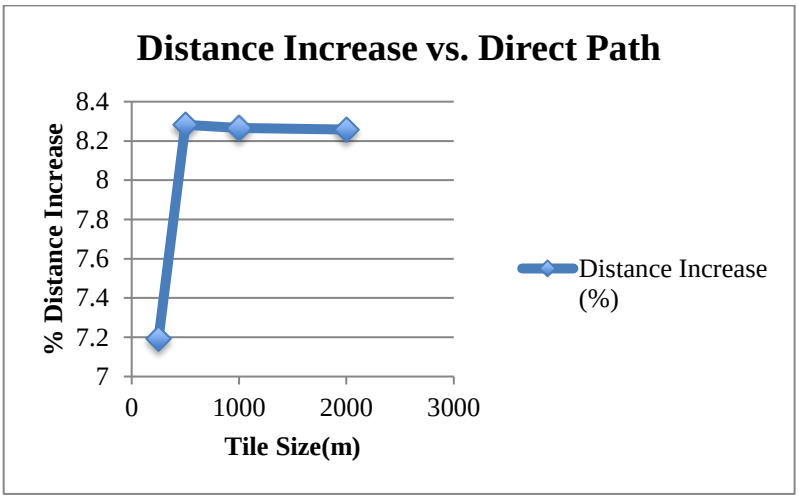

Figure 6-4: Planned Route Distance Increase over Direct Path

Due to discrepancies in the resolution of the different tile size, and the related effective quantization that occurs when placing start and end points into the tile map, it is found that despite having the globally smallest increase in path size, the 250m resolution ends up having the lowest percentage of shortest planned paths across all tile sizes (Figure 6-13).

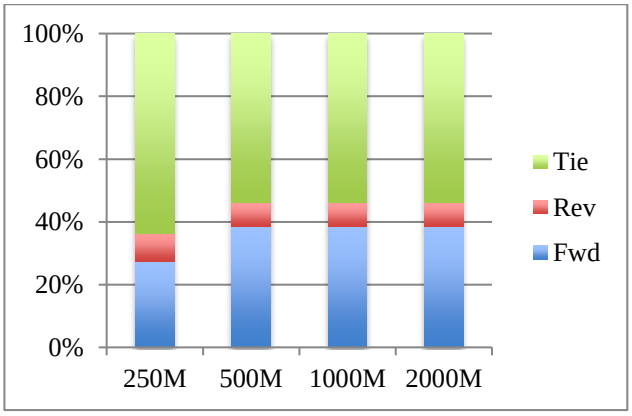

Figure 6-5: Shortest path by planning direction and tile size

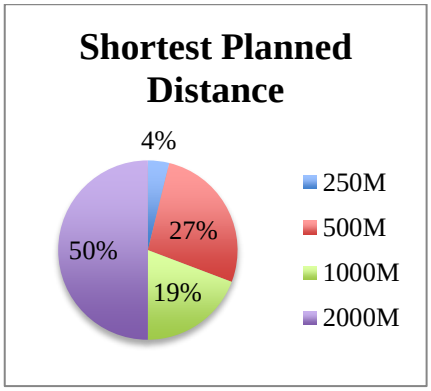

Figure 6-6: Planned Route Distance Increase Over Direct Path

Hypothesis 7 states the planning activities should result in the same distance of path regardless of planning direction. However, this does not hold true, as Figure 6-5 shows that in just over 50% of cases at all altitudes that this is true. In the times when this is not true, the planner plans the shortest routes in the forward direction.

Coverage

Coverage was assessed based on the percentage of path that had some type of cellular signal. Hypothesis 5 states that average coverage should increase with decreases in planning tile size. In Figure 6-7, this trend is shown to be true when comparing the 250m-tile size to the other planning sizes. At all other sizes, the coverage both before and after planning remains mostly constant. The 250m-tile size is of particular note in coverage is it presents both the highest baseline coverage, and the highest planned coverage. However, it also represents the lowest gain in coverage from baseline at only approximately 2.5%. Based on these trends, it can be found that hypothesis 5 does not hold true.

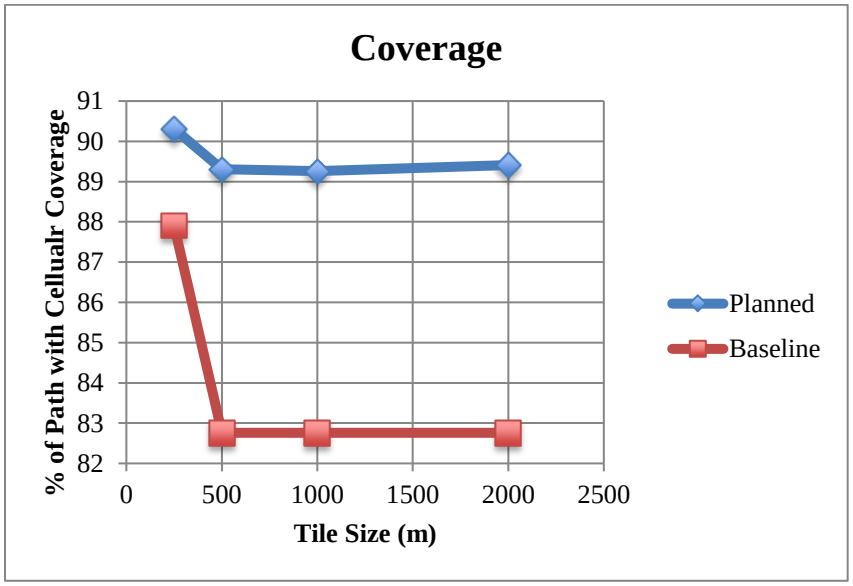

Figure 6-7: Percent Path Coverage Baseline vs. Planned

When assessing the directionality of planning in support of hypothesis 7, it is found that only in 48% that the hypothesis follows reality. In the other 52%, either the forward or reverse direction yields greater coverage (Figure 6-8).

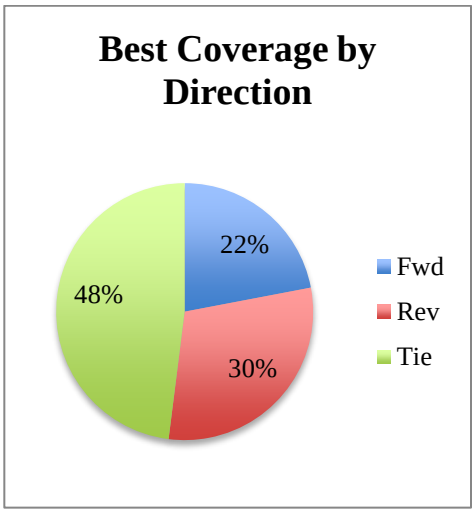

Figure 6-8: Percent Path Coverage Baseline vs. Planned

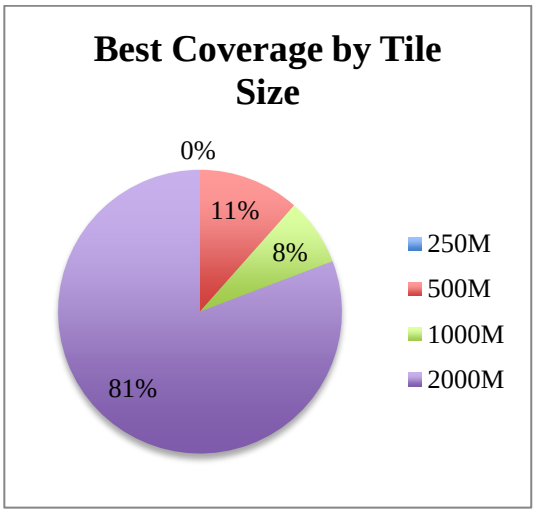

Figure 6-9: Percent Path Coverage Baseline vs. Planned

When assessing the best-planned coverage by cell tower count within each tile on the path by tile size, it is found that the 2000m-tile size most often (81%) yielded the greatest planned coverage (Figure 6-9.).

Time

As stated in hypothesis 4, it is expected that planning time will increase as the planning tile size becomes smaller. Results from planning have been correlated to this as illustrated in Figure 6-10.

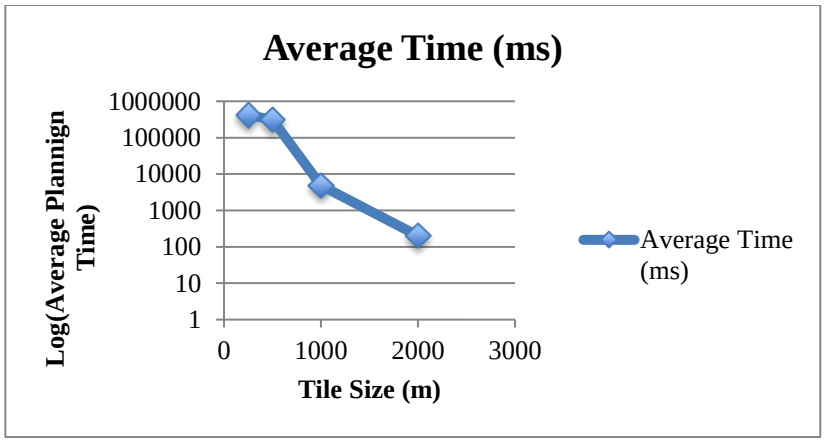

Figure 6-10: Average Planning Time by Tile Size

When planning time is adjusted for both distances, number of points and time, a measure of efficiency in planning is created. When assessing efficiency of planning across the planned tile sizes, it is found that as tile size increases and therefore the effective number of planned point's increases, the overall efficiency of planning goes does. This is illustrated in Figure 6-11

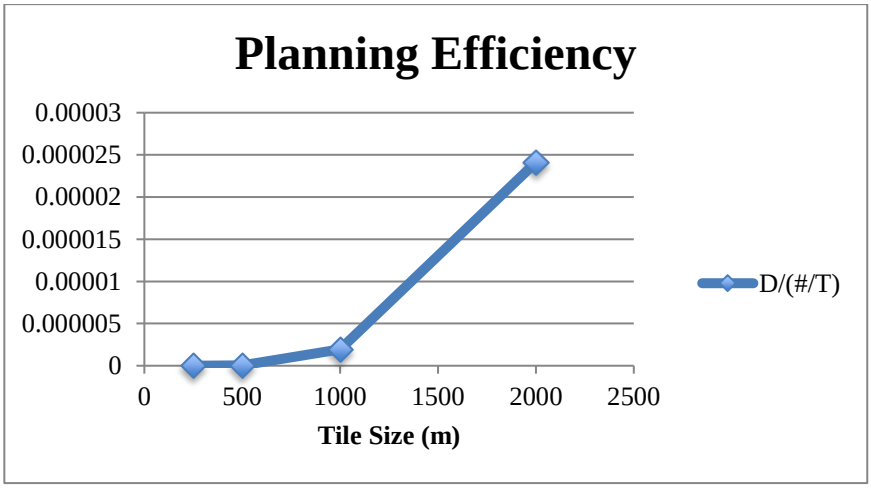

Figure 6-11: Planning Time Efficiency

When comparing planning time to planning direction, it is found that hypothesis 7, which states planning should be the same in all respects in all directions, is not substantiated. In the 250m, 500m, and 1000m planning sizes, it is found that the Reverse

planning direction is only faster than the forward direction in one route, which is the same route planned at all distances. However, in the 2000m planning tile size, it is found that overwhelming the Forward direction is better. Both of these results demonstrate that Hypothesis 7 is invalid.

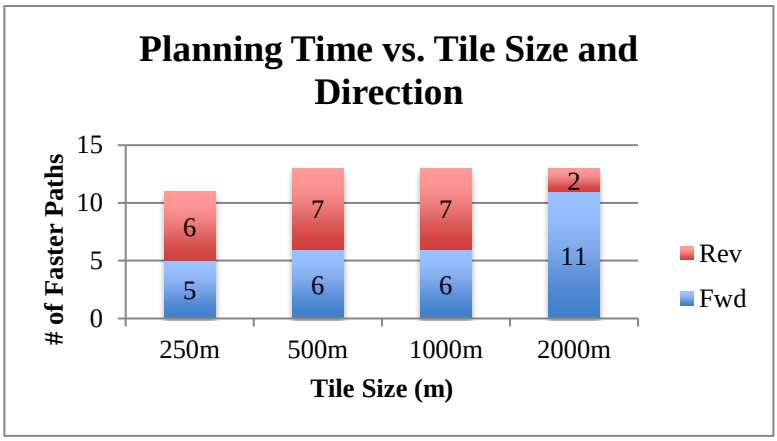

Figure 6-12: Planning Time vs. Tile Size and Direction

6.5.3. Path Smoothing

Path smoothing was completed for each of the routes, in both forward and reverse directions. In the following sections, the results that demonstrate the effects that smoothing has on Time, Coverage, Distance, and Total Number of Points that make up the route are presented. Each of the separate smoothing algorithm methods are presented individually and assessed against one another to determine effectiveness.

Coverage

In chapter 1, it was hypothesized that a smoothing algorithm can be found that can decrease coverage by at most a given percentage while not being affected by planning direction (Hypothesis 10). Furthermore, it is hypothesized that smaller tile sizes will result in a smaller decrease in path coverage from baseline (Hypothesis 12). This section presents

the results based on each of the Ratio and Average smoothing methods in support of these hypotheses.

Ratio

The ratio method assesses the total percentage of the path that has some element of cellular coverage. In Figure 6-13, the Tile Size of 500M is demonstrated as having the greatest average coverage from the baseline, and 2000M the least. There is no demonstrated trend as tile size increases of a smaller coverage reduction.

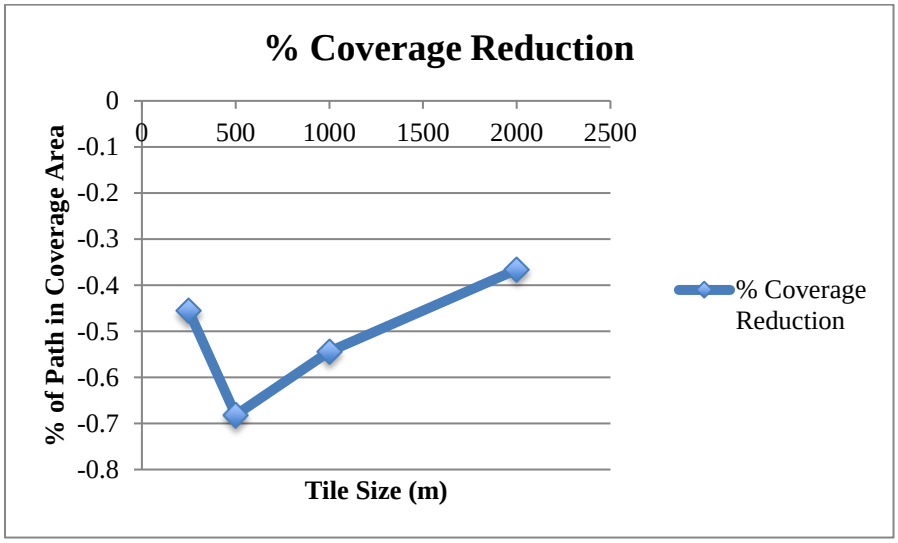

Figure 6-13: Ratio Method Coverage Reduction (%)

When compared across individual path runs, it is found that in 54% of cases, the drop in coverage is the same for all tile lengths and 35% of the non-equal cases, the largest planning tile size of 2000M is found to result in the lowest drop in coverage (Figure 6-15). This demonstrates that hypothesis 12 is not valid, and smaller tile sizes do not result in a lower smoothed coverage drop.

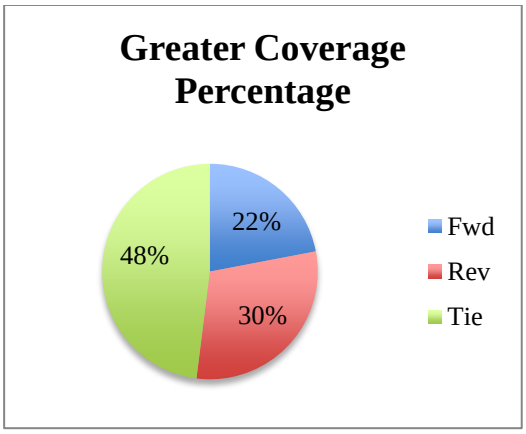

Figure 6-14: Better Smoothed Coverage by Direction

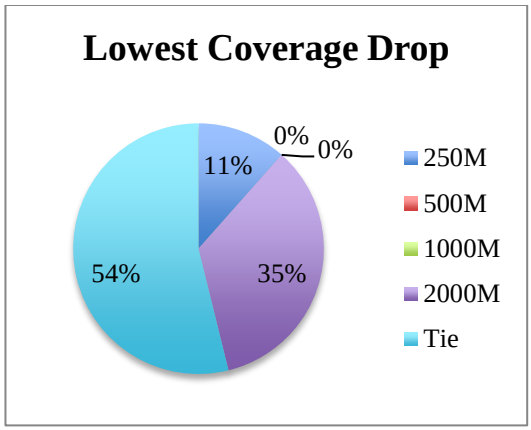

Figure 6-15: Lowest Coverage Reduction by Tile Size

In Figure 6-14 it is shown that only 48% of all cases of smoothing result in the same coverage regardless of direction. This disproves hypothesis 10 and shows that in 78% of cases, smoothing by this method in the reverse direction will yield equal to, or great final coverage than smoothing the path planned in the forward direction.

Average

The average method smoothed the path based on the average number of towers coverage each particular tile of the tile map. Based on hypothesis 12 it is anticipated that coverage will be the best when smoothed based on the smallest tile size. In Figure 6-16, it is shown that the average number of towers is reduced the least based on the smallest number of towers per tile at the 250m size and this progressively increases until the maximum tile size of 2000m.

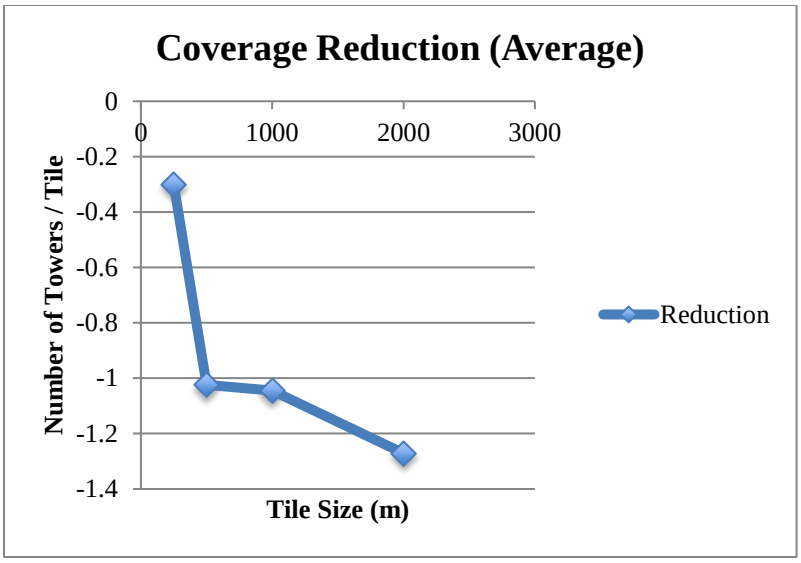

Figure 6-16: Coverage Reduction by Average Method

However, when the smoothed average coverage's are compared to one another, it is found that the highest average coverage comes from the path planned at the larger tile size (Figure 6-18) and thus dispels hypothesis 12.

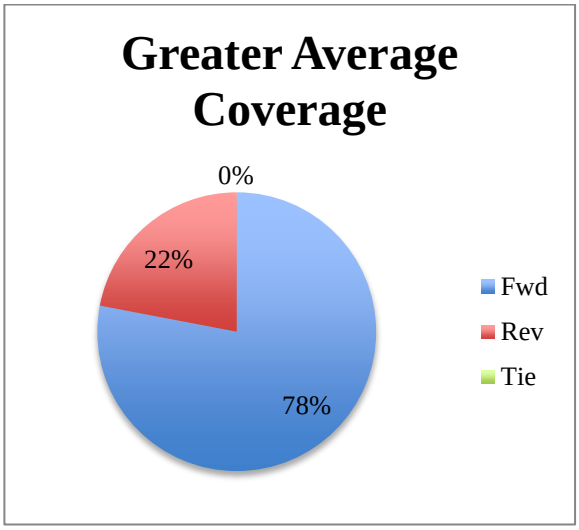

Figure 6-17: Greater Average Coverage by Direction

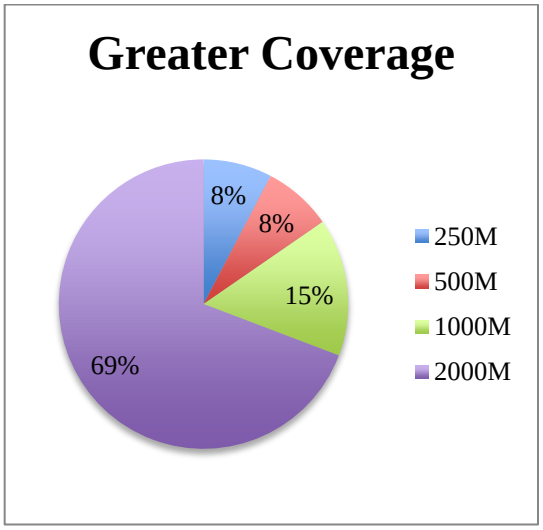

Figure 6-18: Greater Average Coverage by Tile Size

Based on direction, it is found that in 78% of cases, the forward direction is found to have the greater final coverage compared to the reverse direction. This again disproves hypothesis 10.

Distance

In Figure 6-19, the average distance decreases from the original planned paths are presented according to their tile size. Based on analysis, it is found that the average method has the largest average decrease in path distance compared to the ratio method. It is also notable that the average decrease in path length remains consistent across tile sizes except for 250m where the length decrease is much smaller than the others. Further of note, is the correlation between the two different methods, the variance between tile sizes remains consistent across the different methods, but the average method decreases the path length by approximate 3km more on average.

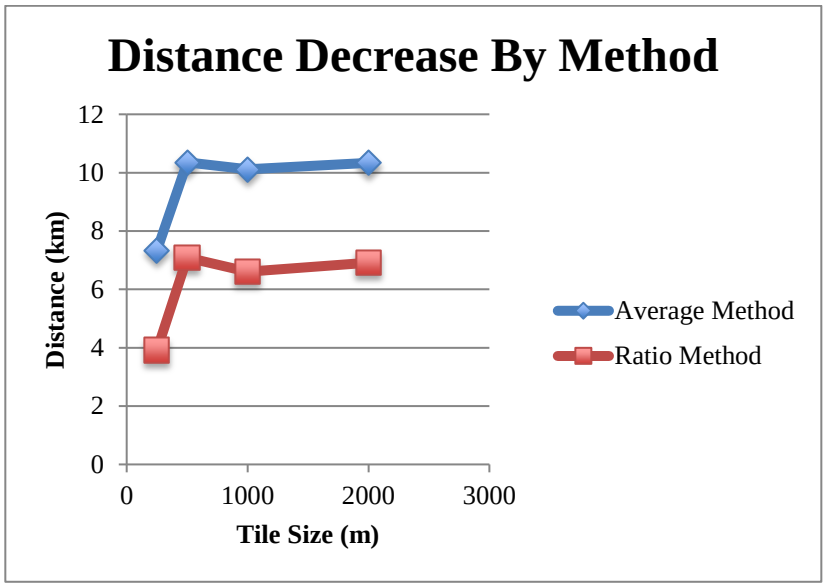

Figure 6-19: Distance Decrease by Method

Based on planning direction, it is found that the two methods are roughly consistent (Figure 6-20). However, the results determined demonstrate that the direction does have an effect on the total distance of the planned path thus disproving hypothesis 10.

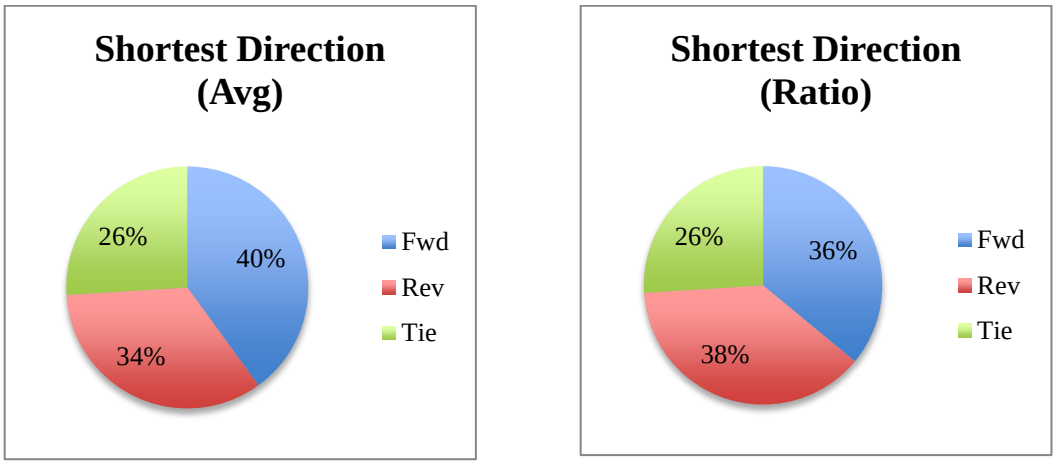

Figure 6-20: Distance Decrease by Planning Direction

When analyzing by average tile size, it is found that initial planning at the 2000m tile size results in the shortest final path after planning. This further negates hypothesis 10. It was also found that there was no direct correlation between the two methods, besides that fact that 2000m were the majority winner in shortest distance for both methods.

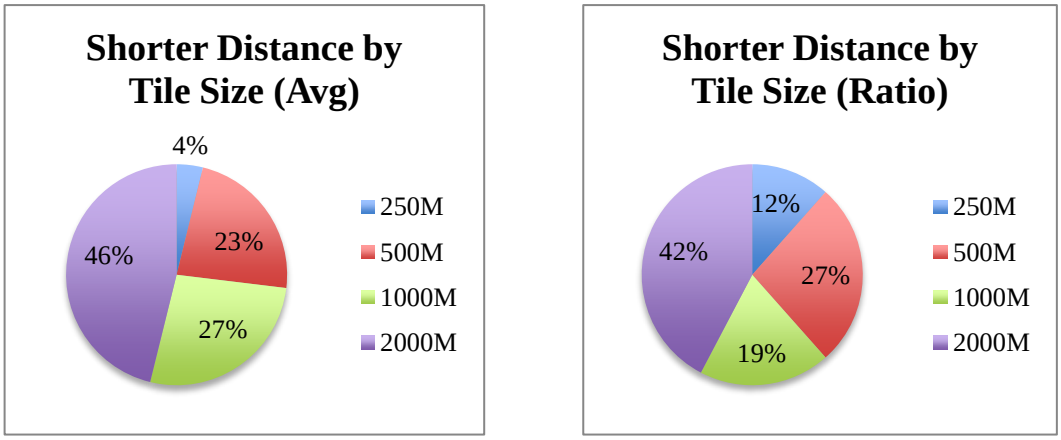

Figure 6-21: Distance Decrease by Planning Direction

When analyzed across all tile sizes, it is found that in the majority of planning resulted in a distance tie between both methods (76%). This is illustrated in Figure 6-22.

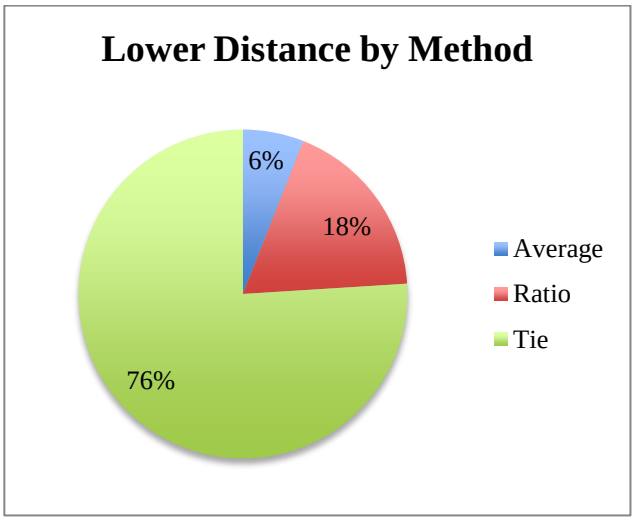

Figure 6-22: Lower Distance by Method

Number of Points

The complexity of the path is a function of the number of points, and therefore line segments that make up the path. It is unrealistic for an aircraft to fly a path that involves changing direction every tile size distance. In order to translate the planned path into a realistic path, the number of points must be reduced accordingly. This aims to evaluate hypothesis 8, which states that the resulting path will contain fewer points when planned originally with a smaller matrix tile size. The planned paths were smoothed according to both the Ratio method, and the Average method and the number of output points recorded. In Figure 6-23, it is shown that there is a corresponding increase in the number of points when planning tile sizes are decreased. However, it is also shown that regardless of the number of planned path points, paths, regardless of method, tend to always be reduced to only ~3-4 points on average. Furthermore, the different smoothing methods yield, on average, the same number of smoothed points. This result demonstrates that hypothesis 8

is invalid as there is no correlation between the planning matrix tile size, and the number of points in the smoothed route.

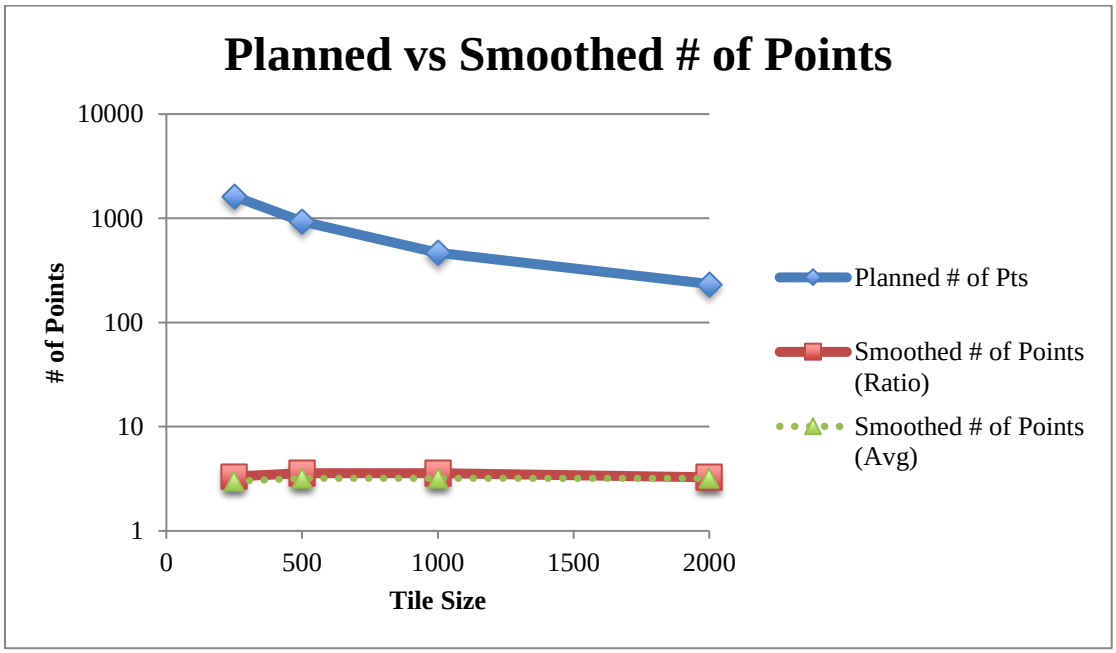

Figure 6-23: Planned vs. Smoothed Number of Points

When comparing point reduction by planning direction for each of the methods, it is found that in the majority of cases, the direction has no bearing on the number of points that exist on the path after smoothing. However, in 30% and 12% for the average and ratio method respectively, Hypothesis 10, is not supported and the resulting paths differ.

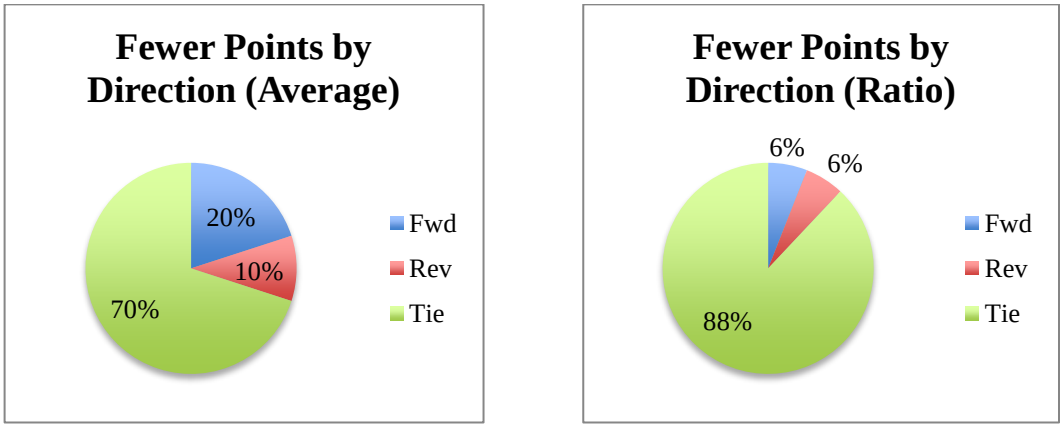

Figure 6-24: Lower Number of Points by Direction

When comparing methods to one another, it is found that 79% of the time, both methods yields a path of the same complexity (Figure 6-26). This trend is also represented fairly evenly across different tile sizes (Figure 6-25).

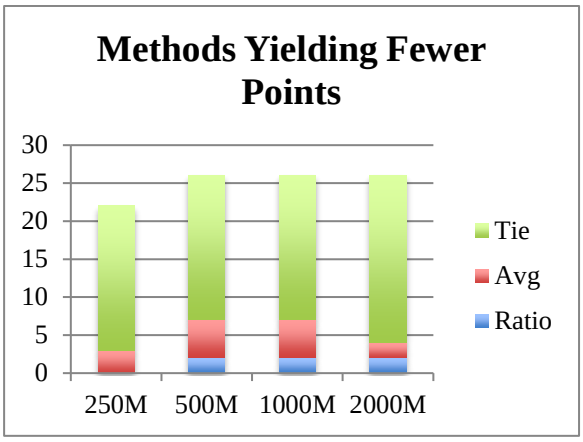

Figure 6-25: Fewer Points by Tile Size and Method

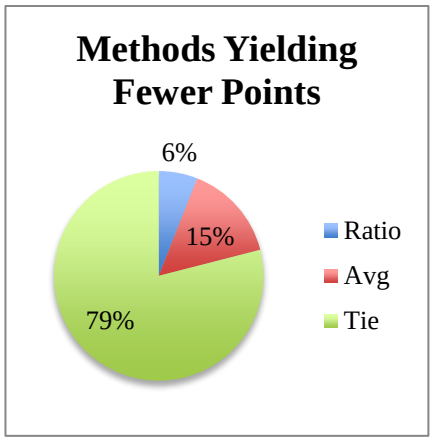

Figure 6-26: Fewer Points by Method

An example of a path planned from Thunder Bay to Hamilton is provided in Appendix IV. This example displays the direct route, planned route, and the smoothed route.

6.6. Discussion

The goal of the case study presented in this section was to validate the approach presented in this thesis by applying it to the field of neonatal transport. By providing a real and tangible application of this work, the hypotheses presented in this work were evaluated in a meaningful way.

One of the key hypotheses presented in this research was that planning could be performed in any direction, and the resulting path would have the same characteristics as each other. However, in planning, it was found that timing, coverage, and distances were not the same in all cases. This pattern continued in the smoothing section. One of the likely reasons for these differences lay in the type and distance of path that exists on some routes.

Route 7 (Kenora to London) is a prime example of a route that was very difficult to plan, and had a large difference between planning directions. Kenora, a Northwestern town has cell coverage within it, but is surrounded by areas of very poor coverage. London, a southern city, has very good coverage both in the city and in the surrounding area. What makes this route particularly unique beyond this, is that the direct path between the two cities is directly over Lake Huron and Lake Superior, which has no coverage at all. The results of this are that the algorithm must create a path that effectively follows the highways that navigate around the highways that have coverage. This causes much difficulty in planning to begin with.

Tile Size	Forward (s)	Reverse (s)
2000m	4002.5	74.5
1000m	105330.4	1336.9
500m	7633646	34610
250m	Unable to plan	Unable to plan

Table 6-16: Kenora to London Planning Times

The directionality trend is also particular prevalent in this route. Planning in the forward direction (Kenora to London) takes much longer, and the resulting path longer, than in the reverse direction (Table 6-16). This trend is also shown in routes 3 and 10. The most likely explanation of this is that planning from areas of relatively low cell coverage to areas of relatively high coverage causes the algorithm much more difficulty than the opposite.

The trend of relatively low area connectivity affecting planning time is also prevalent in other paths. For example when planning between two regions of poor connectivity, such as Route 1 (Hearst to Timmins. Compared to route 9 (Cobourg to Toronto), a route with continuous connectivity between the two points, route 1 has a lower planning time per km of direct distance. Though this sounds counter-intuitive, the reason for this lies in the A* algorithm and the connectivity biasing weighting factor. When there are more paths with high connectivity, the algorithm has much more difficulty pruning the

path tree that it creates. In a region with poor connectivity, the relative quantity of "covered" tile options the algorithm has to explore is much lower, yielding in faster plan times. This trend is illustrated in Table 6-17.

Route	Average Plan Time (ms) / Direct Distance			
	2000m	1000m	500m	250m
1	0.16	0.21	4.36	75.11
9	0.2	0.53	10.53	72.92

Table 6-17: Planning Time Efficiency by Regional Coverage

Another key hypothesis that was evaluated was that smoothing of a planned path would yield a much simpler path that maintains connectivity to be within a defined threshold (5% in this case study). Section 6.4 presents the results of this evaluation. One common theme that presented itself is that both methods, Ratio and Average, both yield the same smoothed route. In a large majority of cases, the method yields the same distance regardless of direction (Figure 6-24) or method (Figure 6-25). Despite these rather uniform results, there is a variance when it comes to comparing across different input route sizes. Regardless of input route size, or the smoothing method used, the output routes tend to be between 2 and 5 points of total size (Figure 6-23). This provides a very interesting conclusion: no matter what tile size is planned with the resulting route generated is nearly always smoothed down to the exact same path. In fact, it was found that larger planning tile sizes generally smooth down to better total path coverage than their smaller tile size counterparts.

When this result is coupled with the exponential increase in planning time when tile sizes are halved (Figure 6-10), it yields a result that goes against one of the main hypothesis' that is proposed: The decrease in tile size will yield more highly covered paths that are shorter. Based on this, the conclusion can be drawn that paths planned at a larger tile sizes are more efficient and there are no benefits to smaller tile sizes.

Broadly, the total planning times can vary dramatically based on both tile size and the distance of the route being planned. These times can vary from a few seconds (short-route with large tile size) to many hours (long route, small tile size). Due to the nature of transport calls often having much lead time before an actual transport flight actually occurs, the hours of planning is not generally seen as a problem. Furthermore, the number of actual possible paths that exist in a constrained area, such as what exists in this case study, is limited. This means that routes could largely be pre-processed meaning the planning time becomes even less important. However, as noted previously, the effect of tile size on the file smoothed path and resulting coverage is minimal. By using larger tile sizes, it is feasible to have planning be globally in the region of seconds rather than minutes or hours. This becomes particularly important in the case that the aircraft is rerouted to another destination while in route. In this case, time to re-plan the route becomes more important.

In a future study, this correlation between larger tile sizes generating more efficient coverage routes should be evaluated to find the upper limit in tile size where the planning becomes less efficient. Based on this, the optimal tile size for planning could be found that provides greatest planning performance, smallest coverage maps, and optimal route coverage.

Overall, a future study should also be completed to follow these routes with actual aircraft. This would allow a measure of how well these theoretical routes translate into reality. The study could use the routes presented in this case study, which are already valid and utilized transport routes, and fly at the altitudes presented in this routes. By keeping track of the coverage every few seconds, a real assessment of path coverage could be found. By comparing this coverage to the theoretical coverage presented in this case study, a gauge of how truly effective these routes are could be realized.

The results presented in this case study have successfully both proven and disproven the various hypotheses that have been presented. The final conclusion from this case study is that there is both vary interesting phenomena that have been found, but also very tangible routes generated. With the notable exception of two routes at the 250m tile

size that were not able to be planned in the allotted time, the case study routes presented were both plan-able and realistic – the main objective of this study.

7. Conclusion

This thesis presents a methodology and set of algorithms to maintain the best possible cellular data connectivity for an aircraft for by determining the shortest path between two airports that maintains the best possible cellular data connectivity for an aircraft. This concluding chapter provides a summary of the work that has been presented in this thesis. In addition, this chapter will discuss the practical implications of this research in the field of neonatal airborne transport, and in the field of neonatology as a whole. Furthermore, the conclusion will revisit and conclude upon on the research contribution that this thesis demonstrates. Finally, the limitations of this thesis are presented and future work that could be completed to further research in this field is outlined.

7.1. Summary

This thesis presents a methodology for creating optimal flight paths for aircraft that maximize cellular network connectivity while minimising total travel distance. The proposed methodology leverages the physical and technical characteristics of ground-based cellular network to create an accurate representation of network coverage at a given altitude for all points of a planning space. This resultant representation of coverage area is then leveraged in path planning in order to optimize the routes planned. The path output from the planning phase is then smoothed into a feasible route for an aircraft to travel. The contributions made to research by this thesis are demonstrated using a case study of Neonatal Critical Care Transport in Ontario and validated over a variety of different possible transport routes, transport aircraft, and flight altitudes.

To establish the current state of research activities in this area, a comprehensive literature review was undertaken. The literature review covered the three fundamental domains that form the basis of this thesis. The first area that was explored was the current state of wireless data communications in aircraft. In this domain, it was found that the predominant trend for wireless communication was the use of satellite networks. These

networks were found to provide adequate bandwidth for this work, but their inability to be utilized on rotary-wing aircraft eliminated their usefulness in the airborne transport. Use of cellular networks was found to be a viable option, as they provide the bandwidth required to support the types of systems needed for airborne telemedicine. With existing research limited to the unmanned aircraft domain, cellular networks utilization in piloted aircraft was identified as an open research area.

The second phase of the literature review focused on path planning activities in aircraft. In this review, it was found that the most common algorithm utilized was A-star. Beyond the most common algorithm, it was found that the vast majority of research related to path planning for aircraft was for the unmanned aircraft field. In fact only a single study was found that pertained to planning for manned aircraft. One of the most common constraints for path planning was connectivity, though only a single study looked at connectivity for cellular signals.

The third and final stage of the literature review focused on the use of telemedicine-type approaches in patient transport. In this review, it was found that all research was with land-based transport. The most predominate means of connectivity in this research was cellular, and they typically transmitted physiological and/or audio and video data. None of the studies specifically set out to support the needs of big data based approaches in telemedicine. Based on this section, it was found that research in the area of airborne transport and wireless telemedicine is both a novel research domain, and one which there is no other work.

Based on the literature review, it has been established that there is a real and pressing need to begin to leverage telemedicine-based approaches to enable big data-based approaches in airborne transport. With this need in mind, the following research goals were created:

I. Maximize cellular data connectivity throughout the airborne portion of the transport;

II. Minimize the total route distance to ensure a rapid transport;

III. Enable best possible telemedicine through the transport;

IV. Demonstrate the feasibility of using cellular networks to provide telemedicine connectivity during airborne transport.

Upon identifying the four goals that motivate this research, four research questions were synthesized to guide this research:

1. **A method to enable a flight path to be found that maintains a higher level of cellular connectivity than a direct path can be quantified;**
2. **The method proposed above is able to determine a flight path that represents the shortest path that maintains highest duration of connectivity;**
3. **The method proposed above is able to determine a flight path that represents a feasible flight path that could be followed by a manned aircraft;**
4. **The method proposed above can be demonstrated in the airborne transport domain and provide a tangible method for maintaining optimal cellular connectivity.**

Following the literature review, the third chapter provides context specifically around neonatal critical care transport. The specific manner in which these transports operate in Ontario, the types of equipment they utilize, and the team structures are presented. This chapter demonstrates the need for more advanced systems that leverage

technology to improve care for patients as the transport system receives an ever-increasing number of patients with more and more severe illness.

In Chapter four, the concept of a coverage map is defined and the methodology for its generation presented. The coverage map consists of a matrix of points at a given density that represents the total travelable area during path planning. The coverage map is generated utilizing the technical and physical characteristics of a cellular network, for a given planning altitude and at a specific matrix density. The methodology presented generates an estimation of the number of cellular towers that cover each point of the matrix. This coverage map is used in chapter five, where the methodology is presented, which leverages this map to do actual path planning.

The methodology presented accepts the parameters of source and target destination and a particular coverage map to utilize. The A-star algorithm is used for planning along with a presented heuristic and path cost function to generate the paths. Following this step, chapter five further presents a method for smoothing the paths into realistic routes for an aircraft to follow.

Finally, the case study of neonatal critical care transport in Ontario is presented in chapter 6 as a means to evaluate the methodologies presented in chapters 4 and 5. Utilising cellular network information from government databases, and typical transport routes and planned altitudes, various optimal routes are generated. These routes are evaluated based on distance, coverage, direction of planning, and timing to validate the research and experimental hypothesis presented.

Based on the work presented in this thesis, the objectives of this have been met:

1. **A method to enable a flight path to be found that maintains a higher level of cellular connectivity than a direct path can be quantified;**
   Leveraging the coverage map methodology, the path planning conducted in this thesis has been found to maintain a higher level of connectivity. This is demonstrated in chapter 6.

2. **The method proposed above is able to determine a flight path that represents the shortest path that maintains highest duration of connectivity;**
   The path planning methodology presented in chapter 5, which leverages the coverage map created in chapter 4, creates paths that maintain the highest duration of coverage. This is demonstrated in the evaluation in the case study presented in chapter 6.

3. **The method proposed above is able to determine a flight path that represents a feasible flight path that could be followed by a manned aircraft;**
   The smoothing methodology presented in chapter 5 enables the paths generated by the path planning algorithm to be down-sampled and smoothed into realistic paths for an aircraft to follow.

4. **The method proposed above can be demonstrated in the airborne transport domain and provide a tangible method for maintaining optimal cellular connectivity.**
   The evaluation of the methodology in the context of neonatal critical care transport, presented in chapter 6, demonstrates that paths can be created that maximize cellular coverage over the total route of a transport.

7.2. Practical Implications

There have been many well-stated benefits from implementing telemedicine solutions in the critical care field [79]. Implementing such solutions in critical care transport also stand to make a positive and direct impact on the quality and timeliness of a patients care [66], [80]. By enabling such systems to function during an airborne transport, the large gap in data that presently exists can be effectively eliminated. Doing this allows for not only better monitoring of a patient's condition, but also allows real-time patient monitoring system to function.

By having a functional analytics system running and monitoring the patient's condition, there are two major benefits that affect a patient's care; decreased workload for the transport care providers, and a better insight into the patient's condition.

By handling the second-by-second monitoring, the care providers conducting the transport will see a decrease in workload. By decreasing the overall workload, the overall transport time can be greatly reduced – which is linked to great medical outcomes [80]. Other benefits from a decrease workload include allowing for more familial interaction, more time to look at big picture care, etc.

By enabling real-time Clinical Decision Support Systems (CDSS), a greater insight into a patient's condition can be achieved. These systems can provide analysis of a patient's condition in ways that are traditionally infeasible in transport. For example, by analyzing the output from patient monitors, a CDSS could detect conditions such as Sepsis, and provide a much earlier diagnosis [81]. This diagnosis would result in the early treatment of the condition, which is of particular importance in the care of neonates. Furthermore, with the transmission of real-time ECG data, it is possible to have a cardiologist diagnosis a condition such as Supraventricular Tachycardia (SVT). This is traditionally only possible with the patients in a hospital ward and a cardiologist present.

7.3. Contributions

The research contributions that are have been made as a result of this research are:

1. Use of advanced link budget calculations to determine realistic cellular coverage regions for path planning presented in section 4.1.3 and demonstrated in section 6.3.1.3
2. Dynamic creation of cellular coverage maps to represent a regions coverage as designed in chapter 4 and demonstrated within the case study in section 6.3.1
3. Use of a path planning approach to maintain cellular connectivity in a manned aircraft through the practical case study example as detailed in section 6.3.2
4. Use of path smoothing to create feasible routes for manned aircraft to utilize as designed in section 5.4 and demonstrated in the case study in section 6.4.4.
5. Demonstration using a clinical problem in the domain of neonatal transport as detailed in chapter 6

7.4. Limitations of Research

There are several limitations within the scope of this research. There are vast numbers of Path Planning algorithms and modifications to them that exist in the computer science field. To limit the scope of this research, research was focused exclusively on the A* algorithm. This was considered an appropriate limitation as the focus was to demonstrate that if techniques were used to create alternate paths that are realistic for aircraft to take, that with a minimal amount of effort, potentially significant improvements to the amount of time where internet connectivity could be achieved. This would have direct impact on the amount of time that telemedicine support of the patient can be provided from a remote location such as the receiving hospital.

Furthermore, due to the extremely complex nature of determining the practical expectations of how a wireless cellular network will perform, there were several assumptions made to decrease the scope of the work and maintain focus on the research hypothesis. These assumptions are:

- Aircraft cruise speeds are below the 500km/h maximum UE velocity defined in the LTE standard [68]
- Cells are unloaded, and therefore there is no usage-based cell radius reduction [68]
- There are no adjacent cell range-limiting interference present [68]
- Aircraft in question contains a single cellular modem only, decreasing the cell network loading and reducing hand-over latency [82]
- Both the cell tower and UE antennas are perfect isotropic radiators and radiate or receive equally in all directions
- If there is a connection, the connection is stable and high-performing

This research is further limited by not providing any means for interacting with a user – there is no user interface. The evaluation of this methodology leveraged a command-line based interface which would not be universally usable to all users. There are also no medical contributions made by this thesis, work presented is proof-of-concept and demonstrates the feasibility of obtaining an Internet connection that could support a telemedicine system.

7.5. Future Research

This thesis by nature is a starting point, leaving much room for future research. The next step would be to execute the future study proposed in 0 to evaluate the practical translation of the theory presented in this thesis. Based on the practicality of this work, future work assessing modifications to the existing cellular infrastructure that would allow better connectivity on airborne platforms would be explored. To overcome the speed

limitations, future research into automatically select next nodes in a cellular network as opposed to allow carrier sense operations to handle the next node.

Future research could also begin to evaluate the usefulness of telemedicine systems during airborne transport could also be conducted. By leveraging existing telemedicine technology and physiological data analytics system, studies could be carried out to examine the effects an air transport has on a patient – in real time.

Within the scope of this particular research, there are several areas of improvement that could be made within future research. The following is a list of potential areas of improvement:

- Improvement of link budget equations to provide more realistic path loss estimations
- Account for the evaluation of tower antennas and the resulting signal attenuation
- Implement more realistic path loss equation than FSPL
- Account for decreased data rates at higher speed and provide optimal cruise speed
- Account for radiation patterns of tower antennas

7.6. Final Conclusion

The utilisation of big data-type approaches to aide clinicians in decision making has long been restricted to the intensive care unit environment. This thesis provides a solution to the main technical barrier preventing these approaches in neonatal airborne critical care transport – connectivity. In this work, a methodology was presented that demonstrates that ground-based cellular networks can provide a feasible means for transmitting the required physiological data to support these approaches.

This contribution demonstrates that by leveraging cellular network properties over a transport area, it is feasible to create flight plans for transport aircraft to enable them to have the best possible connectivity. By enabling connectivity in aircraft, it is possible for critically important physiological and other patient information to be transmitted to a ground-based care team to provide a great insight into a patient's condition. This insight can be used to make quicker and more accurate care decisions, which through the same means, can be transmitted back to the transport teams. This has the ultimate effect to improving the level of care patients receive but can also improve the overall outcome of the patient.

Appendix I – Link Budgets

Field	Description	Typical value
a	UE maximum transmission power for power class 3. Different power classes would have different power levels. The power can be reduced depending on the modulation, see Chapter 11 for details.	23 dBm
b	UE antenna gain depends on the type of device and on the frequency band. Small handheld terminal at a low frequency band (like Band VIII) can have an antenna gain of −5 dBi while a fixed wireless terminal with directive antenna can have a gain of up to 10 dBi.	−5 to 10 dBi
c	Body loss is typically included for voice link budget where the terminal is held close to the user's head.	3 to 5 dB for voice
d	Calculated as a + b − c	
e	Base station RF noise figure. Depends on the implementation design. The minimum performance requirement is approximately 5 dB but the practical performance can be better.	2 dB
f	Terminal noise can be calculated as k (Boltzmann constant) × T (290K) × bandwidth. The bandwidth depends on bit rate, which defines the number of resource blocks. We assume two resource blocks for 64 kbps uplink.	−118.4 dBm for two resource blocks (360 kHz)
g	Calculated as e + f	
h	Signal-to-noise ratio from link simulations or measurements. The value depends on the modulation and coding schemes, which again depend on the data rate and on the number of resource blocks allocated.	−7 dB for 64 kbps and two resource blocks
i	Calculated as g + h	
j	Interference margin accounts for the increase in the terminal noise level caused by the interference from other users. Since LTE uplink is orthogonal, there is no intra-cell interference but we still need a margin for the other cell interference. The interference margin in practice depends heavily on the planned capacity – there is a tradeoff between capacity and coverage. The LTE interference margin can be smaller than in WCDMA/HSUPA where the intra-cell users are not orthogonal. In other words, the cell breathing will be smaller in LTE than in CDMA based systems.	1 to 10 dB
k	Cable loss between the base station antenna and the low noise amplifier. The cable loss value depends on the cable length, cable type and frequency band. Many installations today use RF heads where the RF parts are close to the antenna making the cable loss very small. The cable loss can also be compensated by using mast head amplifiers.	1 to 6 dB
l	Base station antenna gain depends on the antenna size and the number of sectors. Typical 3-sector antenna 1.3 m high at 2 GHz band gives 18 dBi gain. The same size antenna at 900 MHz gives smaller gain.	15 to 21 dBi for sectorized base station
m	Fast fading margin is typically used with WCDMA due to fast power control to allow headroom for the power control operation. LTE does not use fast power control and the fast fading margin is not necessary in LTE.	0 dB
n	Soft handover is not used in LTE	0 dB

Uplink Budget [69]

Field	Description	Typical value
a	Base station maximum transmission power. A typical value for macro cell base station is 20–60 W at the antenna connector.	43–48 dBm
b	Base station antenna gain. See uplink link budget.	
c	Cable loss between the base station antenna connector and the antenna. The cable loss value depends on the cable length, cable thickness and frequency band. Many installations today use RF heads where the power amplifiers are close to the antenna making the cable loss very small.	1–6 dB
d	Calculated as A + B – C	
e	UE RF noise figure. Depends on the frequency band, Duplex separation and on the allocated bandwidth. For details, see Chapter 12.	6–11 dB
f	Terminal noise can be calculated as k (Boltzmann constant) × T (290K) × bandwidth. The bandwidth depends on bit rate, which defines the number of resource blocks. We assume 50 resource blocks, equal to 9 MHz, transmission for 1 Mbps downlink.	–104.5 dBm for 50 resource blocks (9 MHz)
g	Calculated as E + F	
h	Signal-to-noise ratio from link simulations or measurements. The value depends on the modulation and coding schemes, which again depend on the data rate and on the number of resource blocks allocated.	–9 dB for 1 Mbps and 50 resource blocks
i	Calculated as G + H	
j	Interference margin accounts for the increase in the terminal noise level caused by the other cell. If we assume a minimum G-factor of –4 dB, that corresponds to 10*log10(1+10^(4/10)) = 5.5 dB interference margin.	3–8 dB
k	Control channel overhead includes the overhead from reference signals, PBCH, PDCCH and PHICH.	10–25% = 0.4–1.0 dB
l	UE antenna gain. See uplink link budget.	-5–10 dBi
m	Body loss. See uplink link budget.	3.5 dB for voice

Downlink Budget [69]

Appendix II – Cell Towers in Southern Ontario

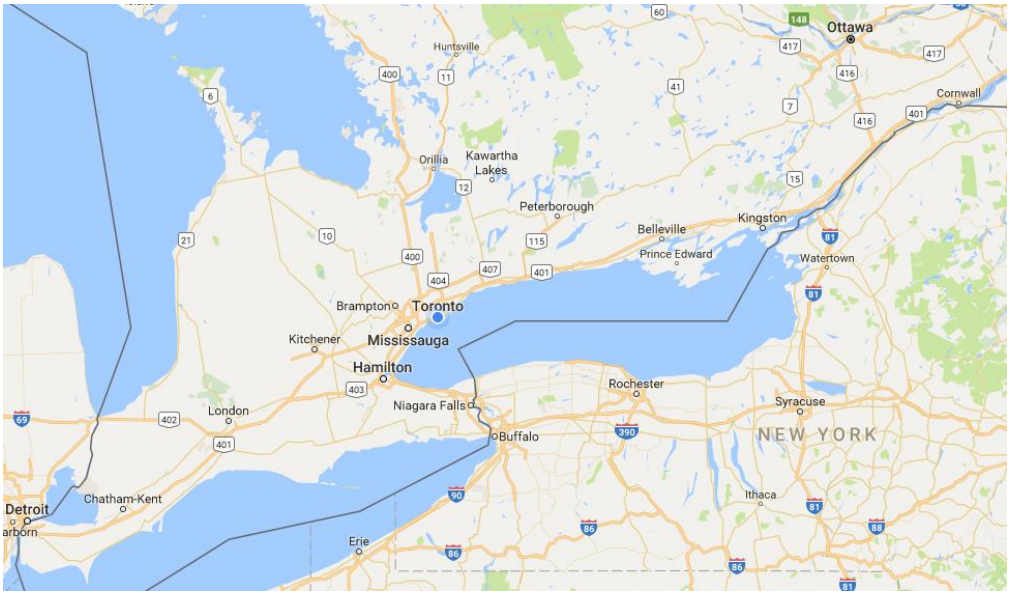

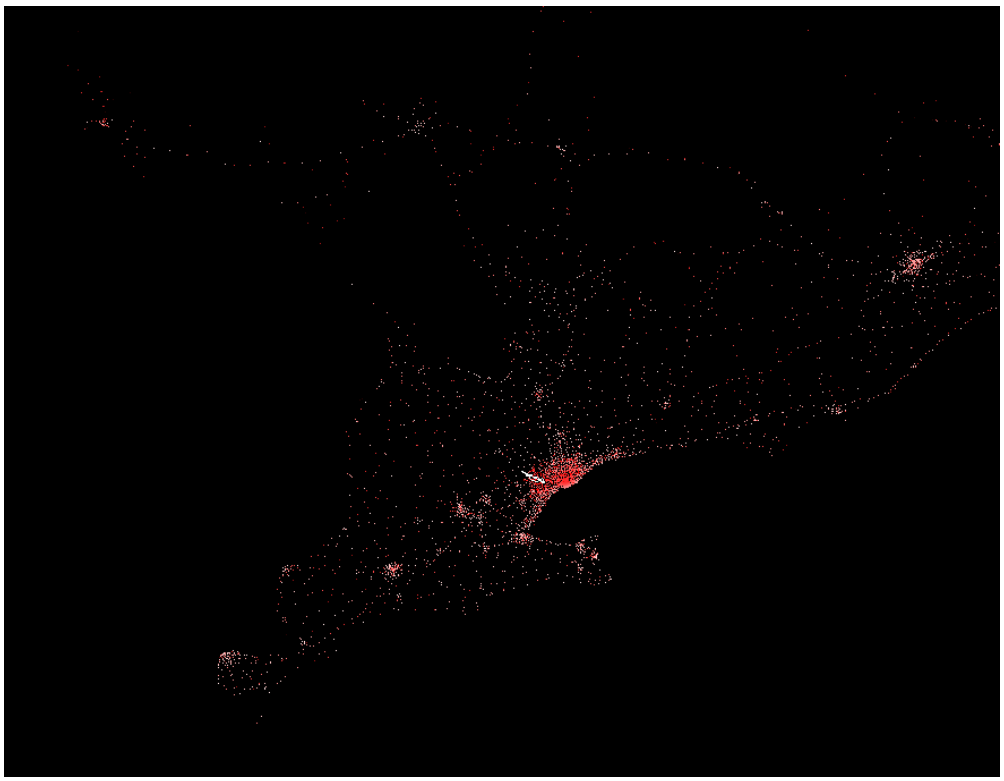

The above image is a map of Southern Ontario. The image below contains a point at the location of each cell tower. Where single points on the coverage grid map contain multiple towers, the colour changes from red (single tower) to white for multiple towers.

Appendix III – Ontario Cell Coverage at 20000ft Altitude

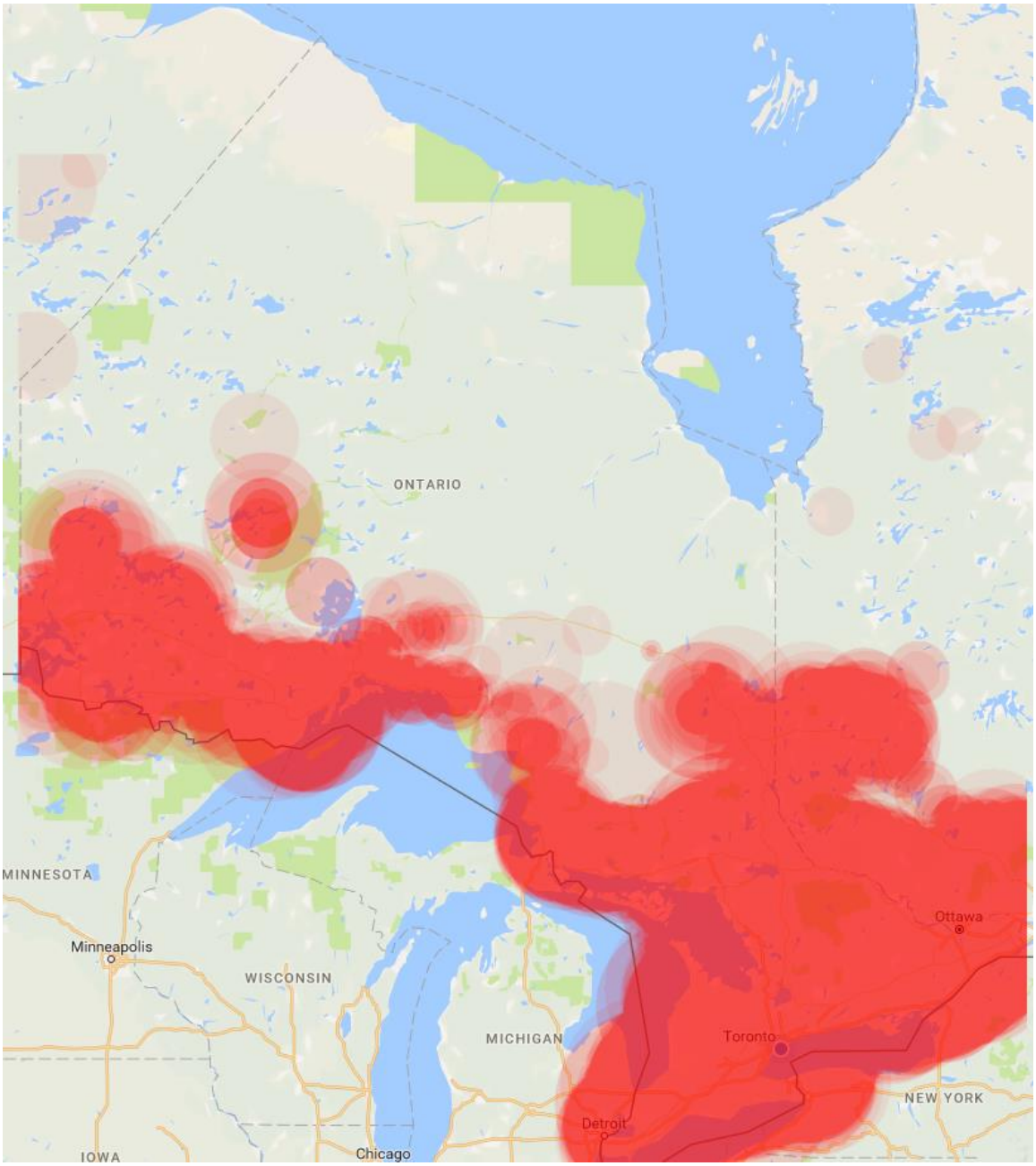

Cell coverage heat map of coverage at 21000 Feet Altitude in Ontario. Darker opacity represents higher number of towers covering the particular area.

Appendix IV – Thunder Bay to Hamilton Path Plan Example

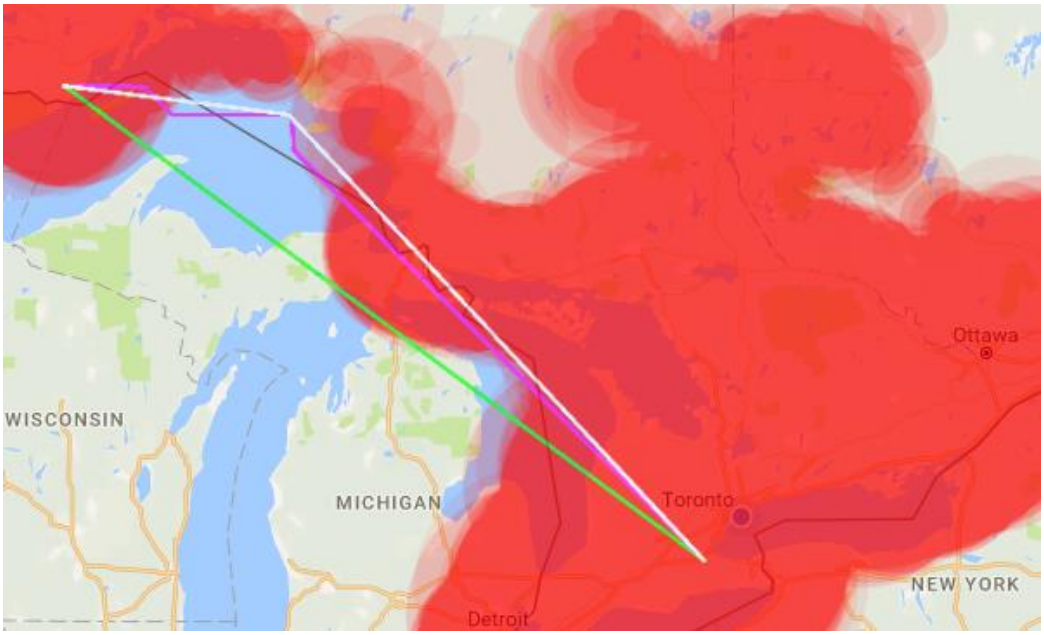

Path plan from Thunder Bay to Hamilton. Direct route is in Green, planned route is in Magenta, and smoothed route in White.

References

[1] C. Abraham, R. T. Watson, and M.-C. Boudreau, “Ubiquitous Access: On the Front Lines of Patient Care and Safety,” *Commun. ACM*, vol. 51, no. 6, pp. 95–99, Jun. 2008.

[2] BCE Inc., “Bell Coverage Map,” 2014. [Online]. Available: http://network.bell.ca/en/coverage. [Accessed: 13-Mar-2014].

[3] Telus Mobility Inc., “TELUS Corporation - Management’s Discussion and Analysis - 2015 Q2,” Vancouver, 2015.

[4] I. Sachpazidis, “Image and Medical Data Communication Protocols for Telemedicine and Teleradiology,” Technische Universit{ä}t, Darmstadt, 2008.

[5] B. A. Lupton and M. R. Pendray, “Regionalized neonatal emergency transport.,” *Semin. Neonatol.*, vol. 9, no. 2, pp. 125–33, Apr. 2004.

[6] E. W. Dijkstra, “A note on two problems in connexion with graphs,” *Numer. Math.*, vol. 1, no. 1, pp. 269–271, Dec. 1959.

[7] S. Even, *Graph Algorithms*, 2nd ed. New York: Cambridge University Press, 2011.

[8] P. Hart, N. Nilsson, and B. Raphael, “A Formal Basis for the Heuristic Determination of Minimum Cost Paths,” *IEEE Trans. Syst. Sci. Cybern.*, vol. 4, no. 2, pp. 100–107, 1968.

[9] E. I. Grøtli and T. A. Johansen, “Path Planning for UAVs Under Communication Constraints Using SPLAT! and MILP,” *J. Intell. Robot. Syst.*, vol. 65, no. 1–4, pp. 265–282, Aug. 2011.

[10] O. M. Hammouri and M. M. Matalgah, “Voronoi path planning technique for recovering communication in UAVs,” in *2008 IEEE/ACS International Conference on Computer Systems and Applications*, 2008, pp. 403–406.

[11] B. Meng and X. Gao, “UAV Path Planning Based on Bidirectional Sparse A* Search Algorithm,” in *2010 International Conference on Intelligent Computation*

Technology and Automation, 2010, vol. 3, pp. 1106–1109.

[12] H. Meng and G. Xin, "UAV route planning based on the genetic simulated annealing algorithm," in *2010 IEEE International Conference on Mechatronics and Automation*, 2010, pp. 788–793.

[13] Z. Wang, L. Liu, T. Long, C. Yu, and J. Kou, "Enhanced sparse A* search for UAV path planning using dubins path estimation," in *Proceedings of the 33rd Chinese Control Conference*, 2014, pp. 738–742.

[14] Xin Yang, Mingyue Ding, and Cheng-Ping Zhou, "Fast Marine Route Planning for UAV Using Improved Sparse A* Algorithm," in *2010 Fourth International Conference on Genetic and Evolutionary Computing*, 2010, pp. 190–193.

[15] C. McGregor, C. Catley, A. James, and J. Padbury, "Next generation neonatal health informatics with Artemis.," *Stud. Health Technol. Inform.*, vol. 169, pp. 115–119, 2011.

[16] M. Blount, M. R. Ebling, J. M. Eklund, A. G. James, C. M. C. Gregor, N. Percival, K. P. Smith, and D. Sow, "Real-time analysis for intensive care: development and deployment of the artemis analytic system," *IEEE Eng. Med. Biol. Mag.*, no. March/April, pp. 110–118, 2010.

[17] R. Greer, C. Olivier, J. E. Pugh, J. M. Eklund, and C. McGregor, "Remote, Real-Time Monitoring and Analysis of Vital Signs of Neonatal Graduate Infants," in *36th Annual International Conference of the IEEE EMBS*, 2014, pp. 1382–5.

[18] G. Dodig-Crnkovic, F. Lüders, M. Höst, and R. Feldt, "Improved Support for Master's Thesis Projects in Software Engineering," Myndigheten för nätverk och samarbete inom högre utbildning, 2010.

[19] GoGo, "Gogo Press Room - Multiple Solutions are a Must," 2015. [Online]. Available: http://gogoair.mediaroom.com/technology. [Accessed: 12-Aug-2015].

[20] OnAir, "About OnAir," 2015. [Online]. Available: http://www.onair.aero/en/about-onair. [Accessed: 12-Aug-2015].

[21] OnAir, "How our global services work," 2015. [Online]. Available:

http://www.onair.aero/en/commercial-airlines-how-it-works. [Accessed: 12-Aug-2015].

[22] P. Thompson, “How In-Flight WiFi Works And Why It Should Get Better,” *Flight Club*, 2014.

[23] J. Stromberg, “Why in-flight wifi is so painfully slow — except on JetBlue and Southwest - Vox,” *Vox*, 2015.

[24] L.-N. Lee, V. Liau, W. Marhefka, and R. Gopal, “Micro Satellite Terminal-Based High Data Rate Communication for Rotary Wing Aircraft,” in *2014 IEEE Military Communications Conference*, 2014, pp. 1698–1703.

[25] Rogers Communications Inc., “Rogers Coverage Map,” 2014. [Online]. Available: http://www.rogers.com/web/content/wireless_network.

[26] K. Daniel, S. Rohde, and C. Wietfeld, “Leveraging public wireless communication infrastructures for UAV-based sensor networks,” in *2010 IEEE International Conference on Technologies for Homeland Security (HST)*, 2010, pp. 179–184.

[27] R. Miura, M. Maruyama, M. Suzuki, H. Tsuji, M. Oodo, and Y. Nishi, “Experiment of telecom/broadcasting mission using a high-altitude solar-powered aerial vehicle Pathfinder Plus,” in *The 5th International Symposium on Wireless Personal Multimedia Communications*, 2002, vol. 2, pp. 469–473.

[28] L. Zhu, D. Yin, J. Yang, and L. Shen, “Research of remote measurement and control technology of UAV based on mobile communication networks,” in *2015 IEEE International Conference on Information and Automation*, 2015, pp. 2517–2522.

[29] BMS Inc., “Broadcast Microwave Services » Blog Archive » Airborne Downlink,” 2015. [Online]. Available: http://www.bms-inc.com/solution/broadcast/airborne-downlink-2/. [Accessed: 12-Aug-2015].

[30] Northrop Grumman, “Understanding Voice and Data Link Networking Understanding Voice and,” 2013.

[31] D. R. Adams and R. E. McKenzie, “System and method for optimizing aircraft flight path,” US 4812990 A, 14-Mar-1989.

[32] S. A. Bortoff, “Path planning for UAVs,” in *Proceedings of the 2000 American Control Conference. ACC (IEEE Cat. No.00CH36334)*, 2000, vol. 1, no. 6, pp. 364–368 vol.1.

[33] P. Kermani and A. A. Afzalian, “Flight path planning using GA and fuzzy logic considering communication constraints,” in *7’th International Symposium on Telecommunications (IST’2014)*, 2014, pp. 6–11.

[34] A. L’Afflitto and C. Sultan, “On the fuel and energy consumption optimization problem in aircraft path planning,” in *49th IEEE Conference on Decision and Control (CDC)*, 2010, pp. 4851–4856.

[35] S. Li and Xiuxia Sun, “A Real-Time UAV Route Planning Algorithm Based on Fuzzy Logic Techniques,” in *2006 6th World Congress on Intelligent Control and Automation*, 2006, vol. 2, pp. 8750–8753.

[36] W. Lingxiao and Z. Deyun, “Effective path planning method for low detectable aircraft,” in *Systems Engineering and Electronics, Journal of*, 2009, vol. 20, no. 4, pp. 784–789.

[37] T. McGee, S. Spry, and K. Hedrick, “Optimal path planning in a constant wind with a bounded turning rate,” in *AIAA Guidance, Navigation, and Control Conference and Exhibit*, 2005, pp. 1–11.

[38] T. Schouwenaars, A. Stubbs, J. Paduano, and E. Feron, “Multivehicle path planning for nonline-of-sight communication,” *J. F. Robot.*, vol. 23, no. 3–4, pp. 269–290, Mar. 2006.

[39] C. Tanil, C. Warty, and E. Obiedat, “Collaborative mission planning for UAV cluster to optimize relay distance,” in *2013 IEEE Aerospace Conference*, 2013, pp. 1–11.

[40] T. Shi, H. Wang, and F. Wang, “Path planning of a four-rotor aircraft based on shortest path algorithm and statistical analysis,” in *2013 10th International Conference on Fuzzy Systems and Knowledge Discovery (FSKD)*, 2013, pp. 627–631.

[41] F. H. Tseng, T. T. Liang, C. H. Lee, L. Der Chou, and H. C. Chao, “A Star Search Algorithm for Civil UAV Path Planning with 3G Communication,” in *2014 Tenth International Conference on Intelligent Information Hiding and Multimedia Signal Processing*, 2014, pp. 942–945.

[42] S. Koch, “Home telehealth--current state and future trends.,” *Int. J. Med. Inform.*, vol. 75, no. 8, pp. 565–76, Aug. 2006.

[43] R. Roine, A. Ohinmaa, and D. Hailey, “Assessing telemedicine: a systematic review of the literature,” *Can. Med. Assoc. J.*, vol. 165, no. 6, pp. 765–771, Sep. 2001.

[44] D. Kofos, R. Pitetti, R. Orr, and A. Thompson, “Telemedicine in Pediatric Transport: A Feasibility Study,” *Pediatrics*, vol. 102, no. 5, p. e58-, Nov. 1998.

[45] V. Anantharaman and L. Swee Han, “Hospital and emergency ambulance link: using IT to enhance emergency pre-hospital care,” *Int. J. Med. Inform.*, vol. 61, no. 2–3, pp. 147–161, May 2001.

[46] G. R. Curry and N. Harrop, “The Lancashire telemedicine ambulance,” *J. Telemed. Telecare*, vol. 4, no. 4, pp. 231–238, Dec. 1998.

[47] M. P. LaMonte, Y. Xiao, P. F. Hu, D. M. Gagliano, M. N. Bahouth, R. D. Gunawardane, C. F. MacKenzie, W. R. Gaasch, and J. Cullen, “Shortening time to stroke treatment using ambulance telemedicine: TeleBAT.,” *J. Stroke Cerebrovasc. Dis.*, vol. 13, no. 4, pp. 148–54, Jan. 2004.

[48] Y.-H. Lin, I.-C. Jan, P. C.-I. Ko, Y.-Y. Chen, J.-M. Wong, and G.-J. Jan, “A wireless PDA-based physiological monitoring system for patient transport.,” *IEEE Trans. Inf. Technol. Biomed.*, vol. 8, no. 4, pp. 439–47, Dec. 2004.

[49] G. J. Mandellos, D. K. Lymperopoulos, M. N. Koukias, A. Tzes, N. Lazarou, and C. Vagianos, “A novel mobile telemedicine system for ambulance transport. Design and evaluation.,” *Conf. Proc. ... Annu. Int. Conf. IEEE Eng. Med. Biol. Soc. IEEE Eng. Med. Biol. Soc. Annu. Conf.*, vol. 4, pp. 3080–3, Jan. 2004.

[50] Y. Yamada, S. Usui, M. Kohn, and M. Mukai, “A vision of ambulance telemedicine services using the Quasi-Zenith Satellite,” in *Proceedings. 6th International*

Workshop on Enterprise Networking and Computing in Healthcare Industry - Healthcom 2004 (IEEE Cat. No.04EX842), 2004, pp. 161–165.

[51] Y. Xiao, D. Gagliano, M. LaMonte, P. Hu, W. Gaasch, R. Gunawadane, and C. Mackenzie, "Design and evaluation of a real-time mobile telemedicine system for ambulance transport," *J. High Speed Networks*, vol. 9, no. 1, pp. 47–56, Jan. 2000.

[52] K. L. Lam, H. Y. Tung, K. F. Tsang, and K. T. Ko, "WiMAX telemedicine system for emergence medical service," in *2009 7th International Conference on Information, Communications and Signal Processing (ICICS)*, 2009, pp. 1–5.

[53] C.-F. Lin, "Mobile telemedicine: a survey study.," *J. Med. Syst.*, vol. 36, no. 2, pp. 511–20, Apr. 2012.

[54] C. McGregor, "Big Data and Opportunities for Critical Care," *IEEE Comput.*, vol. 46, no. 6, pp. 54–9, 2013.

[55] A. Thommandram, J. E. Pugh, J. M. Eklund, C. McGregor, and A. G. James, "Classifying neonatal spells using real-time temporal analysis of physiological data streams: Algorithm development," in *2013 IEEE Point-of-Care Healthcare Technologies (PHT)*, 2013, pp. 240–243.

[56] R. Greer, C. Olivier, J. E. Pugh, J. M. Eklund, and C. McGregor, "Remote, Real-Time Monitoring and Analysis of Vital Signs of Neonatal Graduate Infants," *36th Annu. Int. Conf. IEEE EMBS*, 2014.

[57] D. Konstantas, I. Widya, N. Dokovsky, G. Koprinkov, V. Jones, and R. Herzog, "Mobile Patient Monitoring: The MobiHealth System," *J. Inf. Technol. Healthc.*, vol. 2, no. 5, pp. 365–373, 2004.

[58] R. Kamaleswaran, "CBPsp: Complex Business Processes for Stream Processing," The University of Ontario Institute of Technology, 2012.

[59] Ministry of Health and Long-Term Care, "Ontario Air Ambulance Program," *Ministry of Health and Long-Term Care Public Information*, 2015. [Online]. Available: http://www.health.gov.on.ca/english/public/program/ehs/air/air_mn.html.

[Accessed: 26-Nov-2015].

[60] M. S. Kramer, M. Olivier, F. H. McLean, D. M. Willis, and R. H. Usher, “Impact of intrauterine growth retardation and body proportionality on fetal and neonatal outcome.,” *Pediatrics*, vol. 86, no. 5, pp. 707–713, 1990.

[61] G. W. Chance, J. D. Matthews, J. Gash, G. Williams, and K. Cunningham, “Neonatal transport: A controlled study of skilled assistance,” *J. Pediatr.*, vol. 93, no. 4, pp. 662–666, Oct. 1978.

[62] P. Shah, E. W. Yoon, and P. Chan, “Annual Report 2014 Rapport Annuel,” 2014.

[63] Ornge, “Ornge Annual Report 2012-2013,” Mississauga, 2013.

[64] F. Robitaille, “Picture of the Pilatus PC-12/47E (PC-12 NG) aircraft,” *Airliners.net*, 2009. [Online]. Available: http://www.airliners.net/photo/Ornge/Pilatus-PC-12-47E-(PC-12/1598678/L/. [Accessed: 26-Nov-2015].

[65] J. Bain, “New Air Ambulance Training,” 2011. [Online]. Available: https://www.flickr.com/photos/jasonbain/5821221735/. [Accessed: 26-Nov-2015].

[66] S. P. Nelwan, T. B. van Dam, P. Klootwijk, and S. H. Meij, “Ubiquitous mobile access to real-time patient monitoring data,” in *Computers in Cardiology*, 2002, pp. 557–560.

[67] J. Inman, *Navigation and Nautical Astronomy for the Use of British Seamen*. C & J Rivington, 1835.

[68] H. Holma and A. Toskala, *WCDMA for UMTS - HSPA evolution and LTE*, 4th ed. Chichester, West Sussex: John Wiley & Sons, Ltd, 2007.

[69] H. Holma and A. Toskala, *LTE for UMTS: OFDMA and SC-FDMA based radio access*, 1st ed. Chichester, West Sussex: John Wiley & Sons, Ltd, 2009.

[70] N. Narang and S. Kasera, *2G Mobile Networks: GSM and HSCSD*, 1st ed. New Delhi: Tata McGraw-Hill Publishing Company Ltd., 2007.

[71] T. Chapman, E. Larsson, P. von Wrycza, E. Dahlman, S. Parkvall, and J. Sköld, *HSPA Evolution: The Fundamentals for Mobile Broadband*. Elsevier, 2015.

[72] S. Stefania, T. Issam, and B. Matthew, *LTE, the UMTS long term evolution: from theory to practice*, vol. 6. 2009.

[73] "Motorola Demonstrates Long Range GSM Capability - 300% More Coverage With New Extended Cell Feature.," *Business Wire*, 1998.

[74] A. Ghasemi, A. Abedi, and F. Ghasemi, *Propagation Engineering in Wireless Communications*, 1st ed. New York, NY: Springer New York, 2012.

[75] U. Ramer, "An iterative procedure for the polygonal approximation of plane curves," *Comput. Graph. Image Process.*, vol. 1, no. 3, pp. 244–256, Nov. 1972.

[76] D. H. DOUGLAS and T. K. PEUCKER, "ALGORITHMS FOR THE REDUCTION OF THE NUMBER OF POINTS REQUIRED TO REPRESENT A DIGITIZED LINE OR ITS CARICATURE," *Cartogr. Int. J. Geogr. Inf. Geovisualization*, vol. 10, no. 2, pp. 112–122, Dec. 1973.

[77] Telus Mobility Inc., "Coverage Map," 2016. [Online]. Available: http://www.telus.com/en/on/mobility/network/coverage-map.jsp.

[78] S. J. Opitz, N. Todtenberg, and H. König, "Mobile bandwidth prediction in the context of emergency medical service," in *Proceedings of the 7th International Conference on PErvasive Technologies Related to Assistive Environments - PETRA '14*, 2014, pp. 1–7.

[79] C. McGregor, B. Kneale, and M. Tracy, "Bush Babies Broadband: On-Demand Virtual Neonatal Intensive Care Unit Support for Regional Australia," *Third Int. Conf. Inf. Technol. Appl.*, vol. 2, pp. 113–118, 2005.

[80] R. MORI, M. FUJIMURA, J. U. N. SHIRAISHI, B. EVANS, M. CORKETT, H. NEGISHI, and P. A. T. DOYLE, "Duration of inter-facility neonatal transport and neonatal mortality: Systematic review and cohort study," *Pediatr. Int.*, vol. 49, no. 4, pp. 452–458, Aug. 2007.

[81] C. McGregor, C. Catley, J. Padbury, and A. James, "Late onset neonatal sepsis detection in newborn infants via multiple physiological streams," *J. Crit. Care*, vol. 28, no. 1, pp. e11–e12, Feb. 2013.

[82] A. Parichehreh and U. Spagnolini, “Seamless LTE connectivity in high speed trains,” in *2014 IEEE Wireless Communications and Networking Conference (WCNC)*, 2014, pp. 2067–2072.